平成　29 年　博 士 論 文
[博 士 (工学)

Reconstruction of paleoceanographic significance in the western Pacific and Atlantic Ocean during the Neogene based on calcareous nannofossil productivity and size variations - with special reference to formation of petroleum source rocks

A thesis submitted in fulfillment of the requirements for the Degree of Ph.D, Akita University, AKITA, JAPAN

Santi Dwi Pratiwi
D9514002

ST (B. Eng) (Indonesia), M.Sc. (Akita)

Department of Geosciences, Geotechnology, and Materials Engineering for Resources
Graduate School of Engineering and Resource Sciences
Akita University
2017

ABSTRACT

Source rock is the first logical step to assess a petroleum system because the viability of conventional or unconventional systems depends on its source rocks. The high content of organic materials in the petroleum source rocks reflects the high phytoplankton productivity in paleo-sea surface by upwelling condition. The significance of paleoceanography is the relationship of Ocean surface productivity with the global climatic condition. A high-resolution investigation of Oligocene to Pleistocene calcareous nannofossils stratigraphy was carried out on four ODP Holes in the western Pacific and Bahama Bank of Caribbean Sea to reconstruct the paleoceanography and correlate it with the global events. I compared my results with those of the northwestern Pacific, the western Pacific and the Indian Ocean studies to discuss the paleoceanographic events through the Neogene and interpret the cause of the events based on the correlation to global tectonic and climatic events. This is a new study with special reference to the formation of petroleum source rock based on paleoceanography analysis and the influence of global climatic events from three different Ocean study sites.

Leg 125, Site 782 Hole A in the Izu-Bonin forearc of the western Pacific Ocean, and Leg 166, Site 1006 Hole A and Site 1007, Hole B and Hole C in the Bahama Bank of the Caribbean Sea (Atlantic Ocean) were analyzed for this study. A total of 327 samples from ODP Hole 782A, 1006A, 1007B and Hole 1007C were prepared for microscopic observation and calculation of nannofossil productivity based on the nannofossil assemblages. The biostratigraphic framework consisting of 26 zonal and non-zonal events based on the occurrences of 68 species of calcareous nannofossil. More specifically, an interval at Site 782 Hole A was has correlated within the middle Miocene (13.654 Ma) to Pleistocene (0.265 Ma).

These are as follows: the first occurrence of *Emiliania huxleyi* (NN21/NN20 Zone); the last occurrence of *Pseudoemiliania lacunosa* (NN20/NN19 Zone); the last occurrence of *Discoaster brouweri* (NN19/NN18 Zone); the last occurrence of *Discoaster pentaradiatus* (NN18/NN17 Zone); the last occurrence of *Discoaster surculus* (NN17/NN16 Zone); the last occurrence of *Reticulofenestra pseudoumbilicus* (NN16/NN15 Zone); the first occurrence of *Discoaster asymmetricus* (NN14-NN15 Zone); the last occurrences *Discoaster quingqueramus* and *Discoaster berggrenii* (NN12/NN11 Zone); the first occurrences of *Discoaster berggrenii* (NN11/NN10 Zone); the first occurrence of *Catinaster coalitus* (NN8/NN7 Zone); and the last occurrence of *Cyclicargolithus floridanus* (NN7/NN6 Zone).

Eighteen nannofossil datum species covered the Oligocene (22.824 Ma) to early Pliocene interval (3.77 Ma) at Site 1007, they are; the last occurrence of *Reticulofenestra pseudoumbilicus* (NN16/NN15 Zone); the first occurrence *Discoaster asymmetricus* (NN14-NN15 Zone); the last occurrence of *Discoaster quingqueramus* and *Discoaster berggrenii* (NN12/NN11 Zone); the first occurrence of *Discoaster berggrenii* (NN11/NN10 Zone); first occurrence of *Catinaster coalitus* (NN8/NN7 Zone); the last occurrence of *Cyclicargolithus floridanus* (NN7/NN6 Zone); the last occurrence of *Sphenolithus heteromorphus* (NN6/NN5); the last occurrence of *Helicosphaera ampliaperta* (NN4/NN5); last common occurrence *Sphenolithus belemnos* (NN3/NN4); the first occurrence of *Sphenolithus belemnos* (NN2/NN3); and the first occurrence of *Discoaster druggii* (NN1/NN2).

Ten nannofossil bioevents are correlated with 2.8 Ma (late Pliocene) to 8.52 Ma (late Miocene) at Site 1006 of Bahama Bank of Caribbean Sea, they are; *Reticulofenestra pseudoumbilicus* (NN16/NN15 Zone); the first occurrence of *Discoaster asymmetricus*

(NN14-NN15 Zone); the last occurrence of *Discoaster quingqueramus* and *Discoaster berggrenii* (NN12/NN11 Zone); and the first occurrence of *Discoaster berggrenii* (NN11/NN10 Zone). The calcareous nannofossils are generally abundant and their preservation is moderate to good in both Site 782 and Site 1006. However, calcareous nannofossils in site 1007 are moderately to poorly preserved.

The relationship between the coccolith productivity and relative abundance of *Discoaster* shows the negative correlation throughout the section in Hole 782A and Hole 1006A. The Coccolith number is low in the section of NN6 and NN7, but an increase is found from NN8 to NN16 in Hole 782A. The coccolith productivity in the Pleistocene sequence also drastically increases and reaches the highest peak in NN19 zone to Pleistocene. The relative number of *Discoaster* which is show maximum in NN6 to NN10 in the Miocene experienced a decrease in the sequence above NN10, and it abruptly disappeared in 2.0 Ma at the western Pacific Ocean site. Although the mode of *Reticulofenestra* size is situated around 2 to 3 μm throughout the section from middle Miocene to Pleistocene, bimodal peaks occur in some intervals in this Hole. Larger size mode from 2 to 12 μm appears between 13.5 Ma and 8.8 Ma, 8 Ma and 6 Ma, 6 Ma and 3.8 Ma, and above 3 Ma. The larger mode size increases in these intervals and disappears at the top of the intervals in Hole 782A.

The coccolith productivity increases from NN1 to NN16 in the Bahama Bank but the relative abundance of *Discoaster* indicates no significant changes in the Site 1007. The mode and maximum size of the *Reticulofenestra* increase three times while the mode indicates bimodal in Site 1007 and shows that the mode of *Reticulofenestra* size is situated in 2 to 3 μm throughout the section. The bimodal pattern in the sequence was also observed in the lower part of the section from NN7 to NN10. And in the lower Pliocene

sequence at Site 1007 of Bahama Bank. The coccolith productivity of site 1006A increased from NN10 to NN12 and the relative abundance of *Discoaster* species shows the opposite trends in this interval. The mode and maximum size of the *Reticulofenestra* increased three times while the mode indicates bimodal (NN10, NN12, and NN14-15 Zones) in Hole 1006A.

The dominance of small *Reticulofenestra* at 8.8 Ma shows a positive correlation with coccolith productivity in both sites of studies. The drastic decrease of the maximum size of *Reticulofenestra* at 8.8 Ma in the late middle Miocene and 3.75 Ma in the late early Pliocene was observed in the western Pacific and Caribbean Sea of Atlantic Ocean sites. The maximum size of *Reticulofenestra* increased until 8.8 Ma, which shows the oligotrophic conditions with sea surface stratification and thermocline. The stabilization of the Ocean condition in the western Pacific Ocean collapsed at 8.8 Ma, 5.4 Ma, 3.75 Ma and 2.516 Ma as a result of the change to eutrophic sea surface conditions based on the decrease of the maximum size of *Reticulofenestra*.

Young (1990) demonstrated that there were three bimodal events occurred in the Indian Ocean sites from NN6 to NN16 Zone at 8.8 Ma, 5.4 Ma, and 3.75 Ma. A drastic decrease in the maximum size of *Reticulofenestra* coccoliths was observed at 8.8 Ma. These events are responsible for the change of sea surface stability in the Indian Ocean. Imai *et al*. (2015) studied calcareous nannofossil assemblages from ODP holes 1210A in the northwestern Pacific Ocean and the result also revealed that the large number of *Reticulofenestra* coccolith indicates a shallow thermo- and nutricline had drastically changed to the small size in six times (in 8.8 Ma, 6.4 Ma, 5.4 Ma, 3.75 Ma, 3.4 Ma and 2.75 Ma) in this sites.

Comparison of the present investigated results of the size variation of

Reticulofenestra in the western Pacific Ocean and Caribbean sea with those in Indian Ocean and northwestern Pacific Ocean show that these changes in *Reticulofenestra* maximum size strongly related to the collapse of stability of Ocean surface and are clearly traceable in the Bahama Bank, the western and the northwestern Pacific Ocean and the Indian Ocean. Based on the relationship between size variability and nutrient condition, these nannofossil events are interpreted as a change to a high nutrient condition caused by changes in the global climate system. Among them, two events found in 8.8 Ma and 3.75 Ma are correlated to the intensification of the Asian Monsoon and closure of Panama Isthmus respectively.

Event 1 recognized in 8.8 Ma in the Indian Ocean, Bahama Bank of Atlantic Ocean, and the western Pacific Ocean is strongly influenced by the intensification of the Asian Monsoon. Event 4 of 3.75 Ma is strongly related to the formation of Panama Isthmus. The final closure of Panama Isthmus was established around 2.75 Ma based on nannofossil assemblages and isotope stratigraphy. On the basis of these facts, a drastic decrease of the maximum size of *Reticulofenestra* occurred in 3.75 Ma is strongly influenced by the closure of Panama Isthmus.

The additional event 2 (6.4 Ma) found in the northwestern Pacific and the Indian Ocean and additional event 3 (5.4 Ma) found in both the aforementioned sites and the Bahama Bank indicated by maximum size changes of *Reticulofenestra* is correlated to the formation of hiatus in the western Pacific Ocean and Bahama Bank. The ages of these events are also showing correlation to global events such as the formation of western Antarctic ice sheet. Additionally, the event 3 in 5.4 Ma indicated by size changes of *Reticulofenestra* is strongly influenced by Messinian Salinity Crisis.

These results indicate that nannofossil events recognized in this study reflect the

drastic changes in global paleoceanography, which occurred four times throughout the Neogene. Rising sea level promotes retention of nutrients in marginal seas through several possible mechanisms, leading to higher organic production and/or eutrophic conditions.

On the one hand, the increase of coccolith productivity was superimposed on the change of stratigraphic records (sequence stratigraphy) composed of several sequences and transgressive – regressive cycles deposit in a dynamically changing basin and sub-basin of a petroleum system. On the other hand, the stability of sedimentation rate and high phytoplankton productivity has become important factors for the development of petroleum source rocks. Also, the unconformity zone is crucial data for the source rock deposition and is related with the trap of oil and gas. Hokkaido, Niigata and Akita in Japan, Monterey Formation on Santa Barbara, Los Angeles basin, Palos Verdes Hills and Santa Monica Mountains basin are examples of the areas where the source rocks were formed during the middle to the late Miocene age and correlated with the timing of eutrophication during the late Miocene (8.8 Ma). Based on those results and investigation, I suggest that the results from this study are available for the special references of the formation of petroleum source rocks.

Keyword: Paleoceanography; calcareous nannofossils; *Discoaster*; *Reticulofenestra*; nutricline; thermo-cline; oligotrophic; eutrophic; closure of Panama Isthmus; Intensify of the Asian Monsoon; Messinian Salinity Crisis; formation of petroleum source rocks.

ACKNOWLEDGMENTS

I wish to express my gratitude to Professor Tokiyuki Sato, who gives me the opportunity to study ‘nannofossil’ in his laboratory at Akita University. I extremely thank him for most advice, assistance, and learning in research. Besides that, he always supports and understands me both in my study and life during in Akita.

I would like to thank Dr. Makoto Yamasaki for assistance and advice. I really appreciate all the helps during my study at Akita University.

My gratitude also goes to the Leading Program Grant Akita University for being the biggest sponsor during my master course in Japan. Thank you for the financial and moral support. Without their supports, I might not have an opportunity to pursue and complete my Doctoral program.

Great thanks to Engineering and Resources Science Faculty of Akita University that has given me the opportunity to study nannofossils in Doctoral Course.

Samples for this research were provided by ODP (Ocean Drilling Program) Leg 125 Site 782 Hole A and Leg 166 Site 1007 Hole B.C and Site 1006 Hole A.

Thanks to Basuki Tjahja Purnama.MM (Governor of Jakarta City, Indonesia) for his supports and helps.

My warm thanks to the graduate and undergraduate students (2014-2016) in our laboratory and Leading Program, and special thank to Leading Program officer for the help, support and thoughtful discussions both of in research and life. There are many people and colleagues who have inspired, helped, discussed with me during I am staying in Akita.

And finally, my high appreciate to my mother “Surya” in heaven, I have kept my promise to mom, my father “Saleh.S’, and my sister Susiamsih.

Contents

List Figures

List Tables

Chapter I. Introduction

One of the important factors for the quality of marine source rocks is the abundance of organic matter (OM) supply which is controlled by paleoclimate, sedimentation rate, and paleocurrent system. The high production of organic matter in the petroleum source rocks is reflected by the upwelling condition. High phytoplankton production is an essential factor for the development of petroleum source rocks. Previous paleoceanography studies demonstrate that stratigraphical distribution patterns of calcareous nannofossils were strongly influenced by climatic fluctuations of the oceans stabilities throughout the Neogene. Changes in nutricline and thermocline conditions in the surface Ocean can cause a breakdown of the stratification. Coccolithophorids, which live in the photic zone of the world's Oceans are considered to be sensitive to changes in sea surface temperature and nutrient conditions. This explains why nannofossils, fossil of coccolithophorids, are useful not only for biostratigraphy but also for paleoceanographic reconstruction of Mesozoic and Cenozoic ages.

The difference of geographic distribution pattern of calcareous nannofossil assemblages in sedimentary records has been controlled by sea surface water mass conditions and is influenced by global climatic events. A significant paleoceanographic highlight related to Ocean surface productivity is linked with the global climatic condition in the worldwide. Coccolithophores productivity is low in extreme oligotrophic conditions and poor nutrient supply. In contrast, eutrophic conditions and high nutrient supply in the sea surface Ocean, make productivity high. Although the coccolithophorids live in the upper photic zone in the recent ocean, a few species such as *Florisphaera profunda* are present in the lower photic zone in recent stable Ocean (Okada & Honjo, 1973; Molfino &

McIntyre, 1990). The ecological characteristic of *Florisphaera profunda* is applicable to the reconstruction of paleoceanographic conditions such as stability and nutrient conditions of sea surface Ocean. However, as the occurrence of *Florisphaera profunda* is limited in the interval of Pliocene to Quaternary, it is difficult to apply and reconstruct the stability of surface Ocean to the Neogene sequence based on the ecology of *Florisphaera profunda*.

Scientists had been focusing on the paleoecology of discoasters which were considered as warm water species based on limited distribution in lower latitude region (Haq and Lohmann, 1976; Bukry, 1978). Aubry (1992) interpreted the discoasters as lower photic zone species based on their distributions. Stoll et al (2007) interpreted that *Discoaster* lived in lower photic zone based on Sr of discoasters in the Paleogene sequence. These characteristics indicate that the discoasters are useful tool for reconstruction of paleoceanographic conditions such as ocean surface stability.

Takahashi and Okada (2000) showed that coccolith size is a good indicator of sea surface nutrient conditions. Recently, Sato and Chiyonobu (2009) reconstruct the history of surface ocean stability based on coccolith size and *Discoaster* abundance. Farida et al. (2012) and Imai e al. (2015) also discussed the Neogene paleoceanography of Pacific Ocean based on *Discoaster* abundance, nannofossil productivity, and *Reticulofenestra* size. However, the problems regarding the interpretation of the cause of these paleoceanography changes and the relationship between other areas are yet to be resolved.

The purpose of this study is focused on the reconstruction of the Neogene paleoceanography of western Pacific and Caribbean Sea (Figure 1) based on *Discoaster* abundance and *Reticulofenestra* size variability. On the basis of the comparison of this study results with those of the Indian Ocean (Young, 1990), and northwestern Pacific Ocean (Imai et al., 2015) studies, I discuss the paleoceanographic events through the

Neogene, and interpret the cause of the events based on the correlation with global tectonic and climatic events. In addition, paleoceanography results were correlated with the timing of global tectonic events in the worldwide from those study sites and this study aims at the interpretation of special reference to formation of petroleum source rocks based on the timing of changes of calcareous nannofossils assemblage and product ivy distribution.

Also, this study will be focusing more on high-resolution absolute and relative abundance of species assemblages of nannofossil and the pattern of mode size variation because those two parameters are strongly influenced by the changes in Ocean climate and are related to the events of accumulation of petroleum source rock. Based on four different oceanography settings, the results of this study are not just applicable for a regional study but also on a global scale.

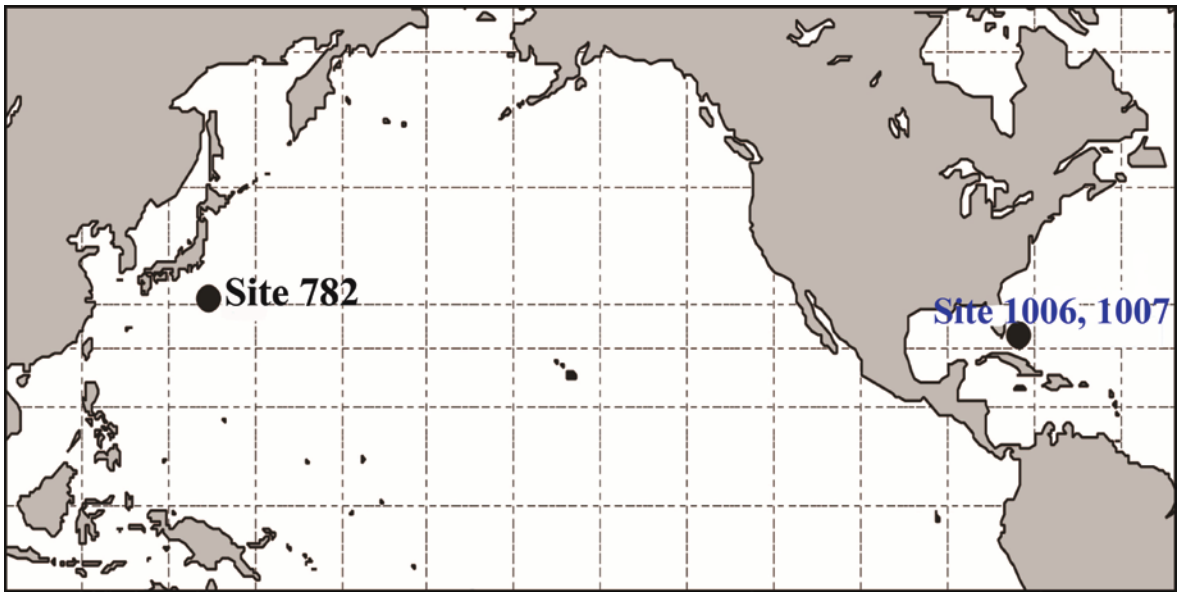

Figure 1.1. Map showing the location of ODP Site 782 in the Western Pacific Ocean and ODP Site 1007 in the Bahama Bank of Caribbean Sea.

Chapter II. Background of Study

2.1 Recent Oceanographic Setting

Leg 125, Site 782 Hole A in the Izu-Bonin forearc of the western Pacific Ocean, and Leg 166, Site 1006 Hole A, Site 1007, Hole B and Hole C in the Bahama Bank of Caribbean Sea are analyzed for this study.

2.1.1 ODP Leg 125 Site 782

The study area is located in Hole 782A Izu-Bonin, which is included in Leg 125 Site 782 conducted in 1990 (latitude 30°51.66’ N, longitude 141°18.85’ E). Site 782 is situated on the outer half of the Izu-Bonin forearc, about 70 km west of the axis of the Izu-Bonin Trench (Figure 2.1.1), at a water depth of 2958.9 m. Hole 782A was drilled to 476.8 mbsf (figure 2.1.2), and this site is influenced by the Kuroshio current. The Kuroshio Current is the major western boundary current of the North Pacific Ocean gyre and is formed at the western end of the North Equatorial Current (NEC). It is situated along the northeastern edge of the Kuroshio at approximately 200 m depth contour at the edge of the continental shelf from about 26 to 29° N (Qiu et al. 1990).

The Kuroshio Current systems from the fact that the downwelling dominant subtropical North Pacific Ocean is low in biological productivity and is devoid of detritus and other organic material in the surface water. The subarctic North Pacific Ocean, on the other hand, is dominated by upwelling. The Kuroshio Current originates east of the Philippine coast where the westward flowing North Equatorial Current (NEC) bifurcates into the northward-flowing Kuroshio Current and the southward flowing Mindanao Current (Qiu et al. 2000). The Kuroshio Current system is an important component of Earth's climate system. The northward-flowing Kuroshio, the western boundary current

of the wind-driven North Pacific subtropical gyre, transports warm and saline tropical waters to higher latitudes. After leaving the Japanese coast, it flows eastward as the Kuroshio extension, circulation gyre exists to the south of the Kuroshio and its extension. In this region of the Pacific, where cold dry air masses from continental Asia encounter the warm Kuroshio waters, the ocean to atmosphere heat flux is among the highest in the world (Yasuda, 2003).

Just as the current reaches Japan's southeast tip, it flows over the shallow Izu-Bonin Ridge which extends due south from Honshu, Japan's main island. The Kuroshio undergoes complex and little-understood fluctuations near this ridge.

Once past the Izu-Bonin Ridge, the Kuroshio may turn north along Japan's east coast for a short distance, or it may continue to flow almost due east. In either case, it joins the Oyashio current, which flows southward from the Kamchatka Peninsula. Together these two currents leave the coast and from the Kuroshio extension.

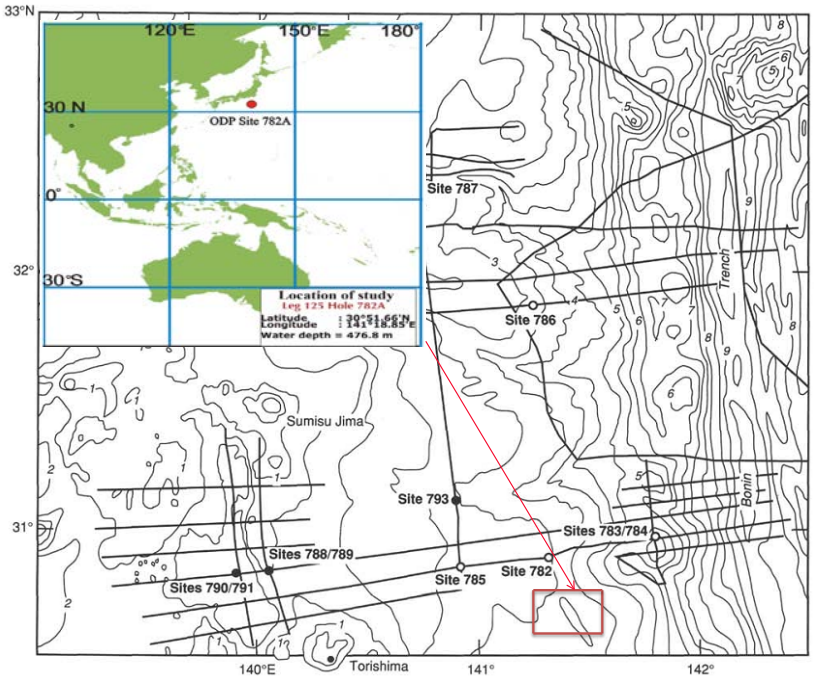

Fig. 2.1. Bathymetry map of the Izu Bonin forearc and forearc areas from about 30.5°N to 33°N. Contour interval is 0.5 km (Fryer et al., 1990)

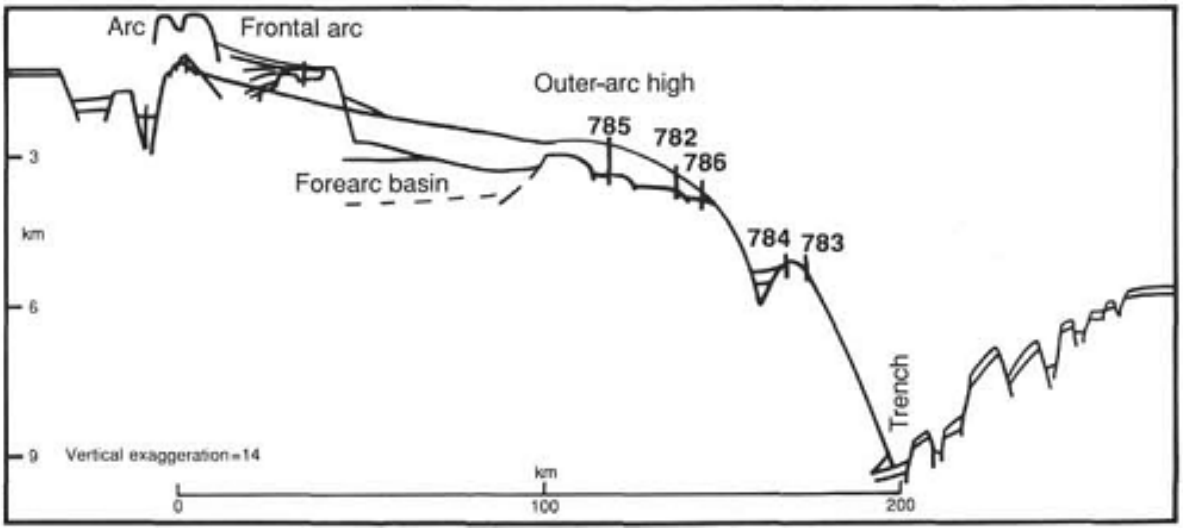

Figure 2.2. Location of Sites 782 through 786 in the Izu-Bonin forearc, as seen in schematic cross section

2.1.2 ODP Leg 125 Site 1006 and 1007

Site 1006 (24°23.989'N, 79°27.541'W) is located at a depth of 658 m approximately 30 km from the western platform edge of the Great Bahama Bank (GBB) (Figure 2.3). A nearly continuous section of Pleistocene to middle Miocene sediments was recovered at Site 1006, drilled in the Straits of Florida at the distal end of the Bahamas Transect (Eberli et al., 1997). Site 1007 (24°30.261’N, 79°19.34’W) is situated at the crossing of seismic Lines 106 and 102B and located on the toe-of-slope of the western Great Bahama Bank (GBB) at 647 m (Figure 2.3) in the Bahama Bank of the Caribbean Sea in the Atlantic Ocean. Site 1006 is positioned on a thick continuous sequence of Neogene-aged drift sediments (Fig. 2.4).In the Caribbean Sea, the main current is the western extension of the North and the South Equatorial current at the Atlantic Ocean while the surface water in the Caribbean is generally characterized by low productivity except in coastal regions, such as off the Venezuelan Coast (Muller et al, 1993). The Atlantic equatorial current branches off the Lesser Antilles Island and one of them invades into the Caribbean Sea. The Caribbean

Current, one of the western boundary currents at the Atlantic Ocean, flows westward across the Caribbean Sea. The Caribbean Current passes through the Yucatan Channel and flows into the Gulf of Mexico (The Loop Current). The Loop Current goes out from the Gulf of Mexico and becomes strong Gulf Stream, which extends to the eastern end of the North American Continent. The western boundary current contributed by the Gulf Stream at the North Atlantic Ocean is apparently strengthened by the presence of the Loop Current. The Central American Seaway would play an important role in the past climate events and it also influenced the tectonic history around the Caribbean and the eastern equatorial Pacific region linked to the circulation of the world oceans.

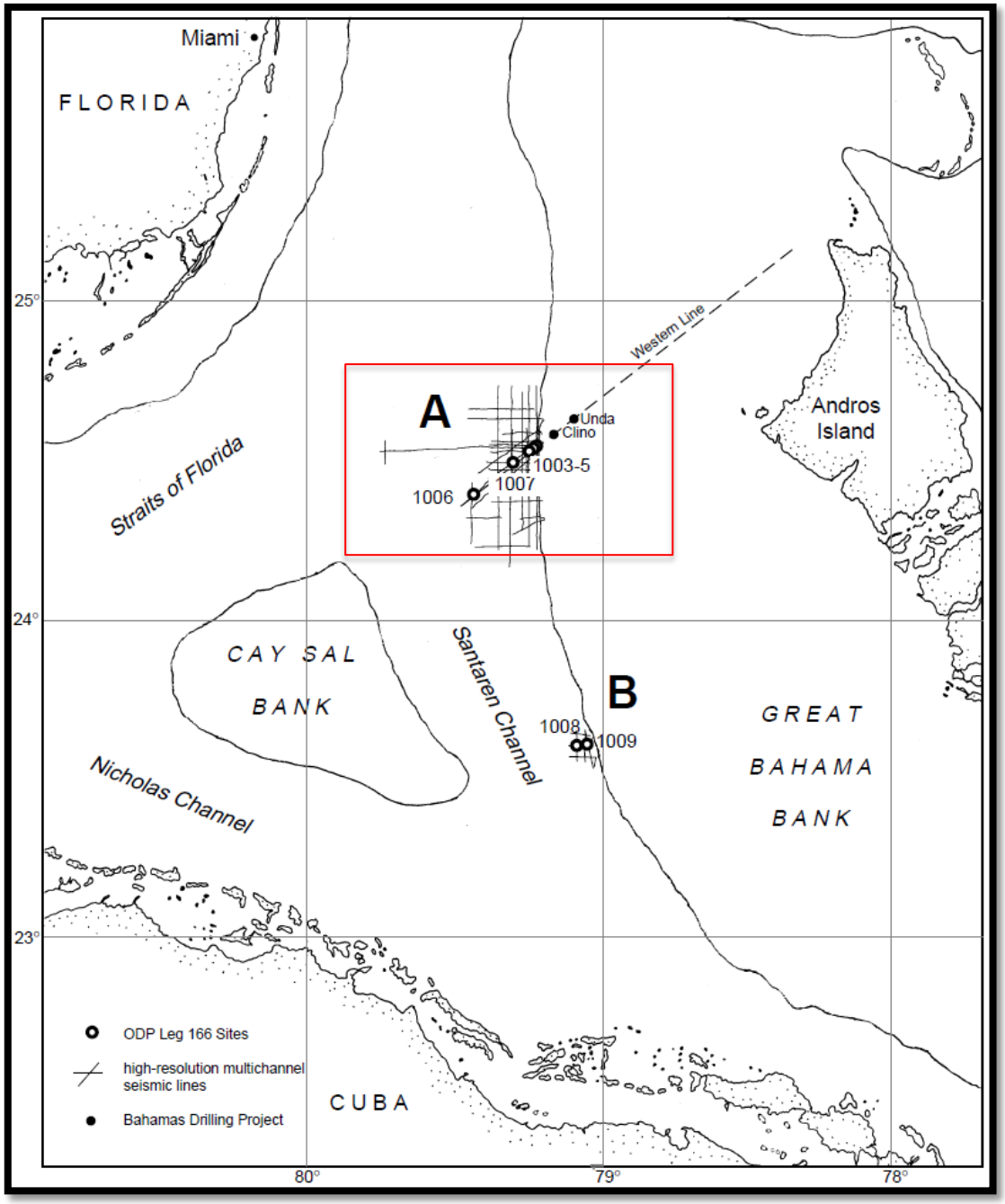

Figure 2.3. Location map of the Bahamas showing Leg 166 sites survey-line. Site 1006 and 1007 are located in area A (Eberli et al., 1997).

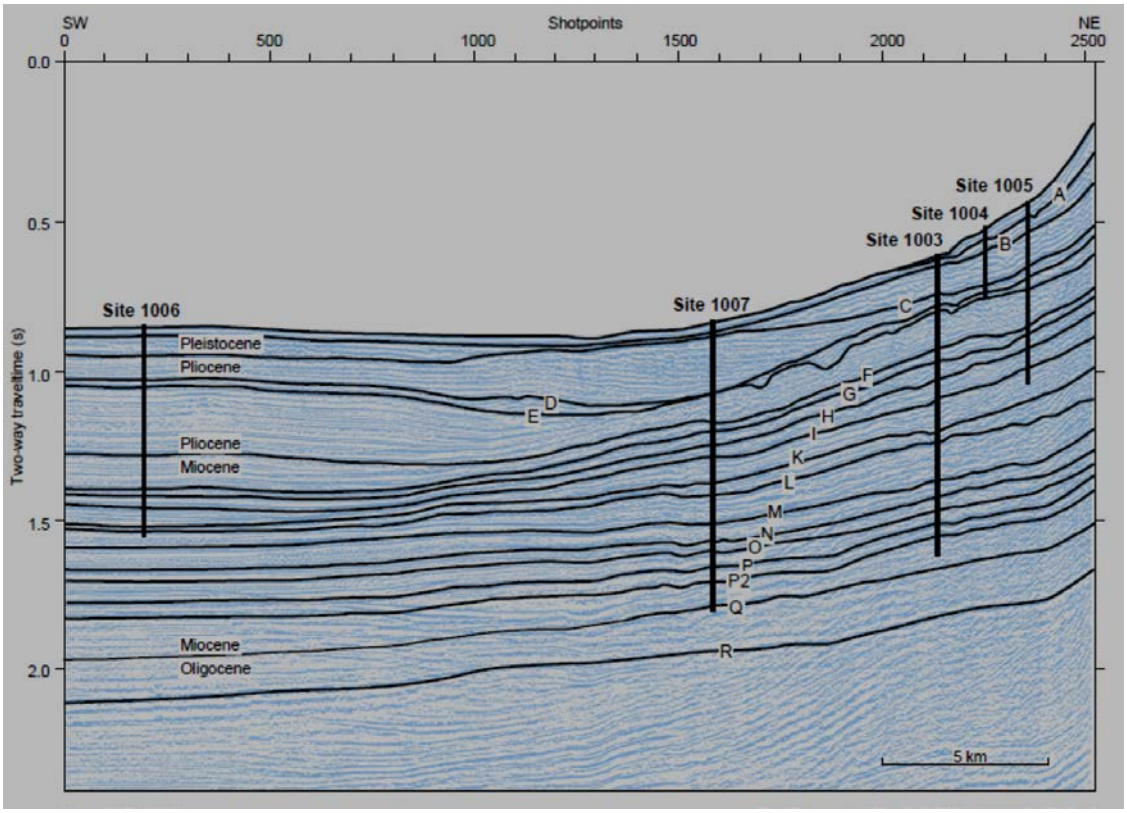

Figure 2.4. Portion of the high-resolution multichannel seismic Line 106 that retraced the cross-bank Western Geophysical seismic line with the positions of Sites 1003, 1004, 1005, and 1007 (Eberli et al., 1997).

2.2 Cenozoic Oceanography Setting

The Pacific and Atlantic region are important areas to resolve major geological problems, especially for petroleum source rocks because of their tectonic/climatic events and significance changes of paleoceanographic events. The closing of the Indonesian Seaways (van Andel et al., 1975), Asian Monsoon intensification and final closure of the Panama Isthmus are the most obvious examples. The development of ocean circulation was strongly controlled by the disappearance of major equatorial seaways which was affected by tectonic events. Opening and closing of oceanic gateway affected ocean circulation, climate, marine productivity, and nutrient distribution (Nathan and Leckie, 2009; Sumata et al., 20004). The current system influences the zonal distribution pattern of the coccolithophorid species in the surface and near-surface water (Honjo, 1977). Zachos et al. (2001), presented that global climatic events during Miocene, as follows;

Mid-Miocene Climatic Optimum, East Antarctic ice-sheet, Asian Monsoons intensify and West Antarctic ice sheet (respectively), as well as tectonic events such as Himalaya uplift and Panama seaway closure (Figure 2.4).

These events significantly influenced ocean circulation, nutrient supply, and thus on the productivity of the oceans (Krammer et al., 2006). One of the tectonic events that significantly changed the Caribbean circulation pattern was the final closure of the Isthmus of Panama. Duque-Caro (1990) discussed a strong cooling episode considered as the invasion of the California current and the final closure of the Panama Isthmus and was estimated at 3.7 to 3.1 Ma. Haug and Tiedman (1998) described that current system across the Panama Seaway changed at 4.6 Ma and intensification of the northern hemisphere glaciation between 3.1 Ma and 2.5 Ma.

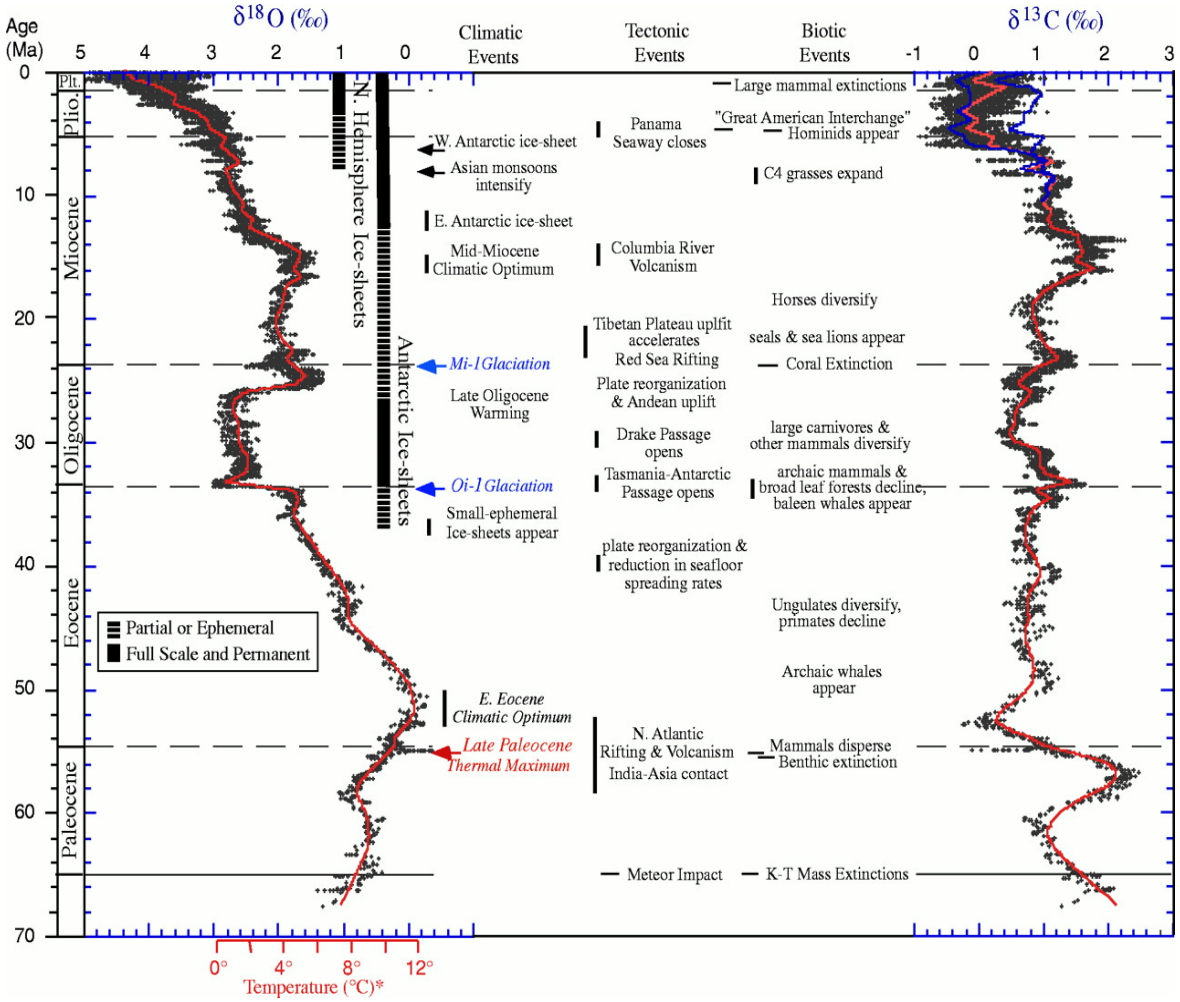

Figure 2.5. Global deep-sea oxygen and carbon isotope records based on data compiled from more than 40 DSDP and ODP sites (Zachos et al., 2001).

Kameo and Sato (2000), Sato et al. (2004), and Bartoli et al. (2005) also described the final closure of Panama Isthmus was established around 2.75 Ma based on nannofossil assemblages and isotope stratigraphy. Krijgsman et al. (1999) presented astronomically calibrated chronology for the Messinian salinity crisis. They showed that the onset of the Messinian salinity crisis was at 5.96±0.02 Ma and the isolation from the Atlantic Ocean has established between 5.59 and 5.33 Ma. Messinian salinity crisis event influenced the changes of sea surface stability conditions in the global sea level (Hodell et al., 2001; Warny et al., 2003). Cane and Molnar (2001) suggested that closure of the Indonesia

seaway 3-4 Ma could be responsible for the global climate changes. During 8 Ma and 10 Ma is characterized by the intensification of the Asian Monsoon caused by uplift of Tibetan Plateau (Burbank et al., 1993; Filipelli, 1997; Zhisheng et al., 2001; Zachos et al., 2001). Uplift of plateaus and mountains has been proposed as a cause of large-scale changes in climate through the action of the carbon cycle (Ruddiman, 1997). The nutrient pulse to the ocean would be expected to increase net primary productivity during these times, and an increase in organic matter production and burial in the ocean due to an increase in the nutrient flux is an additional sink for atmosphere carbon (Filipelli, 1997).

The Mid-Miocene Climatic Optimum occurred in the late early Miocene at ~16 Ma and was associated with a mid-latitude warming of about 6°C relative to the present (Flower and Kennett, 1994). This suggests that early stage of this climatic transition from ~16 to 14.8 Ma, was marked by major short-term variations in global climates, East Antarctic Ice Sheet (EAIS) volume, sea level, and deep ocean circulation.

2.3 Calcareous nannofossil stratigraphy and its application to paleoceanography

The earth has undergone several climatic events over geological time scales and these changes affect the petroleum source rocks distribution in the worldwide. The Pacific and Atlantic region are important areas to resolve major geological problems attributed to these major climatic events and significance changes of paleoceanographic events. Uplift and climate change are intricately linked and can alter regional and global climates due to changes in the ocean circulation and Earth's atmosphere (W.F. Ruddiman, 1997). Ruddiman (1997) explained two basic categories of uplift effect on climate are recognized by two impacts: direct physical impact on climate by means of changes in the circulation of the atmosphere and ocean, and indirect biochemical effects on climate via changes in

atmospheric CO2 and global temperature caused by chemical weathering of siliceous rocks. Climatic and tectonic events influence the structure and productivity of ecosystem or disappearance of organisms and microorganism. Coccolithophores are widespread in the euphotic zone of the global oceans and are the most important part of the marine phytoplankton community, derive energy from photosynthesis and are considered to be sensitive to changes in sea-surface temperature and nutrient levels (McIntyre and Bé, 1967; Winter et al., 1994).

De Vargas et al. (2007) discussed that coccolithophores actively participate in gas exchange (CO2, DMS) between seawater and the atmosphere and in the export of organic matter and carbonate to deep oceanic layers and deep-sea sediments (Figure 2.5).

The organic carbon pump thereby causes a net drawdown of CO_2 from the atmosphere to the ocean and the production of calcium carbonate causing a net release of CO_2 to the atmosphere (Figure 2.5). The biogenic carbonate produced by coccolithophores constitutes of an ideal material for aggregating with the huge reservoir of particulate organic carbon created by photosynthesis in the upper oceanic layers (de Vargas et al., 2007). The climate changes are induced by changes in surface ocean temperature, stratification and the changes in mixed layer light conditions and nutrient cycling. These changes will have a profound effect on the biological carbon pumps. McIntyre and Bé (1967), and Okada and Honjo (1973) divided the assemblages of coccolithophores into five assemblages which are strongly controlled by sea surface temperature in the modern coccolithophores studies from Atlantic and Pacific Ocean. Their results showed that the distribution pattern of recent coccolithophores is clearly related to a latitudinal temperature gradient and to water masses. Changes in the size distribution of coccoliths that covered coccolithophorids are well known throughout various geological periods.

Reticulofenestra specimens are typically found in upwelling areas and are commonly used as an indicator of eutrophic conditions (Flores et al., 1995; Takahashi and Okada, 2000; Kameo, 2002; Chiyonobu et al., 2006). Recently, Sato and Chiyonobu (2009) studied the size variations of *Reticulofenestra* in the middle Miocene sequence in the Pacific Ocean and described that the presence of large size *Reticulofenestra* shows the stable and oligotrophic sea surface condition. Sato and Chiyonobu (2009) presented schematic representations of the vertical distribution of nannofossil assemblages in the Neogene oceans (Figure 2.6). Based on this the abundance of lower photic zone taxa (e.g., *Discoaster*) is shown to increase in response to thermocline and nutricline deepening, and stratification at the sea surface ocean, in both recent times and during the Neogene.

During the stratification (stable condition) waters above the thermocline and nutricline are shown to be oligotrophic, as characterized by decreases in coccolith production and relative abundance of small *Reticulofenestra* coccolith. The opposite character in the mixing or eutrophic condition, a shoaling of the thermocline and nutricline is shown to result in a decrease in *Discoaster* abundance, and increases in coccolith production and the relative abundance of small *Reticulofenestra*, owing to enhanced nutrient transport to the sea surface from the lower photic zone.

There has been a list of studies on nannofossil biostratigraphy in the Bahama Bank and the western Pacific Ocean. However, the problems for interpretation on the cause of these paleoceanography changes based on nannofossil assemblages and the relationship between other areas still remains. Investigation of paleoceanography and comparison to global events in the worldwide sites studies is rare, and special references to formation of the petroleum source rocks have been limited. Biostratigraphy of nannofossils and size

change in general only have been observed using qualitative analysis or smear slide with low-resolution samples interval**.**

I present high-resolution biostratigraphy of calcareous nannofossils and distribution of coccolith size variation in detail and their correlate to water masses and nutrient condition. The importance of the correlation between tectonic and climatic events and the relative abundance of coccoliths and mode size distribution pattern during the Neogene between western Pacific and Atlantic Ocean will be provided in this study.

Finally, these paleoceanographic studies based on a percentage of size variation of coccolith between western Pacific, northwestern Pacific, Indian and Atlantic Ocean clearly demonstrate a relationship between sea surface stability conditions and the influence of global events in the worldwide with implication to the formation of petroleum source rocks. I can see a critical overview of the time interval is direct impacts on climate by changes in the ocean stratification based on assemblages of calcareous nannofossil from this worldwide study sites data. And the timing of drastic changes of paleoceanography in the world occurred based on nannofossil investigated is one of the important references to the formation of petroleum source rocks will be the goals of the present study.

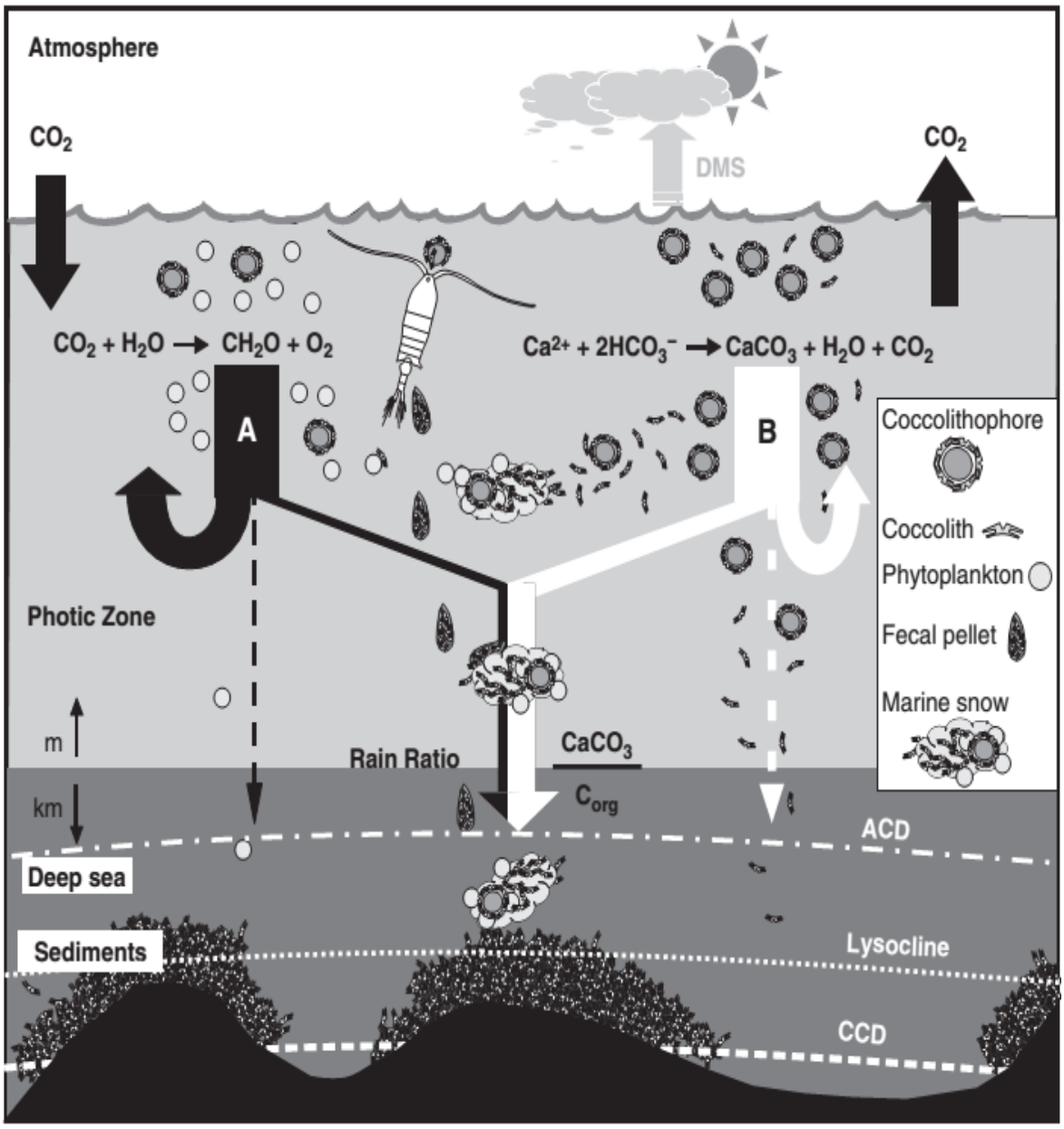

Figure 2.6. Role of coccolithophores in biogeochemical cycles. Through the production of their CaCO3 coccoliths, coccolithophores plays key a role in the global carbon cycling (de Vargas, 2007).

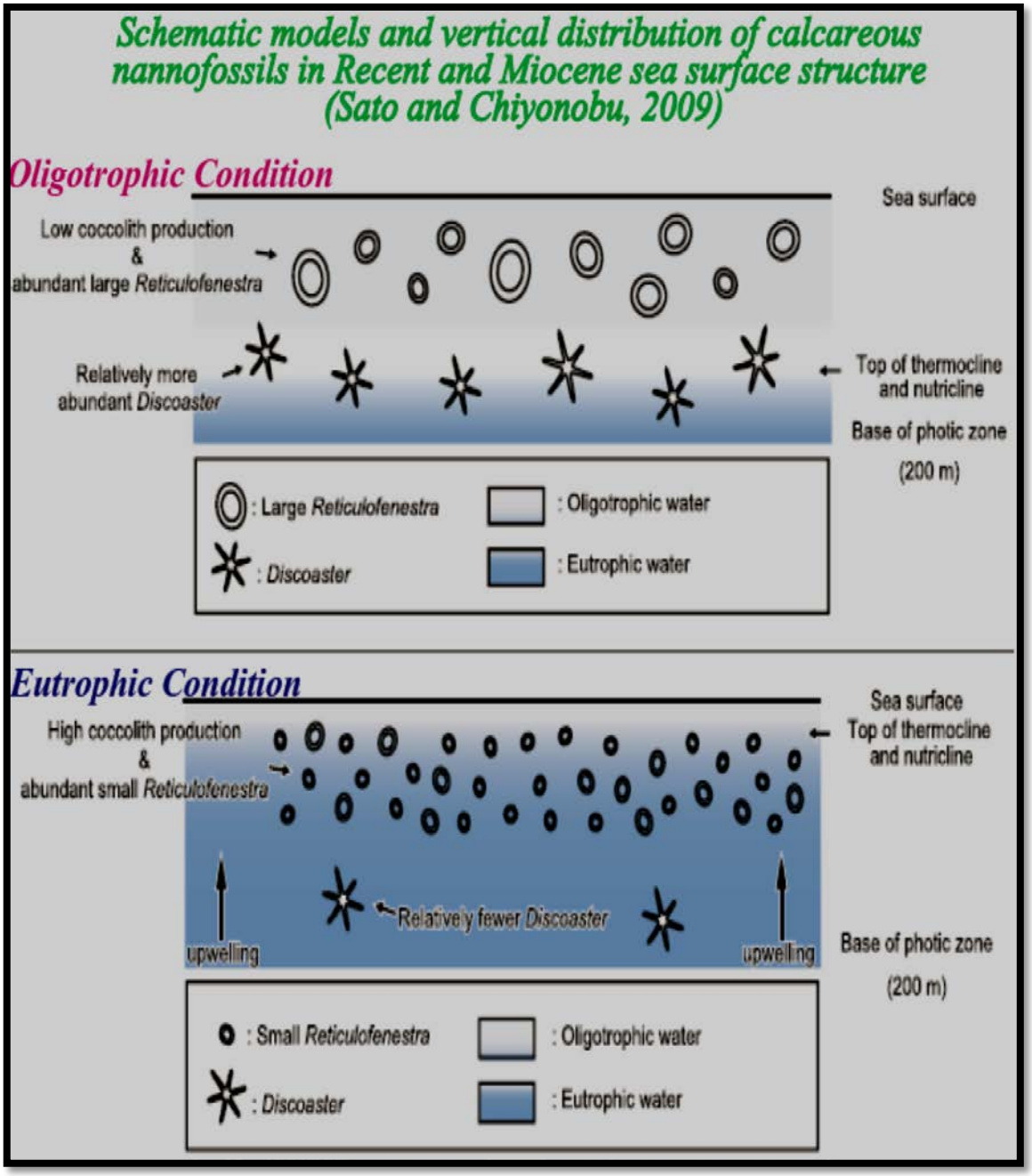

Figure 2.7. Schematic models and vertical distribution of calcareous nannofossils in Recent and Miocene sea surface structure (Sato and Chiyonobu, 2009)

Chapter III
Lithostratigraphy and Previous of Biostratigraphy Records

3 .1 ODP Hole 782A

Ocean Drilling Project Leg 125 was drilled at 9 sites in the Izu-Bonin – Mariana region. Fryer et al. (1990) in ODP Initial Reports explained that Site782 lies on the eastern margin of the Izu-Bonin Forearc basin, about half way between the active volcanic arc and the Izu-Bonin trench. Two holes were drilled: Hole782A was drilled to 476.8 mbsf and Hole 782B was drilled to 468.9 mbsf. As described in ODP Initial Reports that nannofossil marl and vitric nannofossil chalk are the predominant sediment types recovered at Site 782, intervals of foraminifera, radiolarians, nannofossil marl and chalk are also present. The sedimentary section is stratigraphically complete, covering the Pleistocene to the middle Eocene.

The sequence of sediments was divided into two units (I and II), and three subunits from the unit I (IA, IB, and IC) based on the degree of consolidation (Figure 4.1). The unit I is a sedimentary unit from 125-782A-1H-1 to 125-782A-43X-CC (409.2 mbsf) and unit II from 409.2 mbsf to 476.8 mbsf is volcanic basement (andesitic rock).

The subunit IA from cores 125-782A-1H-1 to 125-782A-16X-CC, 9cm is composed of 153.6 mbsf of nannofossil marls (Holocene (?) - lower Pliocene). The subunit IB from cores 125-782A-17X-1 (153.6 mbsf) to 125-782A-35X-5 (337.0 mbsf) is characterized by extensive bioturbation and composed of vitric nannofossil marls (upper Miocene - middle Miocene).

The subunit IC from cores 125-782A-35X-5 (337.0 mbsf) to 125-782A-43X-CC (409.2 mbsf) composed of Nannofossil chalks (upper Oligocene

- middle Eocene). Subunit IC is predominantly vitric nannofossil chalk with frequent intercalations of volcanic ash (Table 3.1). Evidence from calcareous nannofossils, planktonic foraminifers, and diatoms indicates that the sediments overlying the igneous rock range in age from late Pleistocene to middle Eocene (Figure 3.1).

The Cenozoic planktonic foraminifer's stratigraphy for Hole 782A generally low abundance of planktonic foraminifers in the pre-Quaternary, and Diatoms are rare to common and poorly to well preserved in cores 125-782A-1H through 125-782A-34X. Sedimentation a rate in site 782A has been characterized by the late Eocene/earliest Oligocene is extremely low, although only two biostratigraphic events are available for this period (Figure 4.2). The stratigraphy shows continuous of the recovered pelagic sediment, generally high sedimentation rates and increases from Oligocene to Quaternary.

Calcareous Nannofossils Biostratigraphy

Pleistocene nannofossil assemblages are abundant and moderately to well-preserved in Samples 125-782A-1H-1, 20 cm, to 125-782A-4H-CC on the basis of the presence of *Emiliania huxleyi, Gephyrocapsa oceanica, G. caribbeanica, Pseudoemiliania lacunosa, Helicosphaera sellii,* and other species. Samples 125-782A-1H-1, 20 cm, to 125-782A-1H-CC, 125-782A-2H-1, 53 cm, and 125-782A-2H-CC to 125-782A-4H-CC define the late Pleistocene (Zone CN15), middle Pleistocene (CN14b subzone), and early Pleistocene (CN14a subzone), respectively. *Gephyrocapsa oceanica* is absent in Sample 125-782A- 5H-3, 86 cm, whereas *Pseudoemiliania lacunosa, Calcidiscus macintyrei,* and *Gephyrocapsa*

caribbeanica are common; this sample was assigned to the late Pliocene (CN13a subzone), following Backman, Duncan, et al. (1988). Thus, then Pliocene/Pleistocene boundary is located within Sections 125- 782A-5H-1 or 125-782A-5H-2.

Pliocene

Late Pliocene nannofossil assemblages are present from Sample 125-782A-5H-3, 86 cm, to 125-782A-11X-CC. The abundant and moderately to well-preserved assemblages are characterized by marker species of late Pliocene age, *Discoaster asymmetricus, D. brouweri, D. pentaradiatus, D. surculus, D. tamalis,* and *Ceratolithus separatus* (CN12a sub zone). The last occurrence of *Discoaster brouweri,* together with *D. triradiatus,* is present in Sample 125-782A- 6H-CC; the CN12/CN13 boundary thus is present in Core 125-782A-6H.

The last occurrence of *Reticulofenestra pseudoumbilicus* (top of Zone CN11), which coincides approximately with the lower Pliocene/upper Pliocene boundary, is present in Sample 125-782A-12X-CC. This moderately preserved assemblage is characterized by *Sphenolithus abies, Discoaster asymmetricus,* and *Pseudoemiliania lacunosa,* together with *Discoaster brouweri* and *D. pentaradiatus.* The first occurrence of *Discoaster tamalis* and the last occurrence of *Reticulofenestra pseudoumbilicus* and *Sphenolithus* spp. overlap in this sample.

This association, together with *Amaurolithus delicatus* and A. *tricorniculatis,* is common to abundant down to Sample 125- 782A-16X-CC, where the first occurrence of *Ceratolithus acutus* can be found. In Sample 125-782A-17X-CC, the last occurrence of *Discoaster quinqueramus, D. berggreni,* and *Triquetrorhabdulus rugosus,* together with the first occurrence o*f Amaurolithus tricorniculatus,* was

found. Thus, the Miocene/Pliocene boundary is located within Core 125-782 A-17X.

Miocene

Few-to-abundant, moderately preserved late Miocene nannofossil assemblages are present in Samples 125-782A-17XCC to 125-782A-26X-CC. The top of this assemblage has been defined by the last occurrence of *Discoaster quinqueramus* together with *Triquetrorhabdulus rugosus;* the bottom lies between the first occurrence of *Catinaster coalitus* and the first occurrence of *Catinaster calyculus,* within Zone CN6. The first occurrence of *Discoaster quinqueramus* in Sample 125-782A-22X-CC defines the Zone CN8/CN9 boundary.

I expected *Discoaster berggreni*, *D. surculus*, and *D. neohamatus* to appear before *Discoaster quinqueramus,* indicating drilling disturbances in these cores. Sample 125-782A-25X-7, 7 cm, contains the first occurrence of *Discoaster pentaradiatus* together with *D. prepentaradiatus.* Sample 125-782A-26X-4, 92-94 cm, is characterized by the last occurrence of *Discoaster hamatus* (although very rare) and *Catinaster coalitus* (marker species for Zone CN7), together with *Catinaster calyculus* and *Discoaster calcaris.* Therefore, the Zone CN7/CN8 boundary has been placed between Samples 125-782A-25X-7, 7 cm, and 125-782A-26X-4, 92-94 cm.

Middle Miocene nannofossil assemblages were found in Samples 125-782A-27X-1, 110 cm, to 125-782A-35X-5, 125 cm, whereas the early Miocene is completely missing. Sample 125-782A-35X-5, 125 cm, is middle Miocene in age (Zone CN4) on the basis of the occurrence of *Sphenolithus heteromorphus,* together with *Calcidiscus macintyrei, C. leptoporus,* and *Discoaster variabilis.* The presence

of specimens of *Reticulofenestra pseudoumbilicus* larger than 7 mm indicates that this sample is located in the upper part of Zone CN4. Reworked species of Zone CN2 *Discoaster druggi* and *Sphenolithus belemnos* also are present. The top of Zone CN4 can be found in Sample 125-782A-33X-CC, in which the last occurrence of *Spenolithus heteromorphus* was found. The last occurrence of *Cyclicargolithus floridanus* (Sample 125-782 A- 30X-2, 21 cm) and the first occurrence *of Discoaster bugler* (Sample 125-782A-29X-CC) indicate the Zone CN5a/CN5b boundary.

Drilling disturbances are common in middle Miocene cores. However, Sample 125-782A-35X-6, 10 cm, belongs to the late Oligocene on the basis of the last appearance of *Dictyococcites bisectus.* If Zones CN1 to CN4 are partly missing, a hiatus having a duration of more than 7.5 Ma must be present between the middle Miocene and upper Oligocene.

Table 3.1. Lithology summary, Hole 782A (Fryer et al., 1990)

Lithology unit/subunit	Core	Depth (mbsf)	Dominant lithology	Stratigraphic age
IA	125-782A-1H-1 to 125-782A-16X-CC	0-153.6	Nannofossil marls	Holocene (?) - Lower Pliocene
IB	125-782A-17X-1 to 125-782A-35X-5	153.6-337.0	Vitric nannofossil marls	Upper Miocene - Middle Miocene
IC	125-782A-35X-5 to 125-782A-43X-CC	337.0-409.2	Nannofossil chalks, Vitric nannofossil chalks	Upper Oligocene- Middle Eocene
II	125-782A-43X-CC to 125-782A-50X-1	409.2-476.8	Andesitic rocks	(?)

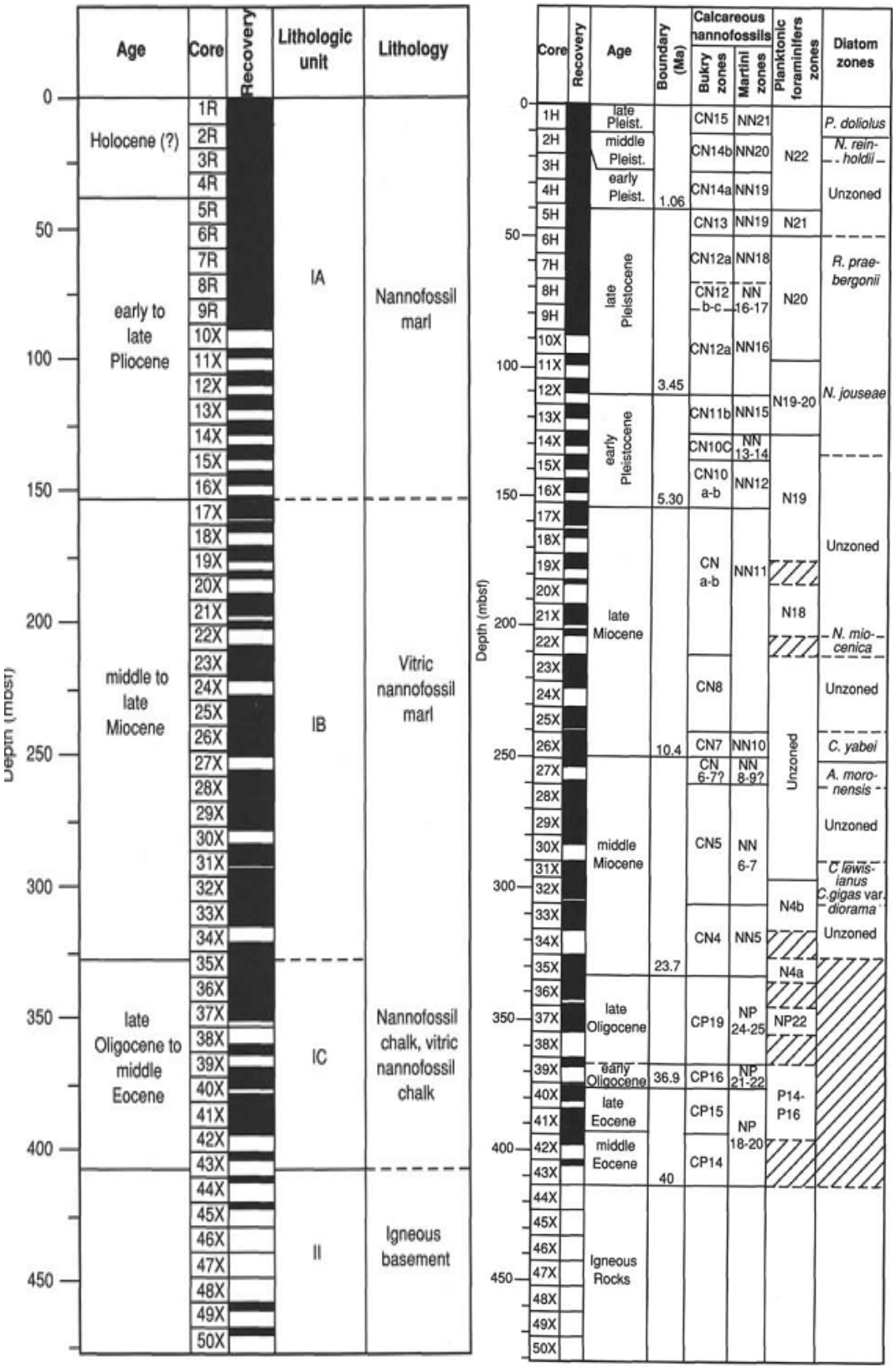

Figure 3.1. Core recovery and lithology summary, Hole 782A (Fryer et al., 1990)

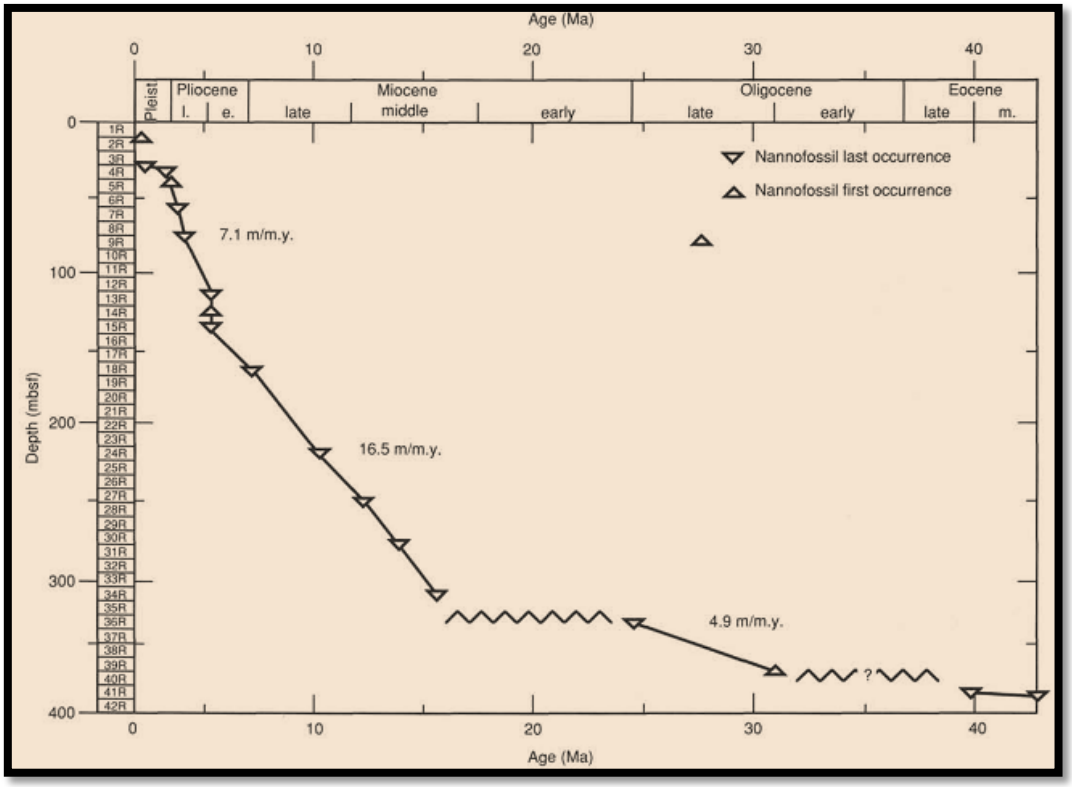

Figure 3.2. Sedimentation rate history, Hole 782A (Fryer et al., 1990)

3.2 ODP Hole 1007B and C

Ocean Drilling Project Leg 166 was drilled at 5 sites in the Bahamas Transect. Eberli et al. (1997) in ODP Initial Reports explained that the Great Bahama Bank is a pure carbonate environment in a subtropical, low-latitude setting and, as such, is an ideal place to evaluate the sedimentary record and timing of global sea-level changes. A larger amount of turbidites and slumps than in the more proximal sites was also recovered in the prograding Miocene sequences. Hole 1007B was drilled to 647.4 mbsf and Hole 1007C was initiated at drilled from 0 to 302.0 mbsf. As described in ODP Initial Reports that 1007B recovered 198.4 m of nannofossil ooze, unlithified to lithified foraminifer and peloidal wackestone and packstone, and foraminifer nannofossil chalk.

Hole 1007C, the deepest of the three holes, penetrated 1235.4 m of foraminifer wackestone, foraminifer nannofossil chalk, and limestone, bioclastic packstone to wackestone, mudstone.

The sedimentary section is stratigraphically complete, covering the Pleistocene to the Oligocene sequences. Sediments at Site 1007 are divided into eight lithostratigraphic units on the basis of compositional and textural changes (Figure 3.3). The upper part of Subunit IA is composed of white to light gray nannofossil ooze that is characterized by moderate bioturbation, which is visible as color mottling or as distinct burrows filled with fine-grained sediment or concentrations of silt- to fine sand-sized skeletal grains.

In the upper part of Subunit IB (Section 166-1007B-2H-1, 139 cm, through Core 166-1007B-3H), light olive brown, silty peloidal wackestone alternates with white nannofossil ooze. Clay- and silt-rich intervals in Core 166- 1007B-4H are relatively thin and thicken downhole through the base of Subunit IB.

Throughout Subunit IC, silt to fine sand-sized peloids is the dominant component. With the exception of the interval of partially lithified foraminifer wackestone (Section 166-1007B-11X-2, 132 cm, through Core 166-1007B-14X), planktonic and benthic foraminifers are rare and poorly preserved. The entire subunit appears mottled as a result of bioturbation. Recovery in the interval containing gray, partially lithified, foraminifer wackestone (Section 166-1007B-11X-2, 132 cm, through Core 166-1007B-14X) was poor. The slumped interval (Cores 166-1007B-15X through Section 166-1007B-16X-3, 135 cm) contains highly contorted interbeds of gray unlithified foraminifer lithoclastic packstone to floatstone with laminated, pale yellow to white, unlithified peloidal wackestone to packstone.

Thin-section analysis (Sample 166-1007B-16X-3, 82-84 cm) shows that, although fine sand-sized planktonic foraminifers are the dominant allochem within the packstone to floatstone, echinoderm debris, micritized bioclasts, fish remains, and shell fragments are also present. Many grains are broken, filled with sediment, or micritized, suggesting that they were reworked. Subunit ID Intervals: 166-1007B-19X-1, 24 cm, through 166-1007B-22X with Age late Pliocene and depth is 165.8 to 203.1 mbsf. Subunit ID consists of a succession of slightly dolomitized wackestone to packstone. Dominant allochems are silt-sized peloids and silt- to fine sand-sized planktonic foraminifers.

The interval from 166-1007B-23X through 33X is covering of early Pliocene age in the depth 203.1 to 302 mbsf. Unit II consists entirely of light gray to pale yellow foraminifer nannofossil chalk. Unit III consists of a succession of light gray to light olive gray foraminifer wackestone, foraminifer nannofossil chalk, and nannofossil limestone. The intervals from 166-1007B-34X through 39X; 166-1007C-1R through 7R-2, 134 cm which covers late Miocene age with depth 302.0-362.6 mbsf.

Lithology Unit IV in the interval 166-1007C-7R-2, 134 cm, through 43R-3, 50 cm cover late to middle Miocene is starting in 362.6-696.4 mbsf. Unit IV consists of a sequence of light gray, gray, and olive gray foraminifer wackestone. Unit V consists primarily of a sequence of light gray to light brownish or olive gray foraminifer wackestone with minor intervals of packstone and mudstone. This unit in interval 166-1007C-42R-1, 0 cm, through 56R-2, 29 cm which cover middle Miocene age (696.4-832.7 mbsf). Unit VI consists of a succession of light gray to light olive or brownish gray foraminifer wackestone with minor intervals of

fine-grained bioclastic packstone and wackestone. The interval of the unit from 166-1007C-56R-2, 29 cm, through 72R-2, 85 cm which covers middle to early Miocene (832.7-986.2 mbsf).

Unit VII consists of a sequence of foraminifer wackestone with minor intervals of mudstone and foraminifer wackestone to packstone, which covers early Miocene sequence. Interval of this unit from 66-1007C-72R-2, 85 cm, through 166-1007C-92R (depth: 986.2-1187.3 mbsf). And Unit VIII consists of pale yellow and light gray foraminifer wackestone and bioclastic wackestone. Interval this unit is formed 166-1007C-93R through 97R which covers early Miocene to late Oligocene in 1187.3-1235.4 mbsf.

Calcareous Nannofossils Biostratigraphy

Samples 166-1007B-23X-CC through 32X-1, 68-69 cm, (212-287 mbsf) contain abundant specimens of *Sphenolithus abies* and *Reticulofenestra pseudoumbilicus,* which define the NN15/16 boundary (3.66 Ma). As *Discoaster asymmetricus* was also found in these samples, this interval is assigned to the lower Pliocene Zone NN14 to NN15. Samples 166-1007B-32X-CC through 33X-CC contain rare and poorly preserved nannofossil specimens, which hampers zonal assignment. Well-preserved specimens of *Discoaster quinqueramus* and *Discoaster berggrenii* were found in Samples 166-1007B-37X-1, 35-37 cm, 166-1007C-3R-1, 105-107 cm, and 166-1007C-3R-CC, which indicates Zone NN11 (5.6 to 8.6 Ma). The absence of the large form *R. pseudoumbilicus* confines this interval to the lower part of Zone NN11 (older than 6.5 Ma).

Discoaster neohamatus and *Discoaster bellus,* which indicate the lower upper Miocene Zone NN10, were found in Samples 166-1007B-37X-1, 35-37 cm, through 41X-CC and 166-1007C-5R-2, 50-52 cm, through 13R-2, 41-44 cm. Samples 166-1007C-15R-1, 37-40 cm, through 19R-1, 67-70 cm, are correlated to the lowermost upper Miocene Zone NN9 on the basis of the presence of *Discoaster hamatus* and *Catinaster calyculus.* Samples 166-1007C-20R-2, 121-123 cm, and 166-1007C-21R-4, 104-106 cm, are characterized by the occurrence of *Catinaster coalitus,* the lowest occurrence of which defines the Zone NN8/7 boundary. *Cyclicargolithus floridanus,* which last appears at the Zone NN6/7 boundary, occurs below Sample 166-1007C-50R-1, 70-72 cm.

The highest occurrences of *Sphenolithus heteromorphus, Helicosphaera ampliaperta,* and *Sphenolithus belemnos,* each of which defines the lower to middle Miocene Zones NN5, NN4, and NN3 are detected in Samples 166-1007C-51R-3, 118-125 cm, 59R-2, 67-71 cm, and 70R-4, 106-109 cm, respectively. The base of NN3 and NN2, defined by the first appearances of *S. belemnos* and *Discoaster druggii,* respectively, were found in Samples 1007C-73R-3, 71-74 cm/74R-3, 46-50 cm, and 85R-2, 150-151 cm/86R-2, 100-102 cm. Below the NN2/1 boundary to bottom sample, the abundance of calcareous nannofossils decreases, and *Braarudosphaera bigelowii,* which lives abundantly in the neritic environment, was found.

The lowermost two samples, Samples 166-1007C-96R-3, 0-1 cm, and 97R-CC, contain the Oligocene species *Sphenolithus ciperoensis,* which defines the Zone NP25/NN1 boundary. This indicates that the bottom of Hole 1007C is correlated to the uppermost Oligocene Zone NP25.

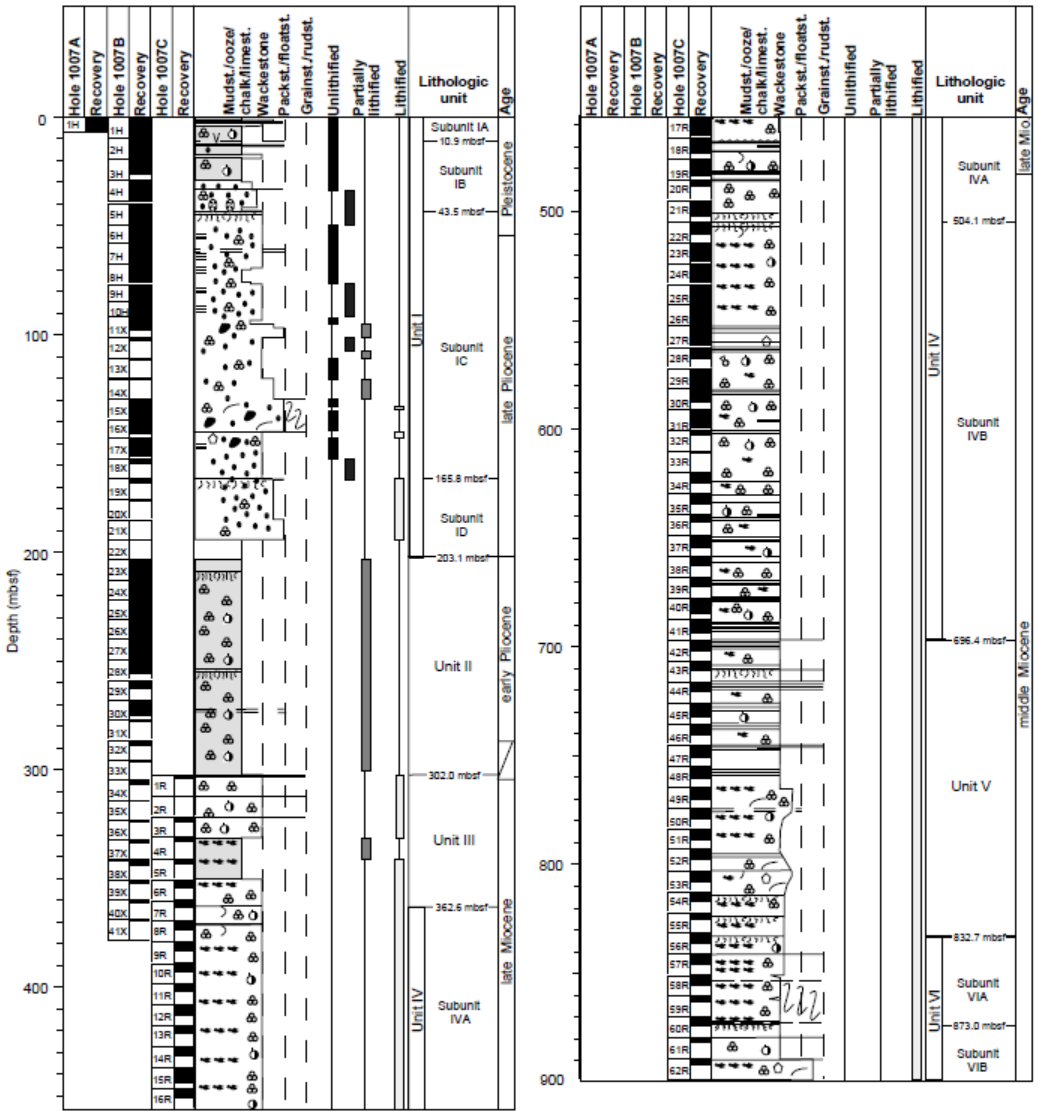

Figure 3.3. Synthesis of dominant texture and component of sedimentary succession at site 1007 (Eberli et al.,1 997).

3.3 ODP Hole 1006A

A 717.3-m-thick Pleistocene to middle Miocene section was recovered at Site 1006 and all nannofossil and planktonic foraminifera zones were present throughout the Pleistocene to middle Miocene section (Eberli et al., 1997). Hole 1006A, the deepest of four holes drilled at Site 1006, recovered 717.3 m of nannofossil ooze, planktonic foraminifer nannofossil ooze, planktonic foraminifer nannofossil chalk, and nannofossil limestone, with variable amounts of admixed silt

and clay. Sediments at Site 1006 are divided into five lithostratigraphic units on the basis of compositional and textural changes (Figure 3.5). Lithology Unit I with intervals: 166-1006A-1H through 14H-4, 35 cm; 166-1006B-1H through 14H-6, 100 cm covering Pleistocene to late Pliocene with depth: 0-125.95 mbsf. The unit I consists of light gray, white, and pale yellow nannofossil ooze interbedded with gray and olive gray clays and silt. Unit II consists of nannofossil ooze and chalk.

Primary allochems include silt to fine sand-sized planktonic and benthic foraminifers, bioclasts, peloids, and fish remains. Intervals from 166-1006A-14H-4, 35 cm, through 40X-2, 40 cm; 166-1006B-14H-6, 102 cm, through 166-1006A-19H which cover late to early Pliocene ages. Unit III is composed primarily of light gray and light greenish gray nannofossil chalk. Major allochems are silt- to fine sand-sized planktonic and benthic foraminifers, bioclasts, echinoderm debris, and rare peloids.

The intervals of this unit are from 1006A-40X-2, 40 cm, through 58X-3, 100 cm which covers early Pliocene to late Miocene (360.0-528.7 mbsf). Lithology unit IV is covered from 166-1006A-58X-5 through 65X-2, 65 cm in late to middle Miocene age (528.70-594.25 mbsf). This unit IV is composed primarily of light gray and greenish gray nannofossil chalk. Dominant components are silt- to fine sand-sized planktonic foraminifers, bioclasts, and benthic foraminifers.

Unit V is composed of alternating intervals of light greenish gray to olive nannofossil chalk and light gray nannofossil chalk with foraminifers. The interval of this unit is from 166-1006A-65X-2, 65 cm, through 77X in the middle Miocene age with depth 594.25-717.3 mbsf.

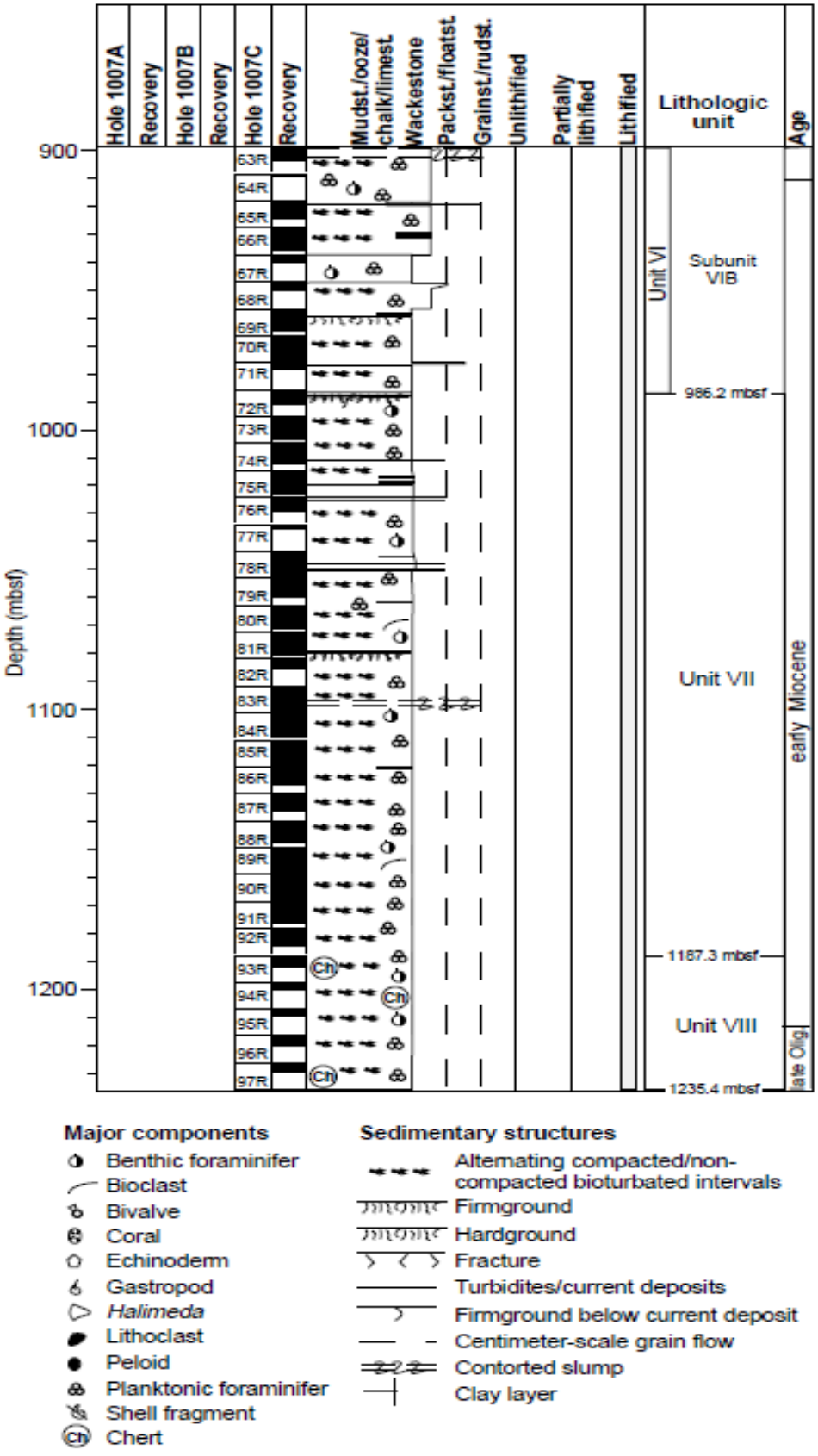

Figure 3.4. Synthesis of dominant texture and component of sedimentary succession at site 1007(Eberli et al., 1997).

Calcareous Nannofossils Biostratigraphy

Sediments recovered from Site 1006 yield common to abundant, upper Pleistocene through middle Miocene calcareous microfossils. Biostratigraphic control at Site 1006 is very good and almost all planktonic foraminifera and nannofossil zones from the Pleistocene to upper middle Miocene are found. The Pleistocene is subdivided into three nannofossil zones, NN21-NN19 (Shipboard Scientific Party, 1997). The uppermost zone, NN21 (0.25 Ma), is marked by the first appearance of *Emiliania huxleyi,* which occurs between Samples 166-1006B-1H-1, 0-1 cm, and 166-1006A-1H-CC (4.24 mbsf).

The last appearance of *Pseudoemiliania lacunosa* defines the base of Zone NN20 (0.41 Ma) and is situated between Samples 166-1006A- 2H-CC and 3H-CC (20.53 mbsf). The lowermost Pleistocene zone and longest in duration (0.41–2.0 Ma) is Zone NN19, which is bounded by the last appearance of *P. lacunosa* above and the last appearance of *Discoaster triradiatus* below. The base of NN19 is recognized between Samples 166-1006B-10H-CC and 166-1006A-10HCC (92 mbsf). Within Zone NN19, several other significant nannofossil events are recognized. The top of *Reticulofenestra asanoi* (0.85 Ma) is placed between Samples 166-1006A-4H-CC and 166-1006B- 5H-CC (39.5 mbsf).

The total range of large-form (>6 μm) *Gephyrocapsa* spp. (1.20–1.44 Ma) is bounded by samples 166-1006A-5HCC and 166-1006B-6H-CC and above samples 166-1006A-7H-CC and 166-1006B-8H-CC below (48.5–68 mbsf). The Pliocene/Pleistocene boundary is marked by the first appearance of *Gephyrocapsa caribbeanica* (1.72 Ma), which is placed between Samples 166- 1006B-10H-CC and 166-1006A-10H-CC (92 mbsf). This datum and the last appearance of *D. triradiatus*

indicate that both the Pliocene/ Pleistocene (1.72 Ma) and NN18/19 (2.0 Ma) boundaries coincide at Site 1006. At present, this cannot resolve whether this reflects the presence of a minor unconformity or a condensed interval.

Three nannofossil zones subdivide the upper Pliocene. The uppermost zone in the Pliocene is Zone NN18, which is constrained by the last appearances of *D. triradiatus* (2.0 Ma) and *Discoaster pentaradiatus* (2.4 Ma). At Site 1006, this interval occurs between 92 and 120 mbsf and is bounded above by Samples 166-1006B-10H-CC and 166-1006A-10H-CC and below by Samples 166-1006B-13H-CC and 166-1006A-13H-CC. Zone NN17 is short in duration (2.40–2.56 Ma), extending down to Samples 166-1006A-14H-CC and 166-1006B-15H-CC (134 mbsf), and is marked by the last appearance of *Discoaster surculus.*

Zone NN16 is the lowermost zone in the upper Pliocene, extending down to the last appearance of *Sphenolithus abies* (3.66 Ma). This datum also defines the upper/lower Pliocene boundary and occurs between Samples 166-1006A-18H-CC and 166-1006B-19H-CC (172.5 mbsf). Within Zone NN16, the last appearance of *Discoaster tamalis* (2.75 Ma) is placed between Samples 166-1006A-16H-CC and 166-1006B-16H-CC. The lower Pliocene is subdivided into three zones: Zones NN15, NN14-13, and NN12. The interval between the last appearances of *S. abies* and *Amaurolithus* spp. defines NN15 (3.66-4.5 Ma). At Site 1006, this interval occurs from the upper/lower Pliocene boundary at 172 mbsf to 259 mbsf, between Samples 166-1006A-27H-CC and 28H-CC.

Zones NN14 and NN13 are combined and are bounded by the last occurrence of *Amaurolithus* spp. above and the first appearance of *Ceratolithus rugosus* (4.7 Ma). At Site 1006, the base of Zone NN14-13 was found between

Samples 166-1006A-35X-CC and 36X-CC (326 mbsf). The short duration of NN14-13 (0.2 Ma) more than 60 m of sediment accumulated. The base of Zone NN12 at the Miocene/Pliocene boundary is defined by the last appearance of *Discoaster quinqueramus* (5.6 Ma) and occurs between Samples 166-1006A-42X-CC and 43X-CC (383 mbsf). At Site 1006, well-preserved specimens of *D. quinqueramus* and *Discoaster berggrenii*, marker species for upper Miocene Zone NN11, were found in contrast to the slope Sites 1003 and 1005. The total range of both species (5.6-8.6 Ma) defines Zone NN11, which extends from the Miocene/Pliocene boundary (383 mbsf) to 501 mbsf, between Samples 166-1006A-54X-CC to 55X-CC. Rare specimens of *D. quinqueramus* are present in Samples 166-1006A-38XCC, 40X-CC, and 42X-CC.

However, these samples also contain the middle Miocene species *Discoaster neorectus* and *Discoaster calcaris,* indicating that these assemblages are reworked. Therefore, Sample 166-1006A-43X-CC is identified as the highest unequivocal level of *D. quinqueramus,* and hence the top of the Miocene. Within upper Miocene Zone NN11, the top of the small *Reticulofenestra* spp. interval (6.5 Ma) provides another useful datum.

This level occurs between Samples 166-1006A-45X-CC and 46X-CC (418 mbsf). The base of this interval is coeval with the base on *D. quinqueramus* in time as well as in depth at Site 1006. In addition, the base of *Amaurolithus primus,* which indicates upper part of Zone NN11, was found in Sample 166-1006A-45X-CC.

Zone NN10 ranges from the base on *D. quinqueramus* (8.6 Ma) to the last appearance of *Discoaster hamatus* (9.4 Ma). The base of NN10 is placed between Samples 166-1006A-57X-CC and 59X-CC (530.5 mbsf). The total range of *D.*

hamatus defines Zone NN9 (9.4-10.7 Ma). The base of this zone defines the middle/upper Miocene boundary and is found between Samples 166-1006A-61X-CC and 62X-CC.

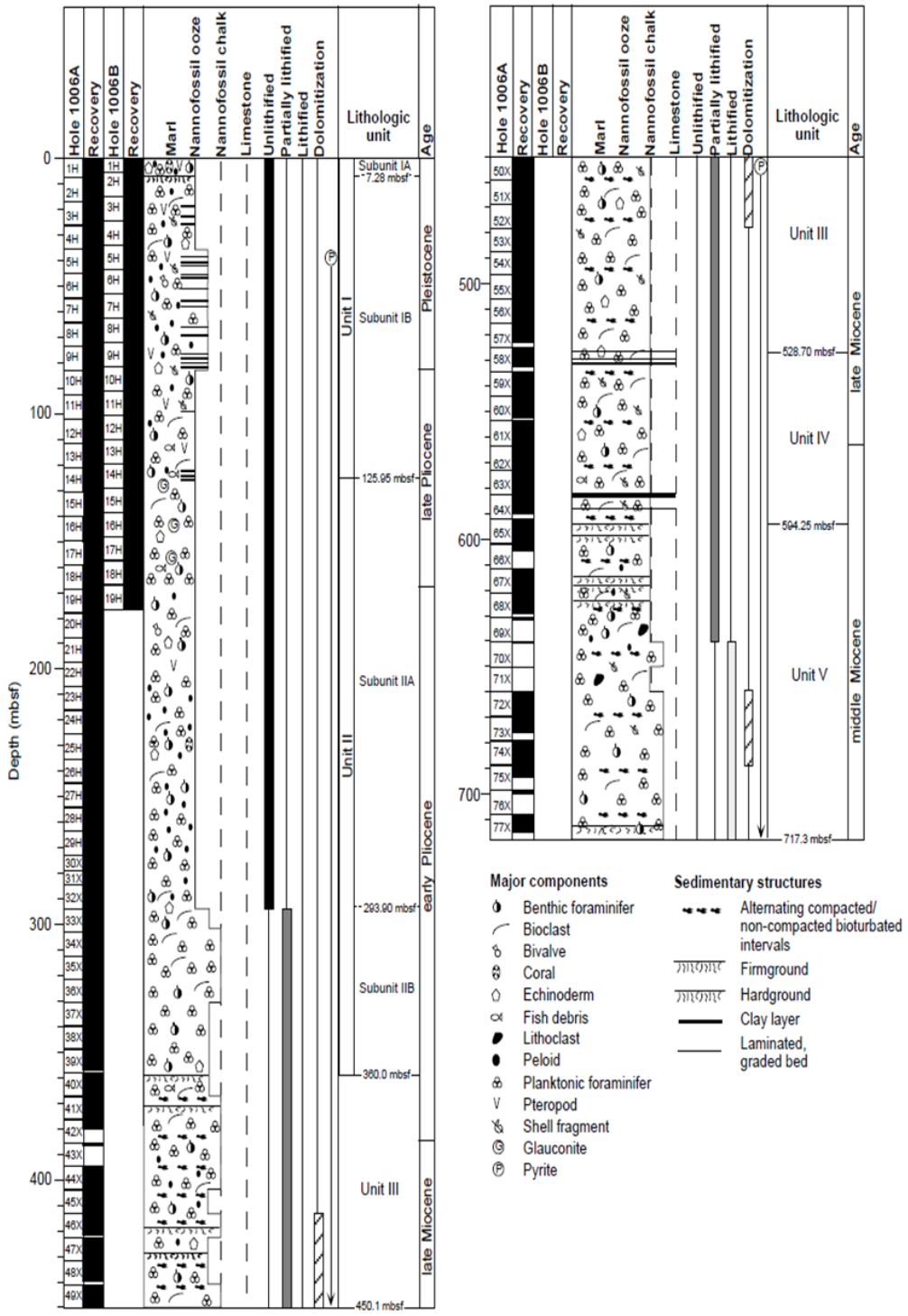

Figure 3.5. Synthesis of the lithostratigraphy Site 1006 (Eberli et al., 1997).

Chapter IV. Materials and Methods

A total of 327 samples was collected from Hole 782 A, 1006A, and Hole 1007B.C, covering the Oligocene to the Pleistocene. The sedimentary section is stratigraphically complete and is composed of nannofossil marl and vitric nannofossil chalk at Site 782 (Shipboard Scientific Party, 1990). Samples were observed with the studied interval extends from sample 1H-1,80-81 cm to sample 35X-6, 77-76 cm (2.3-332.25 m below the sea floor: mbsf) of the middle Miocene to Pleistocene. The sedimentary sequence recovered from ODP Site 1007 (Hole B and C) consists of Pleistocene to upper Oligocene sediments characterized by nannofossil ooze, unlithified to lithified foraminifer and peloidal wackestone and packstone, and foraminifer nannofossil chalk in Hole B and C (Shipboard Scientific Party, 1997).

Two Hole from Site 1007 studied interval was between samples 1007B, 23-1, 99-100 cm through 30X-5, 24-25 cm (204.09-359.95 mbsf) of the late Miocene to Pliocene. And the other Hole studied was between samples 1007C, 8R-CC to 95R-CC (378.9-1216.1 mbsf) which covered the Oligocene to the late Pliocene sequences. Hole 1006A recovered of nannofossil ooze, planktonic foraminifera, nannofossil ooze, planktonic foraminifer nannofossil chalk, and nannofossil limestone, with variable amounts of admixed silt and clay.

At Site 1007, the entire Neogene section and 20 m of Oligocene sediments were penetrated in a 1235.4 mbsf hole, providing the complete sedimentary record of Neogene sea-level changes (Shipboard Scientific Party, 1997).

The studied interval was between samples 1006A, 16H-CC through 57X-CC (149.6-524.7 mbsf) which covered of late Miocene to Pliocene sequences.

Preparation of the microscope slide explained as follows: samples were dried in oven at temperature around 70°C for 24 hours (Figure 4.1); then by using a mortar (Figure 4.2), 0.020- 0.050g (depending on the richness of nannofossil) of powdered were placed in the beaker (Figure 4.3); and 50mL of water were added to make a suspension (Figure 4.4), stir water to make a suspension (Figure 4.5); after stirring, the resulted suspension was measured out 0.5mL using the micropipette (Figure 4.6); to be put carefully and spread over a cover glass (18 mm x 18 mm) and it was dried on a hotplate at 40°C (Figure 4.7 and 4.8); then the cover glass was mounted on a microslide using Norland optical adhesive (Figure 4.9); the cover glass was mounted on a microscope slide using UV-curing adhesive for dry around 2 or 3 minutes (Figure 4.10).

Each microslide was observed under Olympus BX51 binocular polarizing microscope with an oil-immersion objective lens at a magnification of × 1500. I checked all nannofossil species in the microslide to recognize both their first and last occurrence datum planes. Furthermore, I calculate the absolute of coccolith and *Discoaster* and relative abundance of each species. *Florisphaera profunda* was counted another transect in a microslide.

The size distribution of *Reticulofenestra* spp. was also identified by measuring the 50 to 100 of *Reticulofenestra* specimens in a sample. Absolute ages of datums were provided by Sato and Chiyonobu (in prep.) (figure 4.11). Reworked of nannofossil species were not documented in any of the samples.

Figure 4.1 Ocean Drilling Program (ODP) core samples

Figure 4.2. Samples were dried in an oven at a temperature around 70°C for 24 hours and powdered using a mortar.

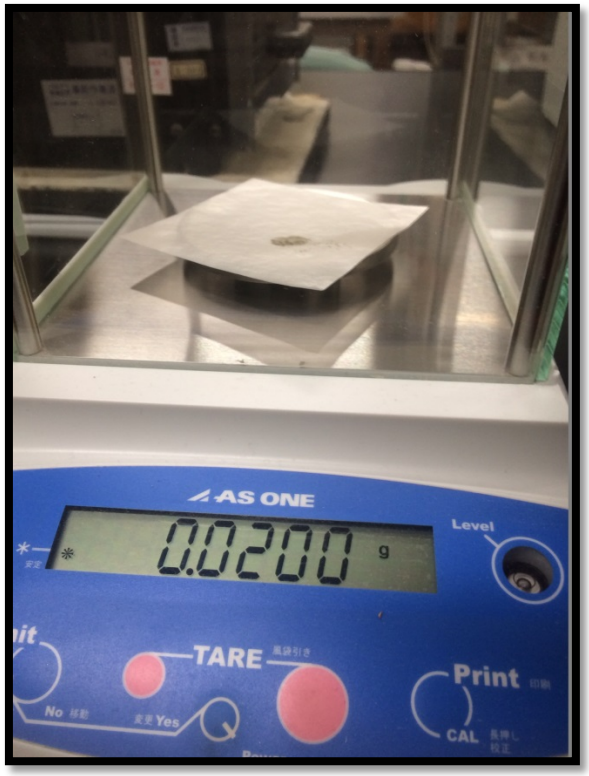

.

Figure 4.3. The powdered sample, weighing around 0.020-0.050g (depending on the richness of nannofossil) was placed in a beaker

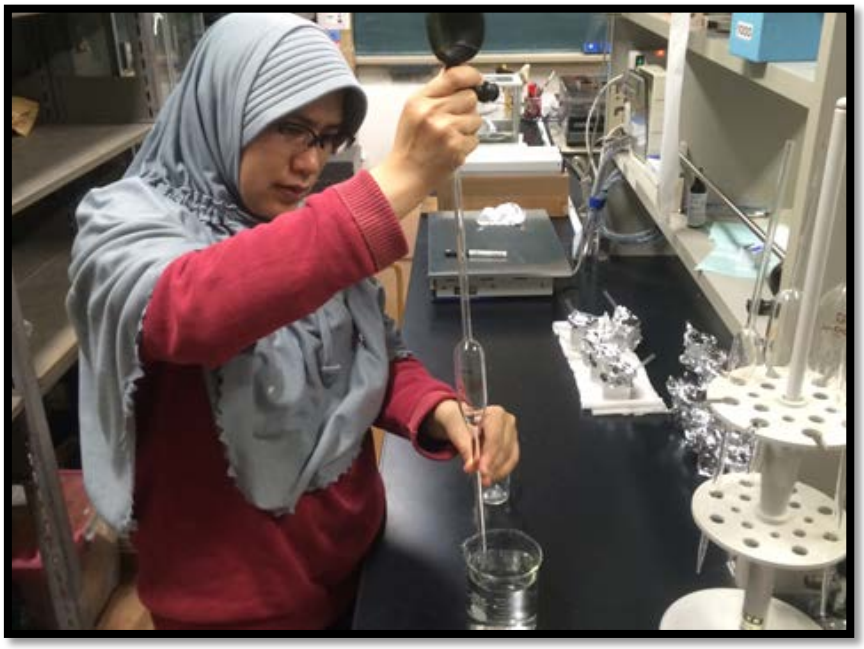

Figure 4.4. 50 mL of water were added to make a suspension.

Figure 4.5. Stir water to make a suspension.

Figure 4.6. Measured out 0.5mL of the suspension using the micropipette.

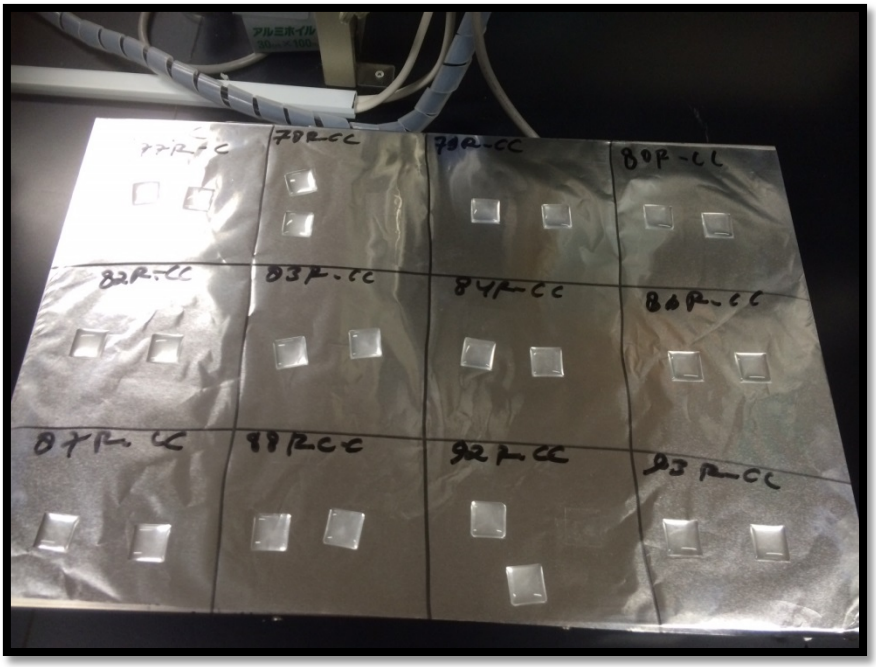

Figure 4.7. Samples are put carefully and spread over a cover glass (18 mm x 18 mm).

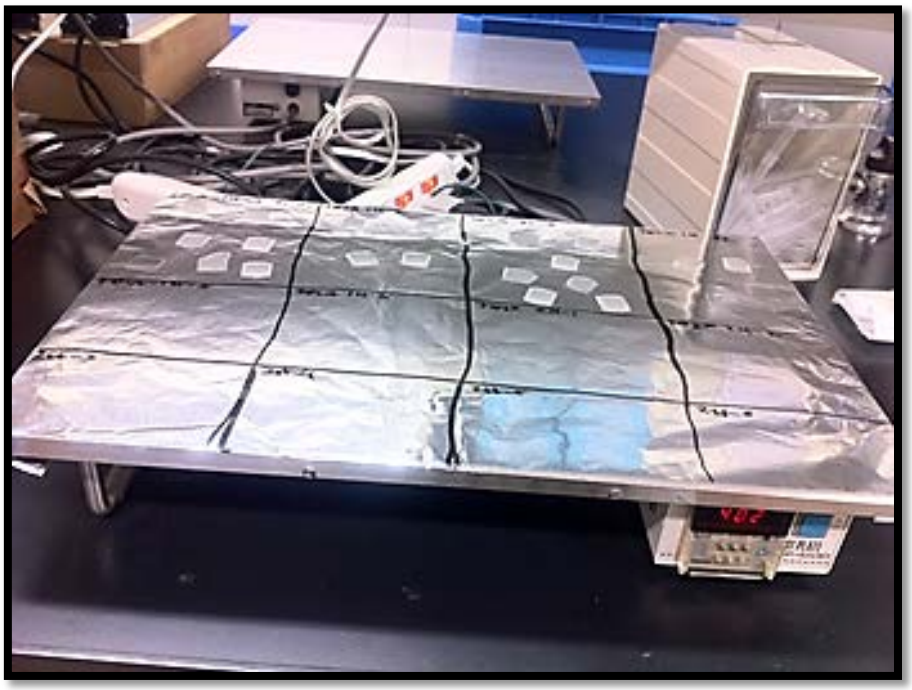

Figure 4.8. Dried on a hotplate at 40°C.

Figure 4.9. The cover glass was mounted on a microslide using Norland optical adhesive.

Figure 4.10. Put the cover glass under UV-curing adhesive for dry around 2 or 3 minutes.

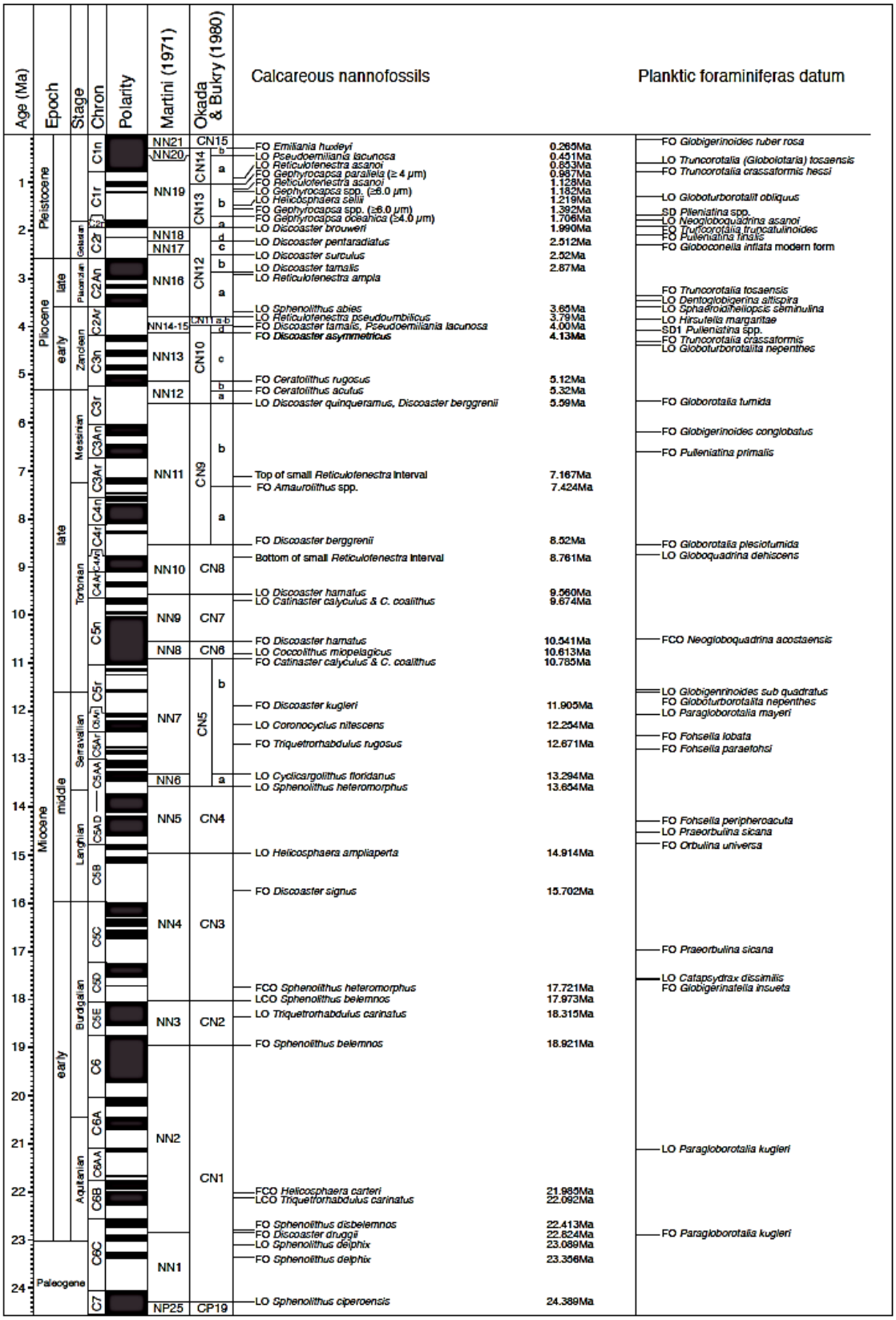

Figure 4.11. Biostratigraphic zonation of calcareous nannofossils (Martini, 1971), and age determination by Sato, T., and Oda, M (2013)

Chapter V. Stratigraphic Distribution of Calcareous Nannofossils

I revised and described in detail nannofossil datums in the western Pacific Ocean sediments (Site 782) and Bahama Bank of Caribbean Sea (Site 1007 and 1006) using qualitative nannofossil analysis. Many nannofossil datums and bioevents were detected based on sequential distribution pattern from Oligocene to Pleistocene nannofossil. Absolute ages of datums in this study were provided by Sato and Chiyonobu (in prep.). The size variations of *Reticulofenestra* and percentage of coccolith were characteristically observed and measured in detail in the all studied sequences. Neogene climatic and tectonic events influenced were correlated with paleoceanographic factors at all sites.

4.1. ODP Site 782 Hole A

The sequence of the Hole is characterized by abundant occurrences of *Reticulofenestra* spp. The typical cold water species, *Coccolithus pelagicus* dominate the lower part of the section. Although *Calcidiscus leptoporus*, and *Pontosphaera* spp. are very rare, they are present throughout the section continuously. The occurrences of *Umbilicosphaera sibogae*, *Syracosphaera pulchra*, and *Rhabdosphaera clavigera* are limited in the upper part of the section (Figure 5.1).

The nannofossil datum planes and their ages described by Sato and Chiyonobu (in press) and its horizons found in this study are shown in Table 5.1.

Among them, the datum planes of marker species which define the NN boundaries of Martini's zonation (Martini, 1971), are as follows:

Emiliania huxleyi which defines the NN20/NN21 boundary first occur in a

sample from 8.4 mbsf. In Zone NN21 are shown nannofossils assemblages such *Gephyrocapsa* spp. and small *Reticulofenestra*. This species is very abundant amount is (~ 46 %) and *Discoaster spp*. (0.1%) is few appear in this zone. At the same time, *Reticulofenestra* spp. (<2µm) also disappear in this zone. In zone NN20, *Reticulofenestra* spp. is very abundant (especially size 2-3µm) amount is (~41.5%), and generally common some species as well as *Gephyrocapsa* spp., *Calcidiscus leptoporus*, *Gephyrocapsa carribbeanica*, *Gephyrocapsa oceanic*, *Gephyrocapsa parallela* and small *Reticulofenestra* (~31%).

The presence of some species such as *Coccolithus pelagicus, Helicosphaera carteri, Pontosphaera japonica*, *Pontosphaera multipora, Rhabdosphaera clavigera*, *Rhabdosphaera longistylis, Syracosphaera pulchra* and *Umbilicosphaera sibogae* also found in this zone. In zone NN20 was observed *Ceratolithus cristatus, Helicosphaera neogranulata, Oolithotus antilarum* and *Umbilicosphaera irregularis* disappeared or absent.

The last occurrence of *Pseudoemiliania lacunosa* which correlate to NN19/NN20 boundaries is found in samples below 18.1 mbsf. And zone NN19 which is defined by 4 nannofossil datum such as FO *Gephyrocapsa parallela* (0.987 Ma), LO *Helicosphaera selli* (1.219 Ma), and *Gephyrocapsa oceanica* (1.706 Ma), which are present in Samples125-782A-4H-2 (32.6 mbsf), 125-782A-4H-5 (37.1 mbsf), 125-782A-5H-2 (42.1 mbsf), and 125-782A-5H-4 (45.1 mbsf). *Reticulofenestra* spp. 3-4µm is still abundance around 58%, and *Discoaster* spp. is abruptly absent. The boundary of NN18/NN19, which is defined by the last occurrence of *Discoaster brouweri*, is found between 54.6 mbsf/56.1 mbsf. In Zone

NN18 *Reticulofenestra* spp. is very abundant (especially size 3-4µm), but smaller size decrease abruptly, and *Reticulofenestra* spp. (4-5µm) disappeared. From this zone to below *Rhabdosphaera clavigera*, *Rhabdosphaera longistylis*, and *Umbilicosphaera irregularis* are absent.

The last occurrences of *Discoaster pentaradiatus*, *D. surculus*, *Reticulofenestra pseudoumbilicus*, and *D. quingqueramus*, which respectively correlated to NN17/NN18, NN16/NN17, NN15/NN16, and NN11/NN12 boundaries are recognized in 67.1 mbsf, 73.6 mbsf, 110.6 mbsf, and 155.85 mbsf.

Zone NN17 is characterized by last appear *Reticulofenestra* spp. (5-6µm) and *Reticulofenestra* spp. (4-5µm) is very abundant amount (~37 %). *Reticulofenestra* spp. small size (<2µm and 2-3 µm) decrease abruptly and the other larger size increase, and *Reticulofenestra pseudoumbilicus* is not found in the below of this zone.

In Zone NN16 characterized by *Reticulofenestra* spp. small size (<2µm and 2-3 µm) is an increase from the top to the bottom this zone, and *Reticulofenestra* spp. (2-3µm) still abundance around 63.5 %. Likewise *Reticulofenestra* spp. large size decrease abruptly, and *Reticulofenestra* spp. (5-6µm) is absent in this zone. *Helicosphaera selli* and *Syracosphaera pulchra* first appears in this range. Moreover, *Discoaster* spp., *Discoaster triradiatus*, *Sphenolithus abies* and *Helicosphaera neogranulata* are absent.

Zonal boundary NN14-NN15 was determined by FO *Discoaster asymmetricus* which was sample observed in 125-782A, 15X-1, 80-81 cm (136.6

mbsf) to 125-782A, 15X-2, 80-81 cm (138.1 mbsf) and it gains an interesting observation result. Some like the zonal boundary NN16, *Reticulofenestra* spp. (2-3µm) still, abundance amount is (65%), but another size (except *Reticulofenestra* spp. <2µm) and *Reticulofenestra pseudoumbilicus* become decline to absent in the 4.00 Ma (FO *Discoaster tamalis* and FO *Pseudoemiliania lacunosa* datum). Most *Discoaster* assemblages were presented in this zonal boundary, such as *Discoaster asymmetricus, Discoaster berggrenii, Discoaster exilis, Discoaster spp., Discoaster surculus, Discoaster triradiatus,* and *Discoaster variabilis. Helicosphaera neogranulata* and *Syracosphaera pulchra* first appear in this zone.

The zonal boundary NN12/NN13 cannot be defined, causing species marker of *Ceratolithus rugosus* is not found. Therefore range zone between NN12-NN13 was determined, and has been identified in 16 species. Some species which the secondary marker of Zone NN11 125-782A, 17X-1, 75-76 cm (155.85 mbsf) first appear in this zone are *Amaurolithus delicatus* and *Amaurolithus tricorniculatus* in the same sample with the datum marker of the NN11/NN12 boundary at 125-782A, 17X-1, 75-76 cm (155.85 mbsf). Based on nannofossil datums, one possible unconformity was identified in the succession from 5.59 Ma to7.424 Ma.

The first occurrence of *Amaurolithus* spp. is also observed in this period. NN11 Zone (late Miocene) is the longest range in the hole. The amount of *Reticulofenestra* spp. is approximately 70% especially *Reticulofenestra* spp. small size (<2µm). All of *Reticulofenestra* spp. decrease abruptly in the bottom this zone. The amount of *Discoaster qingqueramus* and *Discoaster barggrenii* found in this zone is only (~4% and ~2.5%). In addition, *Discoaster triraditus* appeared in this

zone for the first time. The first occurrences of *Discoaster berggrenii* and *Catinaster coalitus*, and the last occurrences of *Cyclicargolithus floridanus* and *Sphenolithus heteromorphus* are respectively found in 234.45 mbsf, 253.75 mbsf, 281.05 mbsf, and 307.27 mbsf. Based on the stratigraphic position of these species, NN10/NN11, NN7/NN18, NN6/NN7, and NN5/NN6 boundaries are traceable to these horizons mentioned above.

The Last occurrence (LO) of *Discoaster hamatus*, which defines the boundaries between NN10 and NN9 boundaries could not be found because of the absence of this species marker in this hole. The range zone NN8-NN10 defined in this hole was characterized by a decline to an absence of *Reticulofenestra* spp. assemblages, which is from a large size to smaller. Likewise, *Reticulofenestra pseudoumbilicus* also decreased from middle to the top of this zone.

Helicosphaera carteri was absent and only two Discoaster species were found in this zone, they are *Discoaster* spp. and *Discoaster varibilis* throughout below this boundary. *Catinaster coalitus* were only found in this zone (approximately 3%), in the last occurrence (LO) in sample 125-782A, 26X-3 (245.55 mbsf) until 125-782A, 26X-4 (247.05 mbsf). *Coccolithus miopelagicus* (last occurrence) were also identified and *Sphenolithus abies* finally disappeared in this zone. Furthermore, below this zone *Reticulofenestra* spp. (<2µm) and *Helicosphaera carteri* were not found.

Zone NN7 (middle/late Miocene boundary) showed an interesting trend. The change from a smaller to larger size characterized by the amount of specimen is absent until very abundant especially *Reticulofenestra pseudoumbilicus*. And moreover, *Coronocyclus nitescens* was the last occurrence of species marker in this

zone approximately (0.5%), which was determined in samples: 782A, 28X-5, 75-76 cm (267.85 mbsf) through 782A, 28X-6, 75-76 cm (269.35mbsf).

The next zone an oldest zone (NN6 and NN5) middle Miocene, has identified 21 species. In this zone, there are interesting observation results of *Reticulofenestra* spp. assemblages which is decreased and it was absent from bottom of the middle of this zone. The percentage of *Reticulofenestra pseudoumbilicus*, *Coccolithus pelagicus*, *Coccolithus miopelagicus*, *Cyclicargolithus* abisectus, *Cyclicargolithus floridanus* and *Discoaster deflandrei* also decreased from bottom to the middle and from top to the middle in this zone (identified in sample 782A, 34X-1, 62-63 cm (315.22mbsf).

Moreover, the last occurrences of *Sphenolithus heteromorphus* was observed in sample 782A, 33X-1, 75-76 cm (305.75 mbsf) to 782A, 33X-2, 77-78 cm (307.27 mbsf) approximately 4.5%. *Helicosphaera scissura* and *Cyclicargolithus abisectus* were only found in this zone. *Cyclicargolithus abisectus* was still abundance around 39%. On the basis of these datums occurrence distribution with 48 species of calcareous nannofossils assemblages were identified, I believe the studied sequence in ODP Site 782 Hole A should be correlated to NN6 to NN21 Zone from the middle Miocene to Pleistocene Zone (Figure 5.1).

Table 5.1. Calcareous nannofossil bioevents and ages in Hole 782A (western Pacific Ocean)

Calcareous nannofossils event	Age (Ma)	Sample	mbsf
FO *Emiliania huxleyi*	0.26	1H-5, 90-91 cm/1H-6, 90-91 cm	8.4/9.9
LO *Pseudoemiliania lacunosa*	0.45	2H-4, 80-81 cm/2H-5, 80-81 cm	16.6/18.1
FO *Gephyrocapsa parallela*	0.98	4H-1, 80-81 cm/4H-2, 80-81 cm	31.1/32.6
LO *Helicosphaera selli*	1.22	4H-5, 80-81 cm/4H-6, 80-81 cm	37.1/38.6
FO *Gephyrocapsa* spp	1.39	5H-1, 80-81 cm/5H-2, 80-81 cm	40.6/42.1
FO *Gephyrocapsa oceanica*	1.71	5H-3, 80-81 cm/5H-4, 80-81 cm	43.6/45.1
LO *Discoaster brouweri*	1.99	6H-4, 80-81 cm/6H-5, 80-81 cm	54.6/56.1
LO *Discoaster pentaradiatus*	2.51	7H-6, 80-81 cm/8H-1, 80-81 cm	67.1/69.1
LO *Discoaster surculus*	2.52	8H-4, 80-81 cm/8H-5, 80-81 cm	73.6/75.1
LO *Discoaster tamalis*	2.87	9X-1, 80-81 cm/9H-2, 80-81 cm	78.6/80.1
LO *Sphenolithus abies*	3.65	12X-1, 80-81 cm/12X-2, 80-81 cm	107.6/109.1
LO *Reticulofenestra pseudoumbilicus*	3.79	12X-3, 80-81 cm/13X-1, 80-81 cm	110.6/117.3
FO *Discoaster tamalis*	4	13X-1, 80-81 cm/13X-2, 80-81 cm	117.3/118.8
FO *Pseudoemiliania lacunosa*	4	13X-1, 80-81 cm/13X-2, 80-81 cm	117.3/118.8
FO *Discoaster asymmetricus*	4.13	15X-1, 80-81 cm/15X-2, 80-81 cm	136.6/138.1
LO *Discoaster quinqueramus*	5.59	17X-1, 75-76 cm/17X-2, 74-75 cm	155.85/157.34
LO *Discoaster berggrenii*	5.59	17X-1, 75-76 cm/17X-2, 74-75 cm	155.85/157.34
FO *Amourolithus* spp	7.42	17X-1, 75-76 cm/17X-2, 74-75 cm	155.85/157.34
FO *Discoaster berggrenii*	8.52	25X-1, 75-76 cm/25X-2, 75-76 cm	232.95/234.45
Bottom of small *Reticulofenestra* interva	8.76	25X-4, 75-76 cm/25X-5, 75-76 cm	237.45/238.95
LO *Catinaster coalitus*	9.67	26X-3, 75-76 cm/26X-4, 75-76 cm	245.55/247.05
LO *Coccolithus miopelagicus*	10.61	26X-5, 75-76 cm/26X-6, 75-76 cm	248.55/250.05
FO *Catinaster coalitus*	10.78	27X-1, 75-76 cm/27X-2, 75-76 cm	252.25/253.75
LO *Coronocyclus nitescens*	12.25	28X-6, 75-76 cm/29X-1, 75-76 cm	269.35/271.45
LO *Cyclicargolithus floridanus*	13.29	30X-1, 75-76 cm/29X-6, 75-76 cm	278.95/281.05
LO *Sphenolithus heteromorphus*	13.65	33X-1, 75-76 cm/33X-2, 77-78 cm	305.75/307.27

FO: first occurrence; LO: last occurrence.
Absolute ages of datums were provided by Sato, T., and Oda, M (2013)

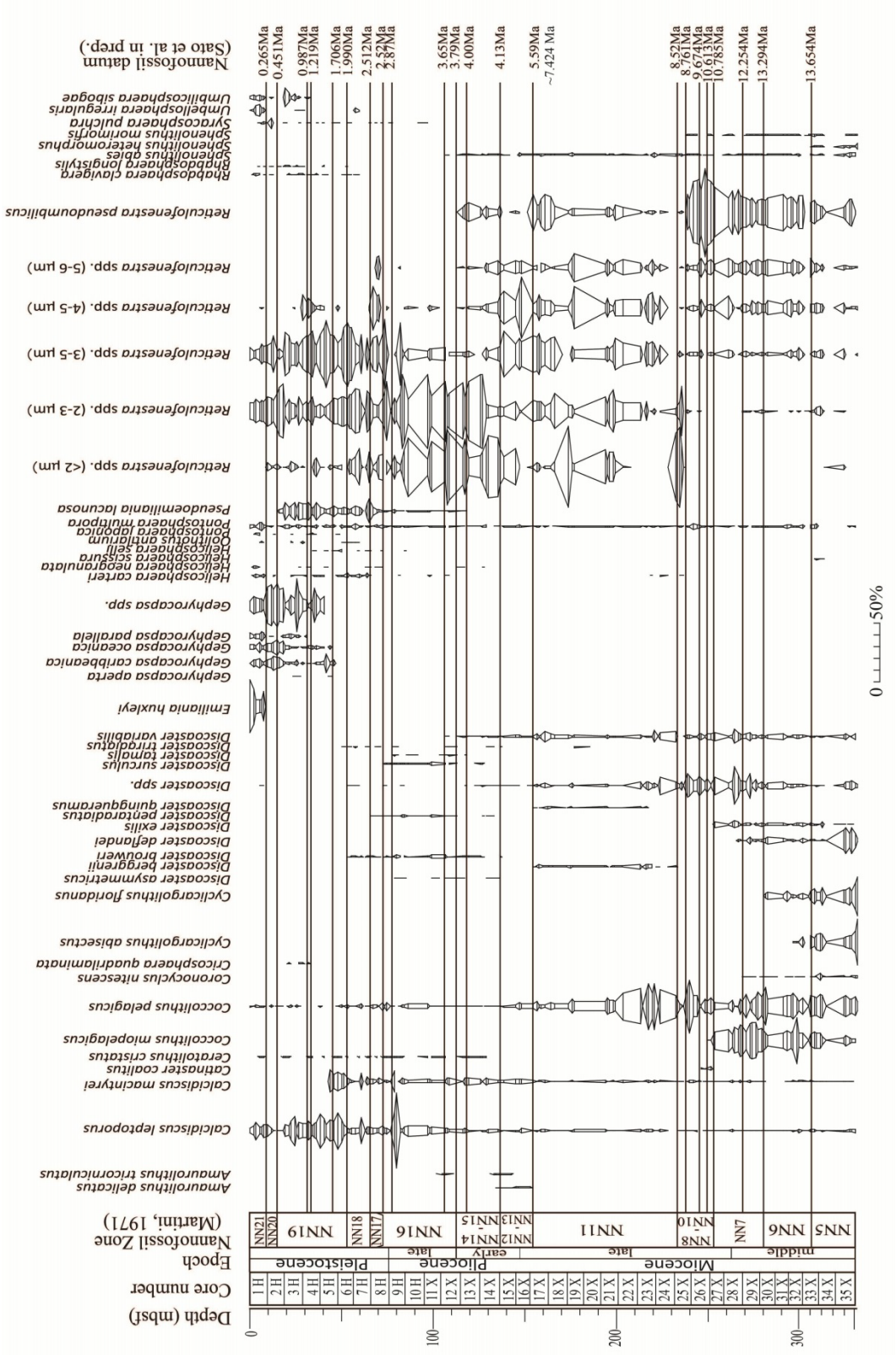

Figure 5.1. Stratigraphic distribution of calcareous nannofossil species in ODP Hole 782A located in the Izu-Bonin of western Pacific Ocean.

Sedimentation Rate ODP Hole 782A

The average sedimentation rates for Hole 782A are provided based on the present of individual datums as listed in Table 5.1. A curve representing the sediment-accumulation rate has been constructed by dividing the thickness of the interval by the time represented (Age-depth relationship of these nannofossils) and the global event's base on the timing interval also shows in figure 5.2, obtained as follows:

- Firstly, the average sedimentation rate from 13.29 Ma (LO *Cyclicargolithus floridanus*) through 8.761 Ma (Bottom of small *Reticulofenestra* interval) is 0.9 cm /kyr. This data of the middle Miocene is related to the end of Mid-Miocene Climate Optimum event and the late Miocene sequence is related to intensification of Asian monsoon event.
- The next sedimentation rate is from 8.76 Ma (Bottom of small *Reticulofenestra* interval) to 7.424 Ma (FO *Amaurolithus* spp.) or between NN10 zone and NN11 zone is 6.0 cm/kyr (Figure 5.2).
- The late Miocene sequence is bounded by a hiatus at 155.8 mbsf interval of undifferentiated sediments (from 7.424 Ma to 5.59 Ma). During the occurrence of hiatus between 5.59 Ma or 5.48 Ma to 7.424 Ma hiatus, the climatic events are shown related to the timing of Messinian Salinity Crisis.
- Between Pliocene and Pleistocene boundary, based on LO *Discoaster quinqueramus, D. berggrenii*) to 2.87 Ma (LO *Discoaster tamalis*) the sedimentation rate decreased to 5.9 cm/kyr.
- Finally, the upper Pliocene interval is highly expanded with an average of Pleistocene sedimentation rate decrease to about 3.0 cm/kyr or between

NN16 zone (2.87 Ma) and NN20/NN21 boundaries (0.265 Ma). Periods of faster deposition occurred in this interval.

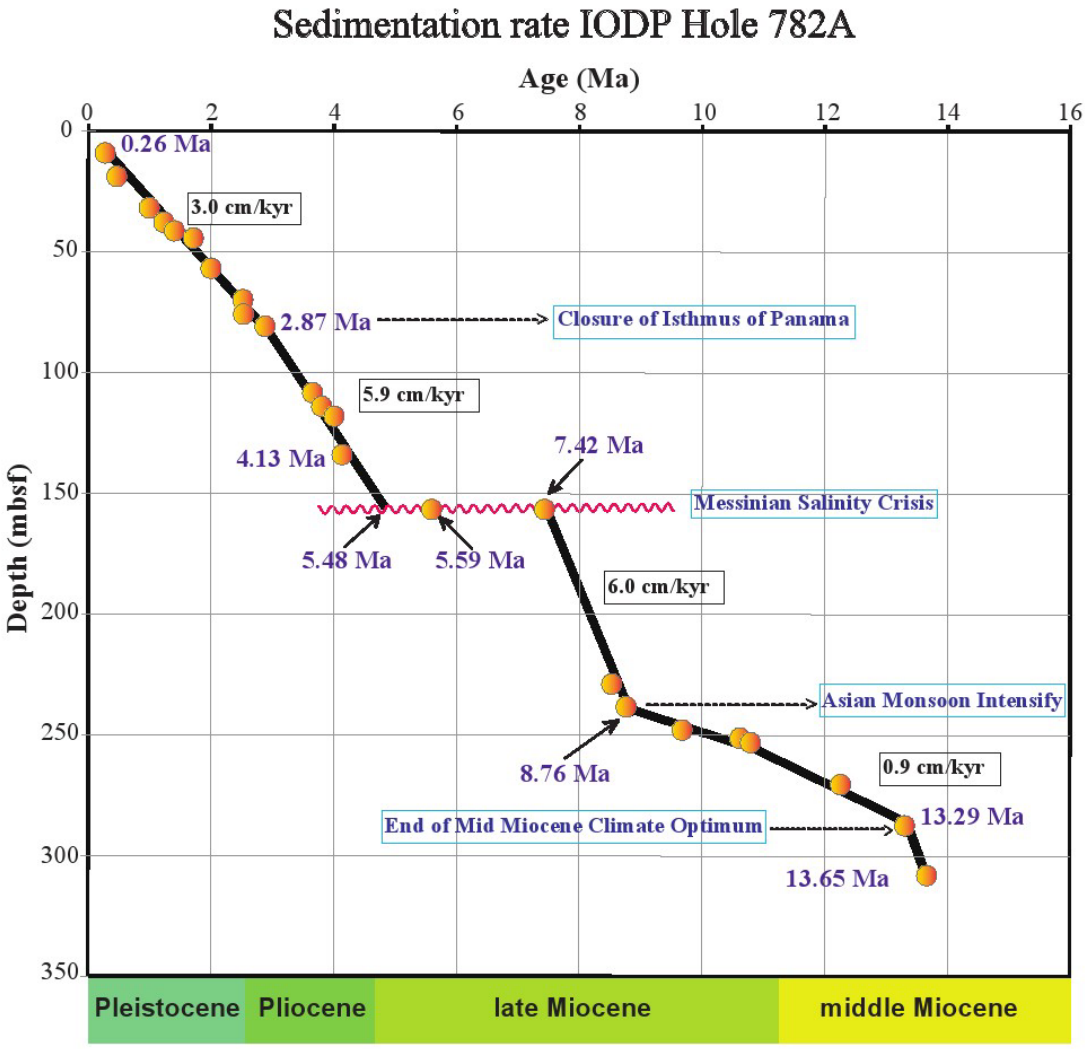

Figure 5.2. Average sedimentation rate of Leg 125 Hole 782A based on calcareous nannofossils datums.

5.2. ODP Site 1007 Hole 1007B, C

The stratigraphic distribution of calcareous nannofossils assemblages from sediment samples of ODP Site 1007 is shown in figure 5.3 where 37 species were identified which were characterized by abundance occurrence of *Reticulofenestra* spp. and *Sphenolithus* spp. throughout the section. The calcareous nannofossils are generally moderately to poorly preserve. The sequence of this site is correlated to Oligocene to early Pliocene from ODP sample 166-1007B, 1H-1,80-81cm to sample 35X-6, 77-76 cm, and 166-1007C, 8R-CC to 95R-CC (Figure 5.3 and 5.4). The abundant of nannofossil are not so common and moderate to the bad preservation of specimens in the sediment of site 1007.

The sedimentary structure indicative of an unconformity was founded in the succession from 7.424 Ma to 8.52 Ma. The sequence of the upper part is characterized by the abundant occurrence of *Sphenolithus abies* which contains 20 to 50 % of the assemblages *Reticulofenestra* spp., which accounts for 30 to 70 % of the assemblages dominates the middle to lower part of the sequences.

Variations abundant of assemblages appeared from NN3 to NN1 boundary and the bottom of NN1 is characterized by the disappearance and the absence of specimens which dissolute the samples. *Cyclicargolithus floridanus* which contains approximately 50% during Miocene-Oligocene ages dominate the lower part of the oldest age. This event is one of the most characteristic events in the middle Miocene assemblages and useful for correlation. *Coronocyclus nitescens*, one of stratigraphically useful species in the middle Miocene, is absence or cannot be found from this site samples.

The First and last occurrences of the marker species are listed in Table 4.2. The zonal boundaries are recognized based on the stratigraphic position of the marker species. NN15/NN16 boundary, defined by the last occurrence of *Reticulofenestra pseudoumbilicus,* is found in 205.59 mbsf. Zone NN15/16 boundary is dominated by assemblages of *Reticulofenestra* spp. (approximately 40.5%) and *Sphenolithus abies* and the common amount is around 16%. In particular, *Reticulofenestra* spp. (<2µm) is decreased to absent in the lower part of NN14-15 Zone and specimens of *Sphenolithus abies* highest appear from the top to the bottom this zone.

The presence of some species such as *Calcidiscus leptoporus, Coccolithus pelagicus, Discoaster* spp., *Helicosphaera carteri*, *Pontosphaera* spp., *Pontosphaera multipora*, *Pontosphaera discopora*, *Rhabdosphaera clavigera*, *Rhabdosphaera longistylis, Thoracosphaera* sp. and *Umbilicosphaera sibogae* are also found in this zone. *Sphenolithus abies* is abundant and dominant with contains 35 % of the assemblages.

Oolithotus antilarum and *Amaurolithus* spp. with a very small percentage (1-3 %) appear in the upper part of this zone and *Hayaster perplexus* appear in the lower part of the zone. The species of *Syracosphaera pulchra* specimen is not present in all sequence from this site studies and percentage of Discoaster species does not show significant changes of abundant from NN15 until NN6 Zone.

The First occurrence of *Discoaster tamalis* as a secondary zonal marker for the NN14-15 zone is not detected and *Pseudoemiliania lacunosa* specimen becomes absently observed in the bottom of this zone, but I found again at sample 27X-1, 99-100cm. *Amaurolithus* spp. is first observed in the sample 26X-4, 99-100 cm

(236.09 mbsf) which occurrence very rare at the studied sites.

Sphenolithus abies is still abundance in NN13 zone, and also the presence of *Umbilicosphaera sibogae*, *Pseudoemiliania lacunosa*, and *Pontosphaera multipora* are disappeared from this zone to below of sequences. The presence of small of *Reticulofenestra* spp. (<2μm), *Pontosphaera* sp., and *Umbilicosphaera sp.,* are absent.

The last occurrence of *Ceratolithus rugosus* is used as zonal boundary NN12/13 zone whereas observed between samples 32X-1, 99-100 cm (286.99 mbsf) and 34X-1, 99-100cm (305.3 mbsf). The next zonal boundary is NN12/NN11 cannot be defined because one remarkable bioevents can identify in the bottom part of NN13 zone mainly by *Discoaster berggrenii* and *Discoaster quingqueramus* in the sample 32X-1, 99-100 cm (286.99 mbsf) which approximately 1% from total identified of 200 specimens.

The last occurrence of *Discoaster quingqueramus* which is correlated to the NN11/NN12 boundary, is found in 286.99 mbsf. The similar pattern of small size *Reticulofenestra* spp. and *Reticulofenestra pseudoumbilicus* continuously appeared in zone NN11-12. *Sphenolithus abies* and *Calcidiscus leptoporus* are dominant with the common species of *Scapholithus fossils* is absent and disappear in the lower part of this zone.

The NN10/NN11, NN7/NN8, and NN6/NN7 boundaries defined by first occurrences of *Discoaster berggrenii*, *Catinaster coalitus*, and last occurrence of *Cyclicargolithus floridanus* are recognized in 332.83 mbsf, 504.1 mbsf, and 783

mbsf. Samples 32X-1, 99-100 cm through 33X-CC contain very rare and poorly preserved nannofossil specimens (Shipboard Scientific Party, 1997), whereas just 218 specimens of nannofossil in the 20μm area of field observed under a microscope (dominated percentage by *Sphenolithus abies*).

In this studied site, the bottom of small *Reticulofenstra* interval which defines the secondary marker of NN11 Zone is not detected. NN8-NN10 boundary is characteristic by the presence of some species such as *Discoaster variabilis*, *Discoaster* spp., *Coccolithus pelagicus, Reticulofenestra pseudoumbilicus, Reticulofenestra* spp., *Helicosphaera carteri, and Rhabdosphaera* sp. *Reticulofenestra* spp. (<2μm) is longest found in this hole and the maximum frequency approximately 60%. *Calcidiscus leptoporus* and *Calcidiscus macintyrei* are absence from NN7 to the bottom interval of this site. The percentage amount species of *Discoaster* is also very rare and not continuously appear during NN8-10 boundary.

The occurrence of *Catinaster coalitus*, which is a secondary marker of Zone NN8-NN10, is observed in samples between 15R-CC (446.3 mbsf) and 16R-CC (455.9 mbsf), but *Catinaster calyculus, which is another secondary datum species,* is undetectable in samples of this site. Small size *Reticulofenestra* spp. (<2μm) is starting abundant of occurrence (~72.5 %) and dominant from this zone more than Sphenolithus abies (~40%). At the same time, specimens of *Coccolithus pelagicus, Discoaster* spp., Umbilicosphaera spp., and *Rhabdosphaera* spp., are decreasing.

Also, *Helicosphaera carteri* are consistently absent throughout the bottom of NN8-NN10 boundary and reappear again from the below of this boundary. Different with Site 782 where a specimen of *Helicosphaera carteri* is disappeared below

NN8-NN10 boundary. The amount of *Reticulofenestra* spp. (<2µm) specimens is very abundant more than another specimen but disappear in the upper part of NN7 zone and *Reticulofenestra pseudoumbilicus* are very rare and decrease abruptly.

Small of *Reticulofenestra (<2µm and* 2-3µm) are increasing in percentage from the middle of NN7 Zone to the bottom but small of *Reticulofenestra* (3-5µm) and *Reticulofenestra pseudoumbilicus* are decreasind and disappear with the amount of percentage around 15 %.

Meanwhile the presence of *Discoaster* spp. appears approximately around 8.5% and this is similar amount condition throughout younger ages. Furthermore, *Calcidiscus macintyrei* and *Discoaster spp.* last appear in the middle part of this boundary were both determined in sample 31R-CC (590.6 mbsf).

The zone NN6 has found 18 species with the abundant amount of *Reticulofenestra* spp. (<3µm) and very rare appearance of *Reticulofenestra* spp. (5-6µm) approximately 2% and *Pontosphaera* spp. approximately 2%. *Reticulofenestra* (2-3µm), *Reticulofenestra* spp. (3-4µm) and *Reticulofenestra* (>2µm) are dominant in the NN6 boundary. Furthermore, *Pontosphaera discopora and Pontosphaera* sp., are absent in the upper part of NN6 boundary and small percentage appearance is detected in the bottom part of this boundary (Figure 5.3).

The last occurrence of *Sphenolithus heteromorphus* which correlates to the NN5/NN6 boundary is respectively found in the sample below 956.1 mbsf (Figure 5.4). The next zonal boundary of NN4/NN5 cannot be defined, caused by the absence of the last occurrence *Helicosphaera ampliaperta*. Zone NN4-5 of the bottom part of

middle Miocene boundary shows increasing amount of specimen *Reticulofenestra* spp. (3-5µm), *Discoaster deflandrei* and *Discoaster* spp., and only 12 specimens of nannofossil with small percentage appear during this boundary.

The boundary of NN3/NN4, which defined by last common occurrence of *Sphenolithus belemnos*, is found between 965.7 mbsf/975.3 mbsf. *Reticulofenestra* spp. (20-3µm) is mostly abundant in NN3 boundary, which amount approximately 65% from the total of assemblages. *Triquetrorhabdulus carinatus* disappear in this boundary. *Triquetrorhabdulus* challenge is a presence from the bottom part of NN3 boundary through below sequences. Otherwise, *Reticulofenestra* spp. (5-6µm) and *Reticulofenestra pseudoumbilicu*s are absent from depth 940 mbsf until 970 mbsf. The species of *Helicosphaera* also disappears from 930 mbsf to 960 mbsf in the bottom part of NN3 boundary. *Umbilicosphaera jafari* and *Hughesius tasmaniae* constantly appeared during NN3 boundary interval.

The next zonal boundary of NN2/NN3 which is defined by the first occurrence of *Sphenolithus belemnos* is recognized in 1004.3 mbsf. The variations of nannofossil assemblages are more abundantand appear in NN2 boundary with consist of 29 species and the abundance amount percentage by *Reticulofenestra* spp. (2-3µm). *Sphenolithus conicus, Helicosphaera intermedia, Helicosphaera oblique, Hughesius gizoensis, Helicosphaera carteri* and *Rhabdosphaera clavigera* finally last appear in this zone, while the disappearance of Reticulofenestra spp. (>2µm) from 110 mbsf until 1130 mbsfis observed in sample 78R-CC to 86R-CC Also, the last appearance of specimen *Sphenolithus abies* at 1139 mbsf between samples 86R-CC and 87R-CC.

The first occurrence of *Sphenolithus disbelemnos* which correlates to lower part of NN2 is present between 1100.6 mbsf/1110.3 mbsf. And the first occurrence of *Discoaster druggii* used as zonal boundary NN1/NN2 was determined in 1100.3 mbsf. The NN1 boundary is shown with abundant of *Cyclicargolithus floridanus* from the upper to the middle part of sequence and *Reticulofenestra spp.* (2-3μm), *Hughesius tasmaniae* and small percentage of *Discoaster* spp. appear continuously.

Sample from 92R-CC to 95R-cc which correlate with the NN1 boundary or Oligocene age are dissolution and just 8 nannofossils can observe and cannot account of abundant. They are *Discoaster* spp., *Coccolithus pelagicus, Coccolithus miopelagicus, Helicosphaera euphratis Cyclicargolithus floridanus, Reticulofenestra spp.* (3-4μm), *Reticulofenestra pseudoumbilicu*s, and *Sphenolithus moriformis.*

Based on distribution of those calcareous nannofossil assemblages, I suggests the studied sequence in ODP Site 1007 Hole B (204.09 mbsf to 359.95 mbsf) and Hole C (378.9 to 1210 mbsf) should be correlated to NN1 to NN15 Zone from the Oligocene to the early Pliocene Zone with the bottom of oldest sequence more than 25Ma (Figure 5.4).

Table 5.2. Calcareous nannofossil bioevents and ages in Site 1007 Hole B and C (Bahama Bank of Caribbean Sea, Atlantic Ocean).

Calcareous nannofossils event	Age (Ma)	Sample	mbsf
LO *Reticulofenestra pseudoumbilicus*	3.79	1007B-23X-2, 99-100 cm/23X-3, 99-100	205.59/207.09
FO *Discoaster asymmetricus*	4.13	26X-1, 99-100cm/26X-2, 99-100cm	231.59/233.09
FO *Ceratolithus rugosus*	5.12	32X-1, 99-100cm/34X-1, 99-100cm	286.99/305.3
LO *Discoaster quinqueramus*	5.59	32X-1, 99-101cm/34X-1, 99-101cm	286.99/305.3
LO *Discoaster berggrenii*	5.59	32X-1, 99-102cm/34X-1, 99-102cm	286.99/305.3
Top of small *Reticulofenestra* interval	7.17	37X-1, 99-103cm/38X-1, 99-103cm	332.82/342.09
FO *Discoaster berggrenii*	8.52	37X-1, 99-104cm/38X-1, 99-104cm	332.82/342.09
Bottom of small *Reticulofenestra* interval	8.76	1007C-9R-CC/10R-CC	388.5/398.1
LO *Catinaster coalitus*	9.67	15R-CC/16R-CC	446.3/455.9
FO *Catinaster coalitus*	10.78	21R-CC/22R-CC	504.1/513.7
LO *Cyclicargolithus floridanus*	13.29	49R-CC/50R-CC	773.3/783
LO *Sphenolithus heteromorphus*	13.65	50R-CC/51R-CC	783/792.6
FCO *Sphenolithus heteromorphus*	17.72	67R-CC/68R-CC	946.5/956.1
LCO *Sphenolithus belemnos*	17.97	69R-CC/70R-CC	965.7/975.3
FO *Sphenolithus belemnos*	18.92	73R-CC/74R-CC	1004.3/1013.9
FO *Sphenolithus disbelemnos*	22.41	83R-CC/84R-CC	1100.6/1110.3
FO *Discoaster druggii*	22.82	84R-CC/85R-CC	1110.3/1119.9

FO: first occurrence; LO: last occurrence.
Absolute ages of datums were provided by Sato, T., and Oda, M (2013)

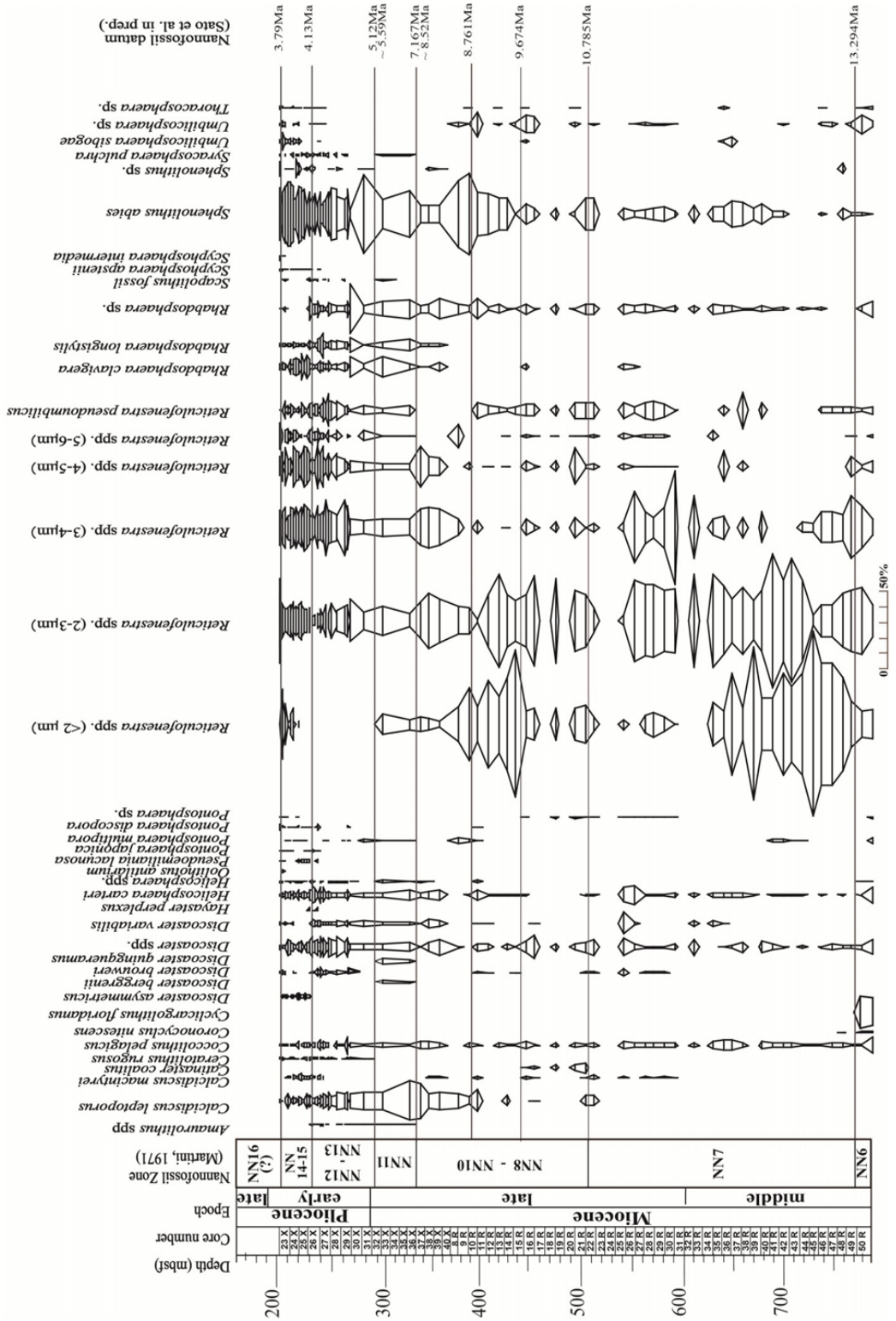

Figure 5.3. Stratigraphic distribution of calcareous nannofossil species (middle Miocene to early Pliocene sequences) in ODP Site 1007 situated in Bahama Bank of the Caribbean Sea in the Atlantic Ocean.

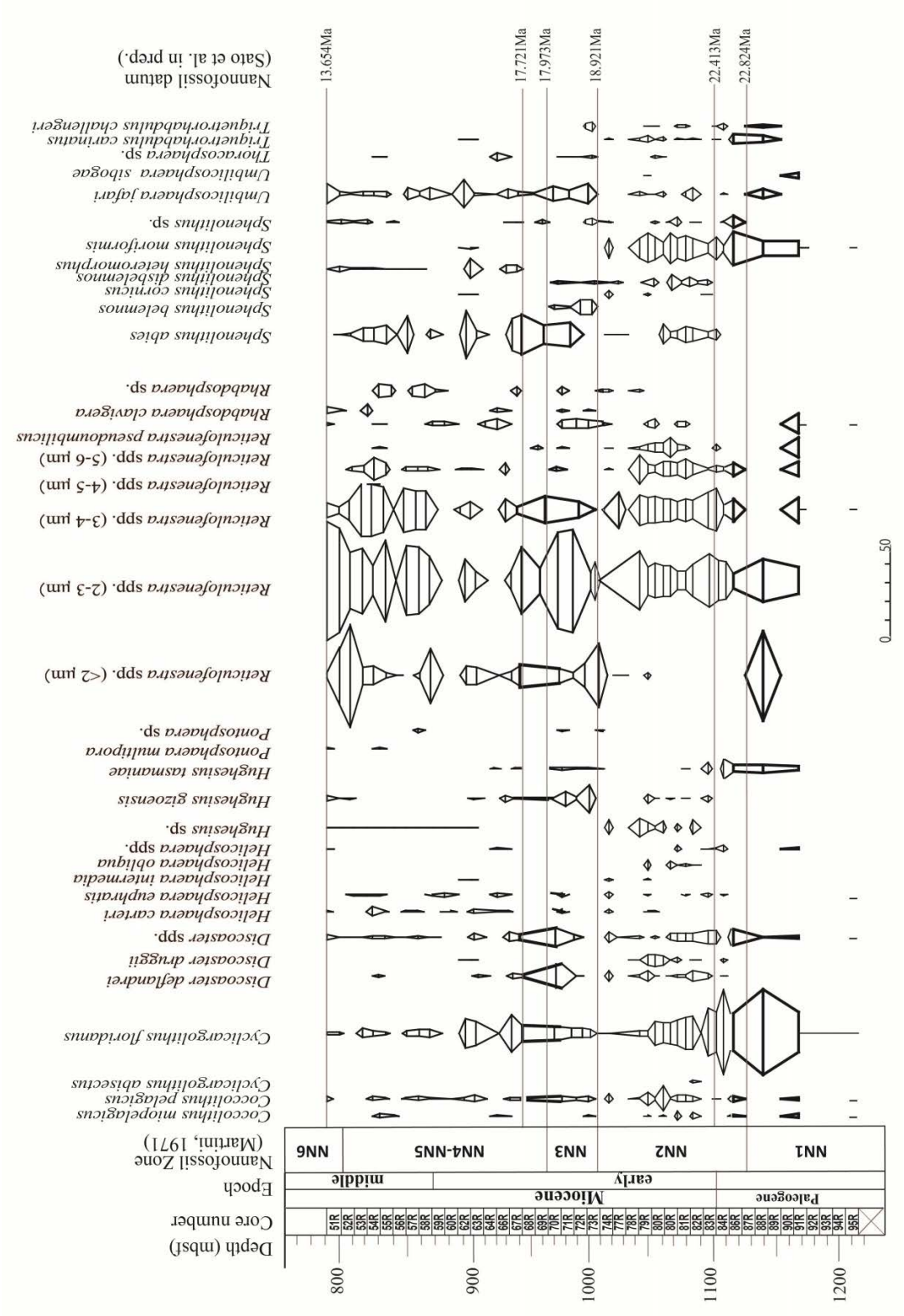

Figure 5.4. Stratigraphic distribution of calcareous nannofossil species (Oligocene to middle Miocene sequences) in ODP Site 1007 situated in Bahama Bank of the Caribbean Sea in the Atlantic Ocean.

Sedimentation Rate ODP Site 1007 Hole B.C

The average sedimentation rate for Site 1007 are provided based on the present of individual datums are listed in Table 5.2. Figure 5.5 shows a representing that the sediment-accumulation rate has been constructed by dividing the thickness of the interval by the time represented (Age-depth relationship of these nannofossils) and the global events base on the timing interval, obtained as follows:

- The sedimentation rate for the Oligocene and early Miocene section (22.824 Ma – 17.973 Ma) based on the first occurrence of *Discoaster druggii* at 1110.3 mbsf and last occurrence of *Sphenolithus heteromorphus* (13.654 Ma) at 946.5 mbsf was 3.6 cm/kyr. The period between 15 and 16 Ma is a significant global tectonic event in the middle Miocene which I call middle Miocene Climatic Optimum (MMCO).
- The average sedimentation rate from 13.6544 Ma (LO *Sphenolithus heteromorphus*) through 10.785 Ma (first occurrence of *Catinaster coalitus*) shows an increase increase to 9.7 cm /kyr.
- The high rate of sedimentation at Site 1007 shown between middle Miocene and late Miocene boundary increased to 7.5 cm/kyr based on the LO *Catinaster coalitus* (10.78 Ma) and the first occurrence of *Discoaster berggrenii* (8.52 Ma). The global event occured during 10 to 8 Ma is the intensification of Asian Monsoon which strongly influence the change of ocean circulation and atmosphere in the world.
- A late Miocene hiatus was detected at approximately 332.8 mbsf that spanned approximately 1.36 Ma and just above this unconformity approximately 50 m of uppermost Miocene sediments were found (8.52 Ma to 7.167 Ma). The

base of this package at Site 1007 lies above a section 287 mbsf to 304 mbsf of undetermined age because of poor preservation of the microfossils. And the second hiatus detected in the lower Pliocene package is bounded by a hiatus at 286 mbsf of undifferentiated sediments. During the occurrence of hiatus between 5.59 Ma/5.48 Ma to 7.42 Ma, the climatic events were shown related to the timing of Messinian Salinity Crisis.

- The next sedimentation rate is between late Miocene to early Pliocene sequence which from 5.12 Ma (FO *Ceratolithus rugosus*) to 3.79 Ma (LO *Reticulofenestra pseudoumbilicus*) or between NN12 zone and NN13 zone is 6.7 cm/kyr (Figure 5.5).

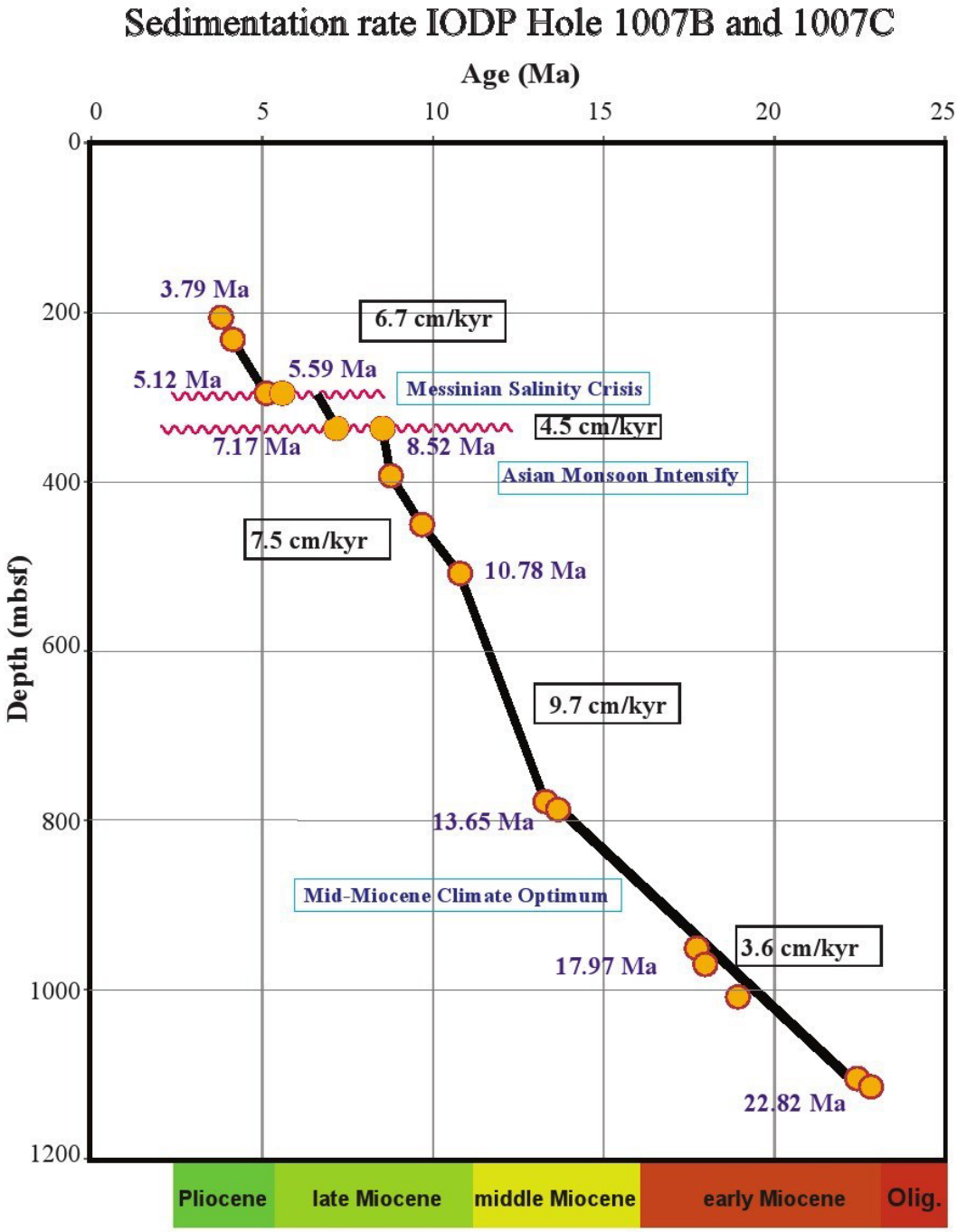

Figure 5.5. Average sedimentation rate of Leg 166 Site 1007 Hole B.C based on calcareous nannofossils datums.

5.3. ODP Site 1006

Calcareous nannofossils in Holes 1007B and 1007C are moderate to poorly preserved based on observed, especially at late Miocene to early Pliocene boundary. The large hiatus at Sites 1007 is not present at Site 1006. I determined sediments recovered from Site 1006 with focus from late Miocene throughout late Pliocene sequence to make clear of productivity nannofossil and provided in detail of nannofossil assemblages distribution. The samples of Hole 1006A yield common to abundant, upper Pleistocene through middle Miocene calcareous microfossils. Biostratigraphic control at Site 1006 is excellent and almost all nannofossil zones from the late Pliocene to lower part of late Miocene are found (Figure 5.6).

The results of the investigation as many as the 10 datum of nannofossil was determined with 61 species of calcareous nannofossils were identified in ODP Hole 1006A (Table 5.3) whereas the absolute ages of datums were provided by Sato and Chiyonobu (in prep.). Ten zonal and non-zonal events were determined in this Hole. Thus, I believe the studied interval in ODP Hole 1006A from samples 16H-CC (149.6mbsf) to 57X-CC (524.7 mbsf) can be correlated with the late Miocene to the late Pliocene.

The sequence of the Hole is characterized by abundant occurrences of *Sphenolithus abies* and *Reticulofenestra* spp. A typical cold water species, *Coccolithus pelagicus* are very rare and are present from the middle part throughout the section not continuously. Although *Reticulofenestra* spp. are abundant, the presencce of this species disappearance in the upper part of late Miocene. The occurrences of *Umbilicosphaera jafari, Umbilicosphaera rotula, Scapolithus fossilis, Umbilicosphaera* sp., and *Hayaster perplexus* are limited in the upper part of the

section (Figure 5. 6). in Zone NN16, small- sized *Reticulofenestra* spp. (3-4µm and 2-3 µm) was observed abundant.. it contains 17 to 45% of the assemblages. However, Reticulofenestra spp. (<2µm) is absent in the upper part of the zone. *Pseudoemiliania lacunosa* has been declining to absent in 190 mbsf which maximum amount is 16%. A small percentage of *Scyphosphaera apsteinii* also occur in the 17H-CC which contains 3.5 % of the assemblages and absent throughout 230 mbsf.

The zonal boundary NN16/NN15 was determined by LO *Reticulofenestra pseudoumbilicus* which was identified in sample 21H-CC/22H-CC (196.9/206.58 mbsf). The maximum frequency of Reticulofenestra *pseudoumbilicus* is approximately 7% of the assemblages and its presence throughout the section is not continuously. Moreover, *Reticulofenestra* spp. (5-6µm) and *Umbilicosphaera jafari* first appeared in this boundary. Generally, the amount of *Discoaster* specimens is rare in the NN14-15 zone and very small of *Reticulofenestra* spp. is absent from the upper part to the middle part of this zone. The first occurrences of *Pseudoemiliania lacunosa* and *Discoaster tamalis* were found in 225.6 mbsf/235.08 mbsf.

In Zone NN13 was observed *Sphenolithus abies* which increase from the top to the bottom of this zone which accounts for around 45 %. Likewise *Reticulofenestra* spp. large size decrease abruptly, and *Pontosphaera multipora* is absent in this zone.

Amaurolithus tricorniculatus, Amaurolithus primus, and *Amaurolithus delicatus* first appear in this range. However *Oolithotus antillarum, Helicosphaera sellii* and *Rhabdosphaera stylifera* finally disappeared in zone NN13.

The boundary of NN13/NN14, which is defines by the last occurrence of *Discoaster asymmetricus* is found between 244.6 mbsf/253.65 mbsf. The first occurrences of *Ceratolithus rugosus* which respectively correlated to the NN12/NN13 boundary are recognized in 321.48 mbsf.

The last occurrences *Discoaster quingqueramus* and *Discoaster berggrenii*, which respectively correlated to the boundary of NN11/NN12 were recognized in between 339.78 mbsf/348.15 mbsf. *Discoaster pentaradiatus, Discoaster surculus* and *Discoaster variabilis* occurrence in the zone NN12 which account for ～3.5%. *Syracosphaera pulchra* is absent and *Sphenolithus abies* is appear with abundance around 30% of the assemblages.

The first occurrences of *Discoaster berggrenii* are respectively found in 478.08 mbsf, which is correlated to the NN11/NN12 boundary. The occurrence of *Amaurolithus amplificus* specimens was only found in NN11 zone. *Reticulofenestra pseudoumbilicus* and *Discoaster surculus* are absent from middle to the bottom of this zone. In between 376.4 mbsf and 385 mbsf was shown the absence of all *Reticulofenestra* spp. small size (<2-5μm) and it only contains around 1% of occurrence assemblages *Reticulofenestra pseudoumbilicus* (Figure 5.6). Likewise, *Sphenolithus abies* also increased from middle to the lower of this zone and abundant with the amount of account approximately 35% of assemblages. Although *the cold water species of Coccolithus pelagicus* is very rare, are present throughout the section continuously and *Sphenolithus moriformis* also first appear and present throughout the section continuously which account for 15% to 28% of the assemblages.

Table 5.3. Calcareous nannofossil bioevents and ages in Site 1006 Hole A (Bahama Bank of Caribbean Sea, Atlantic Ocean).

Calcareous nannofossils event	Age (Ma)	Sample	mbsf
LO *Reticulofenestra pseudoumbilicus*	3.79	166-1006A-21H-CC/22H-CC	196.9/206.58
FO *Discoaster tamalis*	4	166-1006A-24H-CC/25H-CC	225.6/235.08
FO *Pseudoemiliania lacunosa*	4	166-1006A-24H-CC/25H-CC	225.6/235.08
FO *Discoaster asymmetricus*	4.13	166-1006A-26H-CC/27H-CC	244.6/253.65
FO *Ceratolithus rugosus*	5.12	166-1006A-35X-CC/36X-CC	321.48/330.6
FO *Ceratolithus acutus*	5.32	166-1006A-36X-CC/37X-CC	330.6/321.48
LO *Discoaster quinqueramus*	5.59	166-1006A-37X-CC/38X-CC	339.78/348.15
LO *Discoaster berggrenii*	5.59	166-1006A-37X-CC/38X-CC	339.78/348.15
FO *Amourolithus* spp	7.42	166-1006A-45X-CC/46X-CC	413.38/421.72
FO *Discoaster berggrenii*	8.52	166-1006A-52X-CC/53X-CC	478.08/487.18

FO: first occurrence; LO: last occurrence.
Absolute ages of datums were provided by Sato, T., and Oda, M (2013)

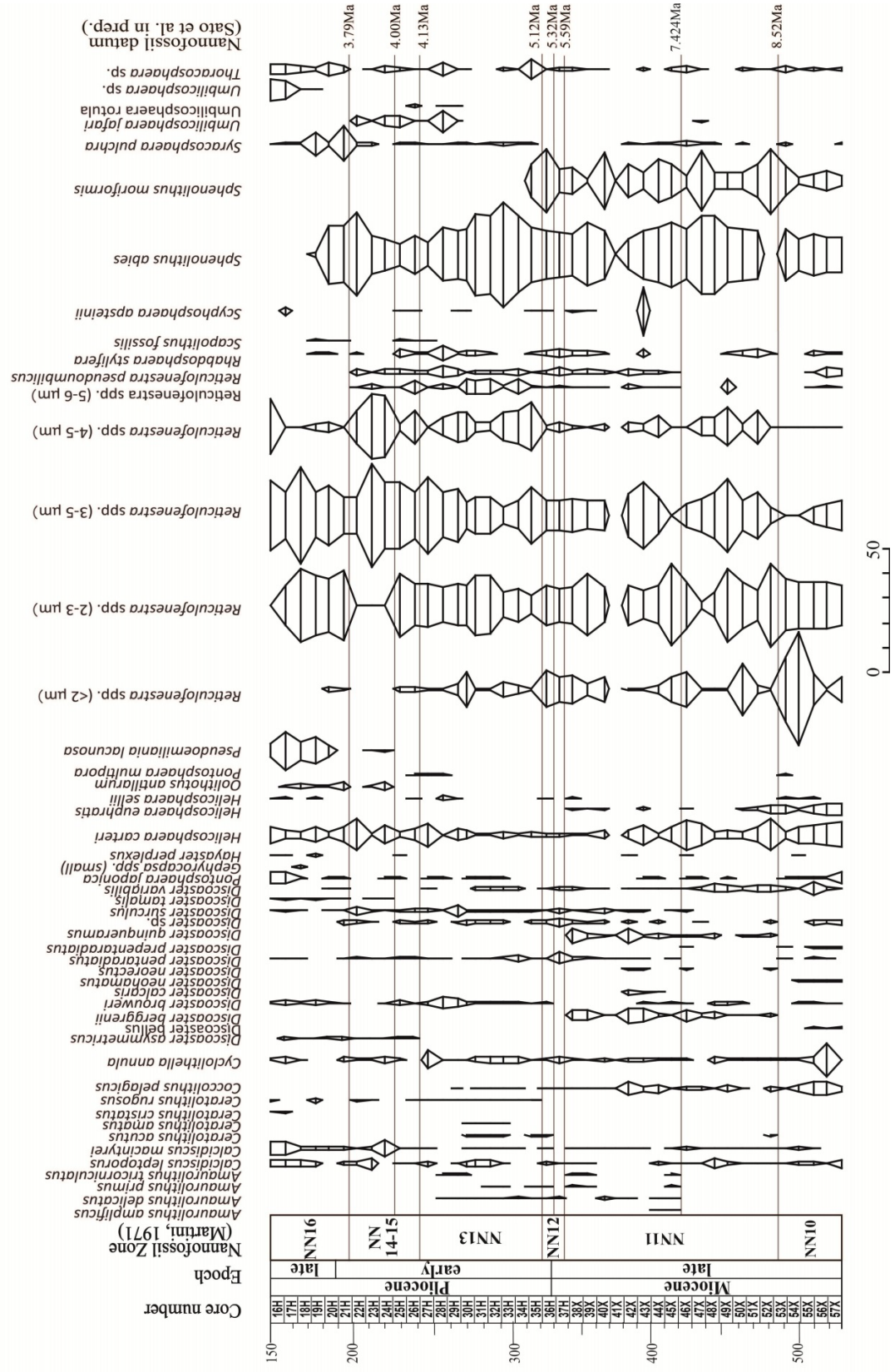

Figure 5.6. Stratigraphic distribution of calcareous nannofossil species (late Pliocene to late Miocene) in ODP Site 1006 situated in Bahama Bank of the Caribbean Sea in the Atlantic Ocean.

Sedimentation Rate ODP Site 1006 Hole A

A curve representing the sediment-accumulation rate for Hole 1006 based on nannofossils zones (Table 5.4) has been constructed by dividing the thickness of the interval by the time represented (Figure 5.7) and relation with the global event, obtained as follows:

- Firstly average sedimentation rate from 8.52 Ma based on the first occurrence of *Discoaster berggrenii* through 5.59 Ma based on the last occurrences of *Discoaster quinqueramus* and *D. berggrenii* is 4.7 cm /kyr. The late Miocene sequence is related to Asian monsoon intensify event which occurred at around 8 Ma to 10 Ma.

- The second sedimentation rate is increasing to 7.8 cm/kyr in the Pliocene sequence based on the last occurrences of *Discoaster quinqueramus* and *Discoaster berggrenii* at 339.78 mbsf/348.15 mbsf, and the last occurrences of *Reticulofenestra pseudoumbilicus* at 196.9 mbsf/206.58 mbsf.

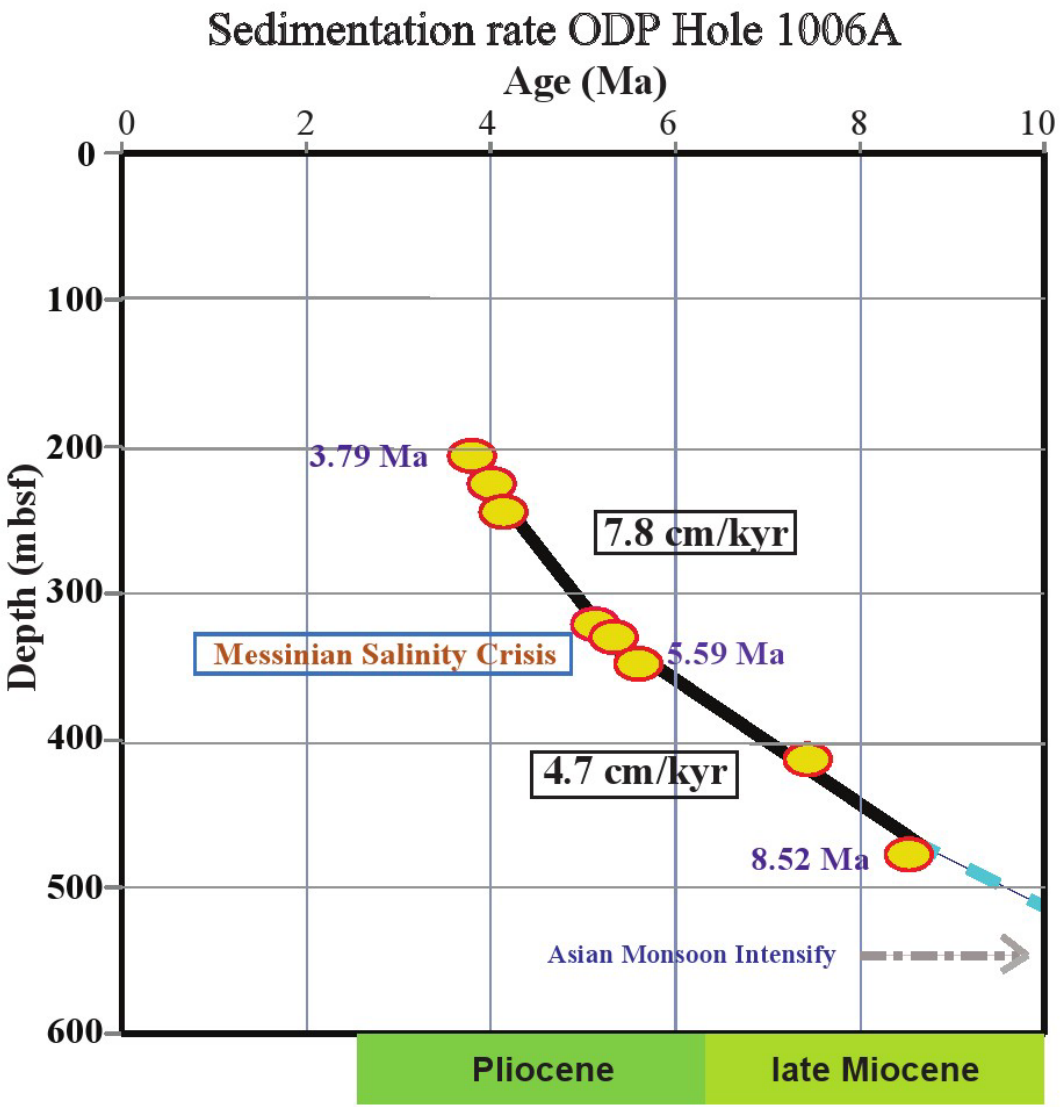

Figure 5.7. Average sedimentation rate of Leg 166 Site 1006 Hole A based on calcareous nannofossils datums.

VI. Coccolith and *Discoaster* Productivity, and *Reticulofenestra* Size Distribution

6.1. ODP Site 782A

The coccolith, *Discoaster* productivity and size variation of *Reticulofenestra* were examined and measured during the middle Miocene to Pleistocene, as shown in Figure 5.1, 5.2, and 5.3 Figure 6.1 shows from the left hand are the number of coccolith productivity, *Discoaster* productivity, and the right hand are percentages of *Discoaster* and size variation including mode of *Reticulofenestra* specimens. From NN5 zone to NN8-NN10 zone, the number of coccolith productivity is around 5.0 x 10^9 N/g, increasing from the upper part of NN8-NN10 Zone (1.2 x 109 N/g) to NN 11 Zone (1.5x 10^9 N/g) and it showed an increase again throughout Pleistocene boundary with the highest peak in NN19 zone (2.4 x 10^9 N/g).

The *Discoaster* species which lived in the lower photic zone under the stable sea with nutricline and thermo-cline are recognized a maximum number in NN6 to NN8-NN10 zone, approximately 7.2 x 10^8 N/g (~50%) and it changed to very rare above NN10 zone (18%). The Negative result with coccolith productivity, the number of *Discoaster* and the mean of *Discoaste*r in the sequence of NN11 Zones decreased abruptly until approximately 8.55 x 10^7 N/g (9%). From NN12-NN13 to the lower part of NN16 Zone (late Pliocene) decreased again until approximately 2.0x107 N/g (~1%), gradually very rare to NN18 Zone (5.0x106 N/g), and *Discoaster* in the upper part of Pleistocene zone is not found (Figure 6.1).

The size of *Reticulofenestra* which is strongly influenced by nutrient level, and in this Site the increase of the maximum size is recognized in five intervals in

NN5 to NN8-NN10 Zone, NN11 Zone to NN12 Zone, NN112-13 to NN15 Zone, NN16 to NN17 Zone and NN18 Zone to NN21 Zone (Figure 6.2). The mode size of the *Reticulofenestra* size is characterized by a positive correlation with the maximum size and the variability of the maximum size of *Reticulofenstra* recorded in the Sites 782 (Figure 4.9). The bimodal pattern distribution is occurred in the every interval before and after the termination of maximization from middle Miocene until Pleistocene Zone.

The upper part of NN8-NN11 interval, the large size is not found, but very small *Reticulofenestra* spp. is start much detected, then continuous increase the number and keep nearly constant through upper part NN11 (Figure 6.2). And the bottom of small *Reticulofenestra* spp. is used as marker 8.761 Ma. The bimodal trend also occurs in size 1-2μm and the next us from this size till 3-4μm during NN12-NN13 Zone, whereas the range of size distribution also shown, which very small size (1-2μm) is dominant.

The very smaller size (1-2μm) mode is not distinct in middle to upper late Miocene sequence (only one specimen mark in NN6 Zone). The small size of *Reticulofenestra* spp. specimens are marked a clear mode in the interval of NN6 to NN11 Zone, and very small size of *Reticulofenestra* spp. specimens is marked in the Interval NN12 to NN21 Zone

Although the mode of *Reticulofenestra* size is situated around 2 to 3 μm throughout the section from middle Miocene to Pleistocene, bimodal peaks occur in some intervals (Figure 6.3). Larger size mode from 2 to 12 μm appears between 13.5 Ma and 8.8 Ma, 8 Ma and 6 Ma, 6 Ma and 3.8 Ma, and above 3 Ma. The larger mode size increases in these intervals, and disappear at the top of the intervals.

The relationship between the coccolith productivity and relative abundance of *Discoaster* shows the negative correlation throughout the section (Figure 6.3). Coccolith number is low in the section of NN6 and NN7 but it increases from NN8 to NN16. It also drastically increases the number in the Pleistocene sequence. The relative number of *Discoaster* which is maximum in NN6 to NN10 in the Miocene, decrease in the sequence above NN10 and abruptly disappeared in 2.0 Ma.

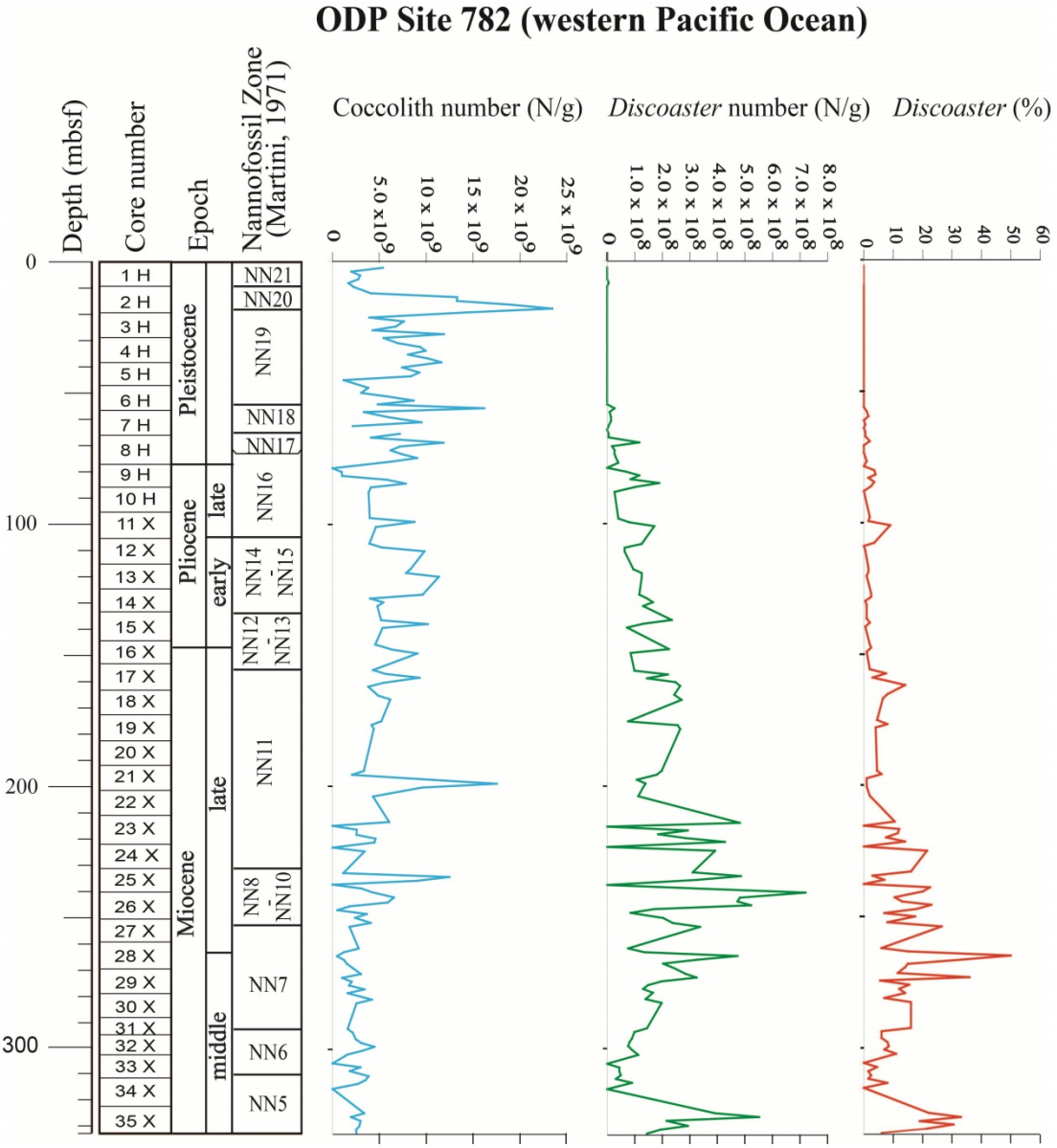

Figure 6.1. Comparison between coccolith and *Discoaster* number (N/g), and relative abundances of *Discoaster* (ODP Site 782, western Pacific Ocean)

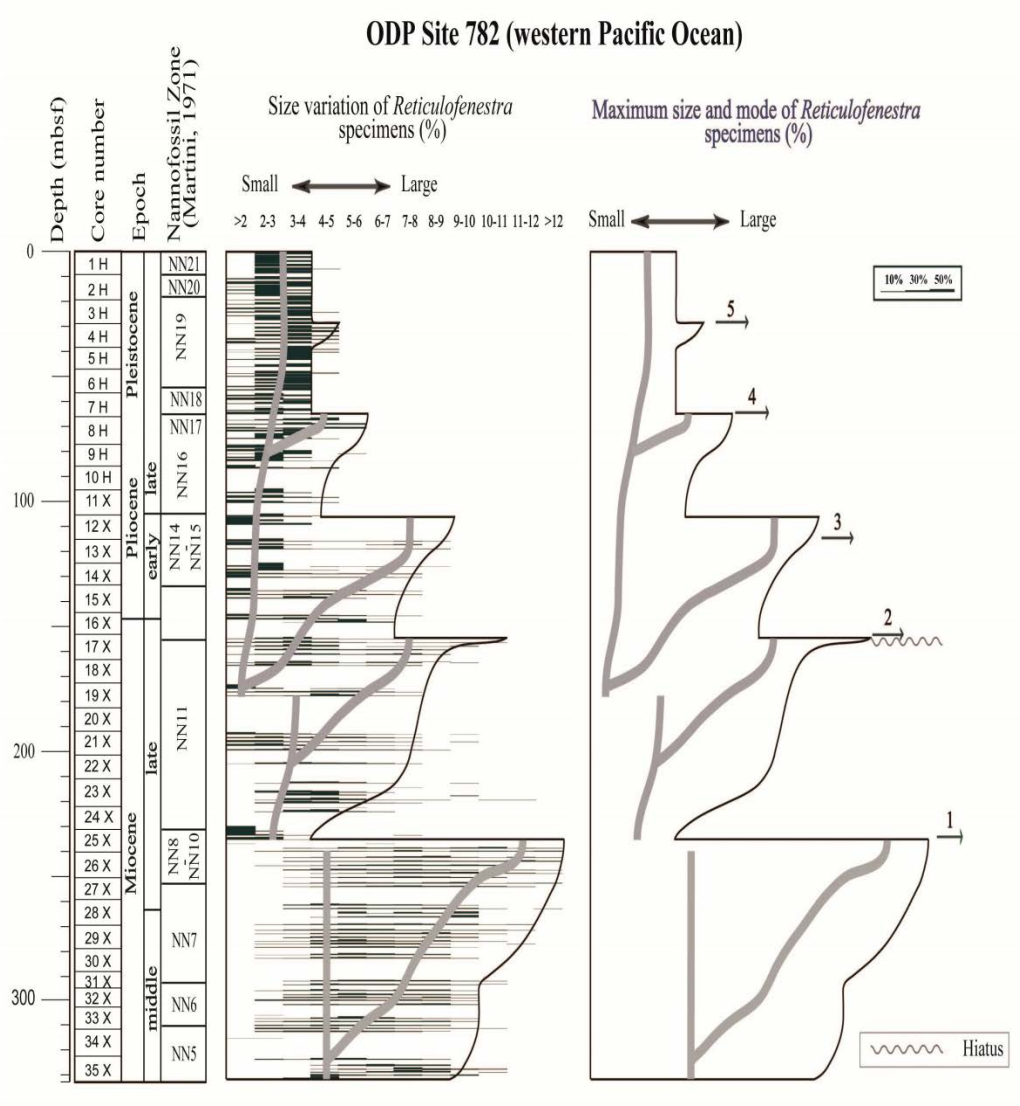

Figure 6.2. Comparison between distributions of size of *Reticulofenestra* specimens (%), and the maximum size of *Reticulofenestra* (ODP Site 782, western Pacific Ocean).

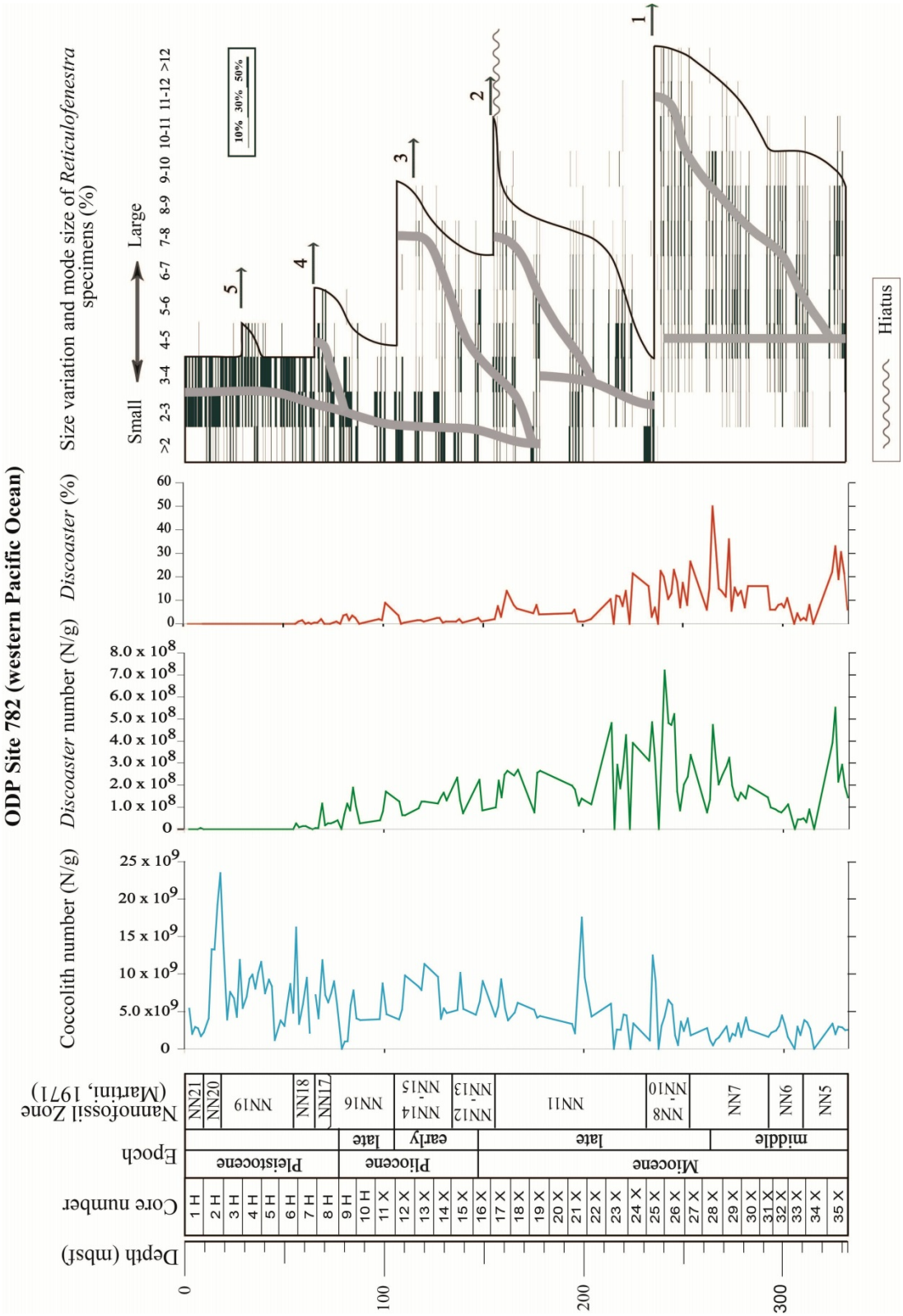

Figure 6.3. A comparison of coccolith number (N/g), *Discoaster* productivity, percentage of *Discoaster*, and mode size variation of *Reticulofenestra*, in ODP Hole 782A (western Pacific Ocean).

6.2. ODP Site 1007

I am using two Hole sediment samples from Site 1007 which consist of Hole 1007B (cover of late Miocene to the late Pliocene) and Hole 1007C (cover of the Oligocene to the late Miocene sequence). The absolute of coccolith and *Discoaster*, and relative abundance of each species was investigated in detail from Oligocene to the late Pliocene sequence (see Appendix B, C, D, and E). The focus of the present study is from NN5 boundary throughout NN21 boundary which cover of the middle Miocene to Pleistocene age between western Pacific Ocean (Site 782A) and Bahama Bank of Caribbean Sea (Site 1007 and 1006). In this chapter will not shows the figure distribution percentages of *Discoaster* and *Reticulofenestra* size variations for the NN1 to NN4 zone from Hole 1007C (see Figure 4.4), but all of data provided in appendix.

The coccolith productivity from Site 1007 is shown increased from the lower part of NN8-NN10 Zone throughout NN14-NN15 Zone with the highest peak approximately 5.0 x 10^9 N/g (Figure 6.4). From NN6 zone to NN8-NN10 zone, the number of coccolith productivity was around 8.4 x 10^8 N/g until 1.0x 10^9 N/g. Otherwise, the amount of *Discoaster* productivity is not significantly change of the number and also a percentage, are was few from NN6 until NN14-NN15 of age study. The highest peak of *Discoaster* productivity is approximately 3.0 x 108 N/g and the maximum percentage around 25% (Figure 6.5).

This study site is situated in the low tropical climates and inferred with the abundant of the cold water species. The coccolith size of *Reticulofenestra* specimens was measured in each sample for clarifying the size distributions of coccolith throughout the sequence which is decreased three times in NN6 to NN8-NN10 Zone,

NN11 Zone to NN12 Zone, and NN112-13 to NN15 Zone.

The all range size occurs from 2µm until 10 µm and the small size of *Reticulofenestra* spp. (2-3µm) specimens are mark a clear mode from NN6 to NN14-NN15 Zone. Focusing to mode size, the mode of the *Reticulofenestra* spp. size is characteristic by a positive correlation with the maximum size whereas showed two bimodal occur in NN7 and NN12-NN13 zone.

The upper part of NN8-NN10, abruptly decrease in maximum size from 8-9µm to 4-5µm, as well as minimum and bimodal also show was recognized. The bottom of small *Reticulofenestra* spp. is used as marker 8.761 Ma as well as same with Site 782. The wide range size occurs in the last termination (NN12-NN13 to NN14-NN15), from 2µm until 10µm, some specimen of *Reticulofenestra* spp. size 9-10µm is found in the upper part of this zone.

The mode of *Reticulofenestra* size is situated in 2 to 3 µm throughout the section (Figure 6.6). The bimodal pattern in the sequence also found in the lower part of the section from NN7 to NN10. Another bimodal pattern is also recognized in the lower Pliocene sequence. Although coccolith productivity increases from NN8 to NN16, the relative abundance of *Discoaster* indicates no significant changes.

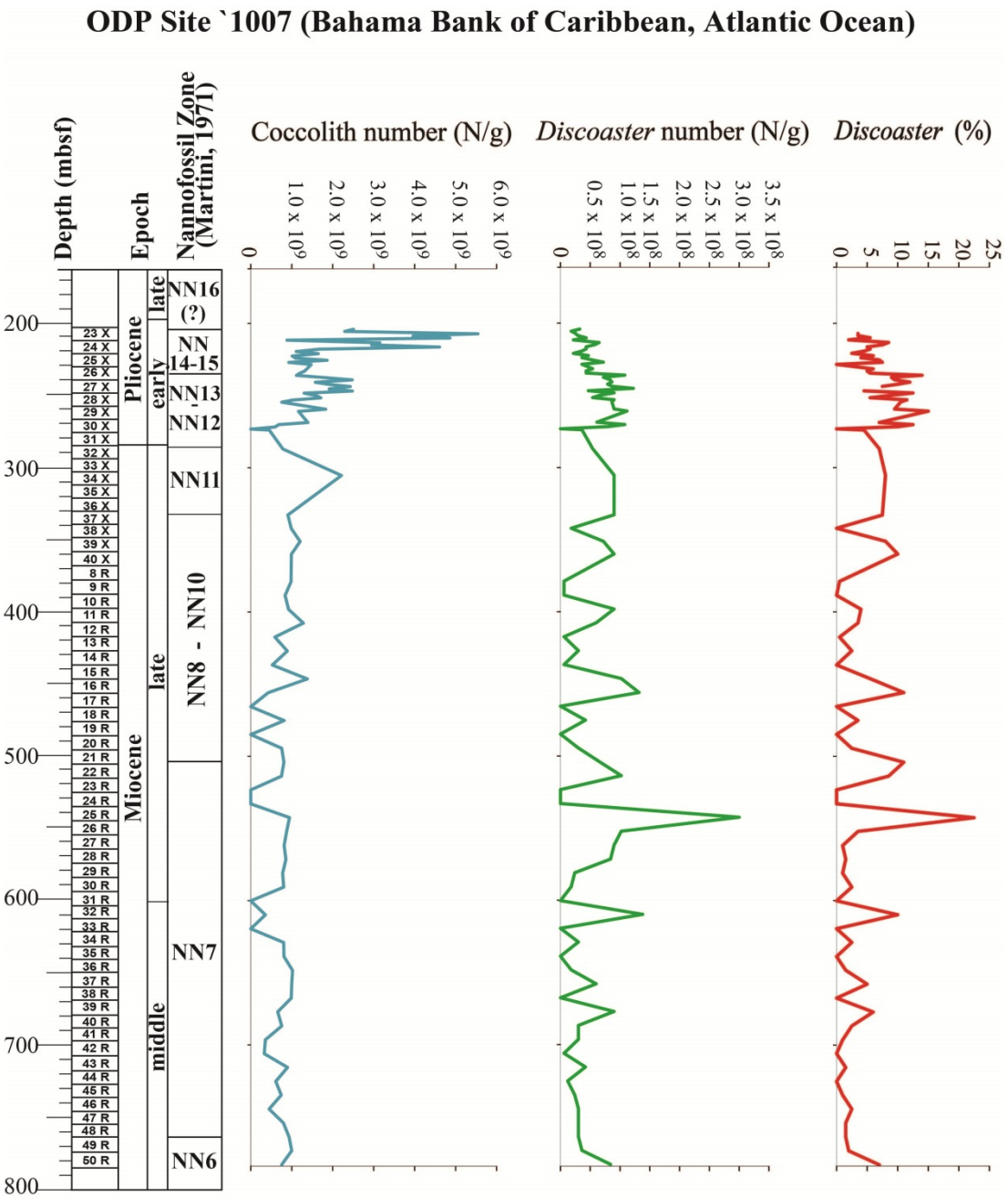

Figure 6.4. Comparison between coccolith and *Discoaster* number (N/g), and relative abundances of *Discoaster* (ODP Site1007, Bahama Bank of Caribbean Sea).

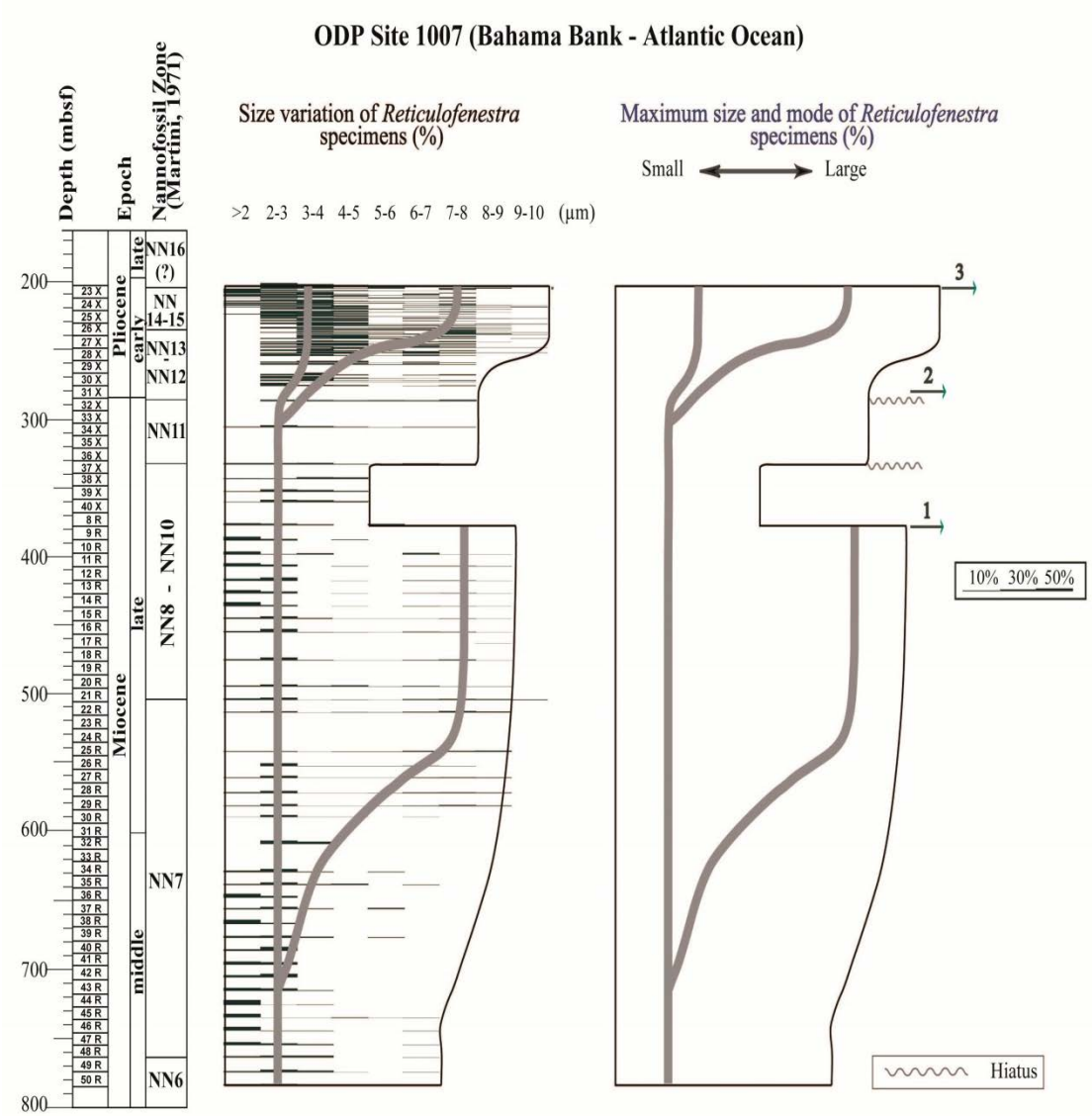

Figure 6.5. Comparison between distributions of size of *Reticulofenestra* specimens (%), and the maximum size of *Reticulofenestra* (ODP Site 1007, Bahama Bank of Caribbean Sea).

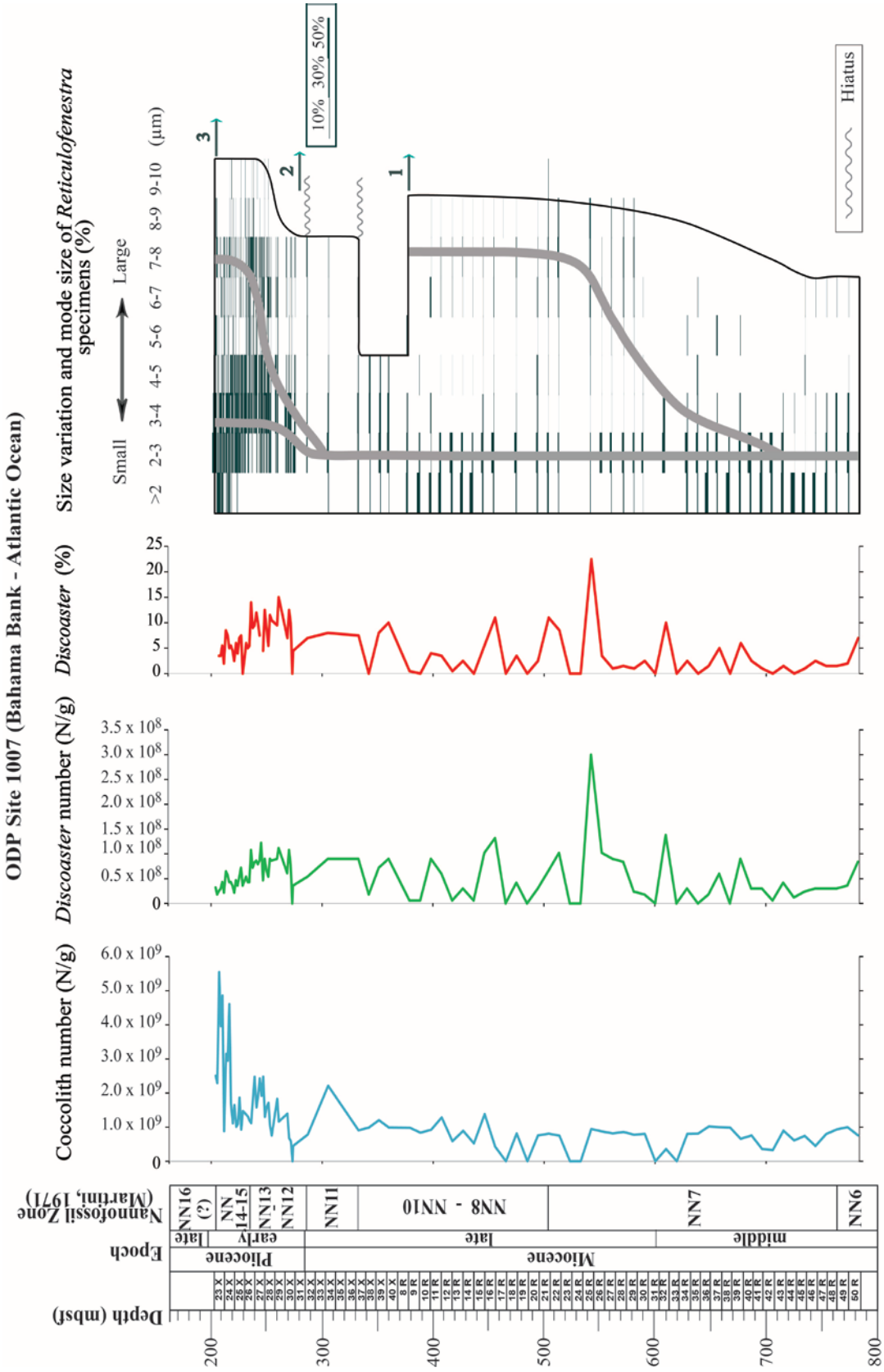

Figure 6.6. A comparison of coccolith number (N/g), *Discoaster* productivity, percentage of *Discoaster*, and mode size variation of *Reticulofenestra*, in ODP Site 1007 (Bahama Bank of Caribbean Sea, Atlantic Ocean).

6.3. ODP Site 1006 Hole A

The coccolith size of *Reticulofenestra* specimens was measured in each sample for clarifying the size distributions of coccolith throughout the sequence show in figure 5.7. The size distribution was divided into four intervals, large (>7μm), medium (5-7μm), small (3-5μm) and very small (<3μm). The increase of the maximum size is recognized in three intervals in NNN10 Zone, NN11 Zone to NN12 Zone, and NN14-15 Zone. Very small size dominance (2-3μm) and contrast occur in NN10 Zone until 82%. The relative abundance of *Discoaster* decreased in between NN11 and NN12 boundary, and it changed to very rare above NN14-15. Focusing on the mean size of *Reticulofenestra* species, it decreased at NN10 zone, NN12 and lower NN14-15 (Figure 6.7). Meanwhile, in the upper part of NN11 show the coccolith productivity increased throughout to NN16. A bimodal size distribution and increases in the modal size of *Reticulofenestra* coccoliths were also found in this period in size 2-3μm (Figure 6.8). The mode of *Reticulofenestra* size is situated in 2 to 3 μm throughout the section (Figure 6.8). The bimodal pattern in the sequence also found in the lower part of the section from NN10 to NN12. Another bimodal pattern is also recognized in the lower Pliocene sequence. The change in relative abundance of *Discoaster* and coccolith are also closely related to the stepwise change in the modal size of *Reticulofenestra* (Figure 6.9). The late – early Miocene period (NNN11/NN12) is characterized by coccolith productivity increase, a low abundance of *Discoaster*, and abundant small *Reticulofenestra* coccoliths (Figure 6.9).

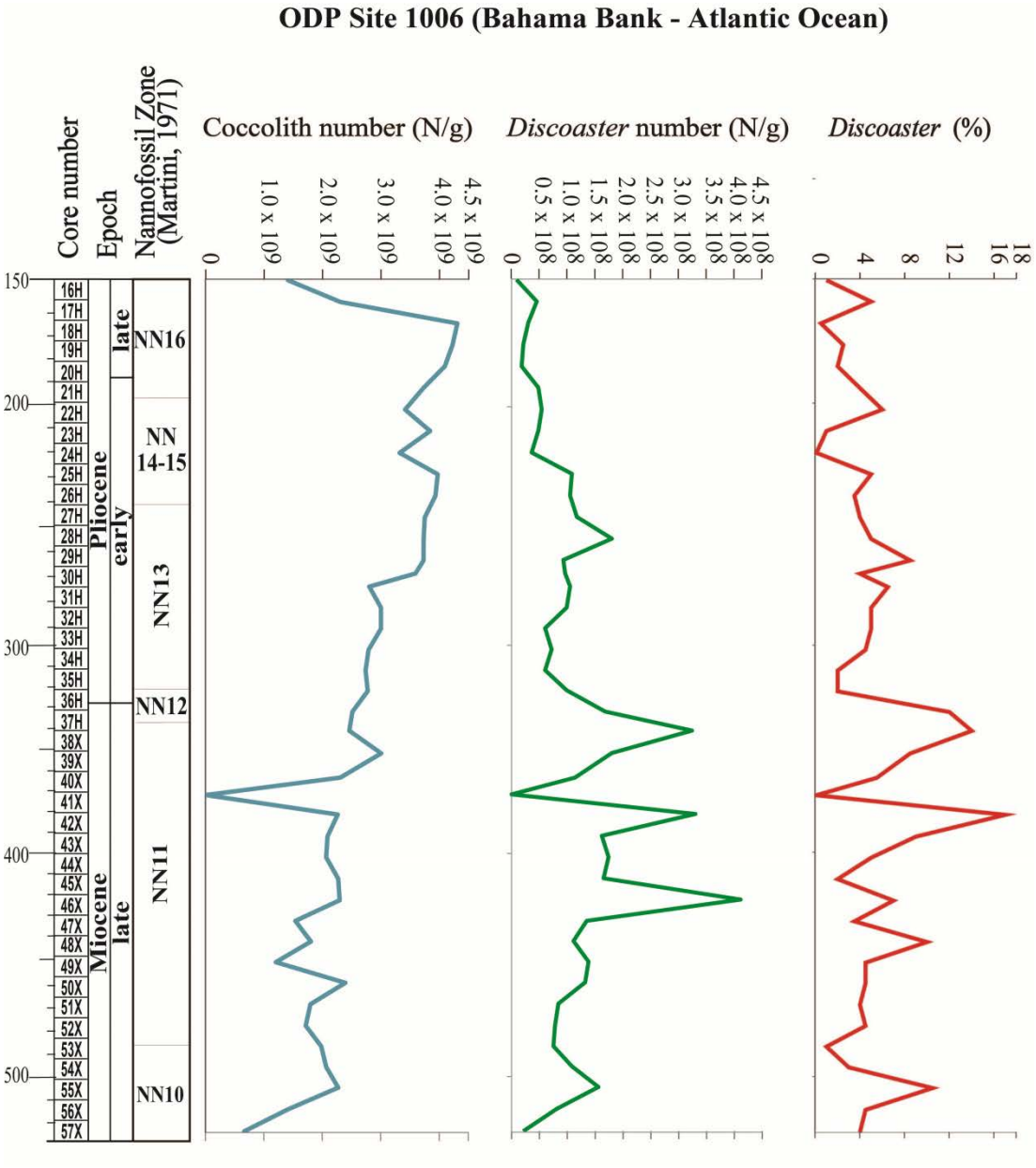

Figure 6.7. Comparison between coccolith and *Discoaster* number (N/g), and relative abundances of *Discoaster* (ODP Site1006, Bahama Bank of Caribbean Sea).

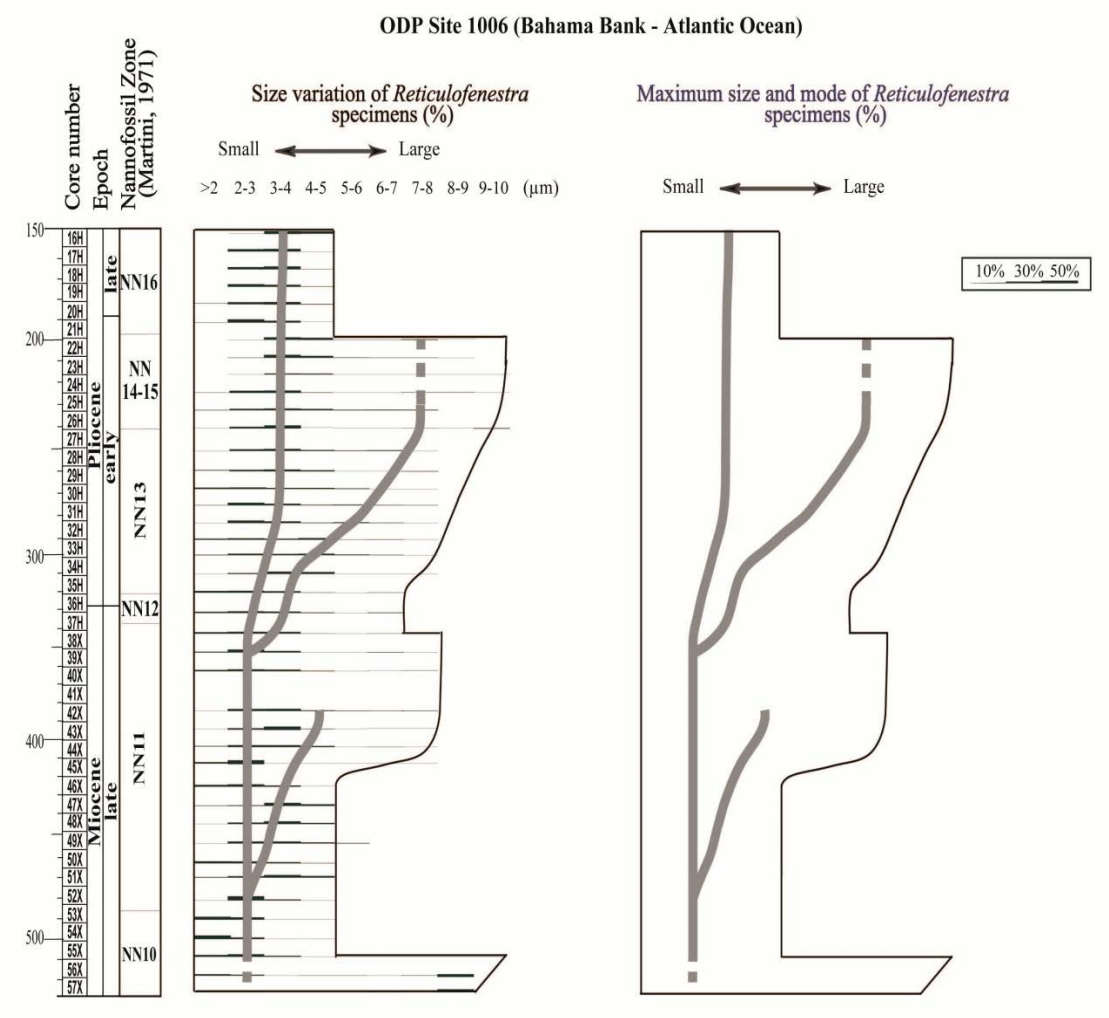

Figure 6.8. Comparison between distributions of size of *Reticulofenestra* specimens (%), and the maximum size of *Reticulofenestra* (ODP Site 1006, Bahama Bank of Caribbean Sea).

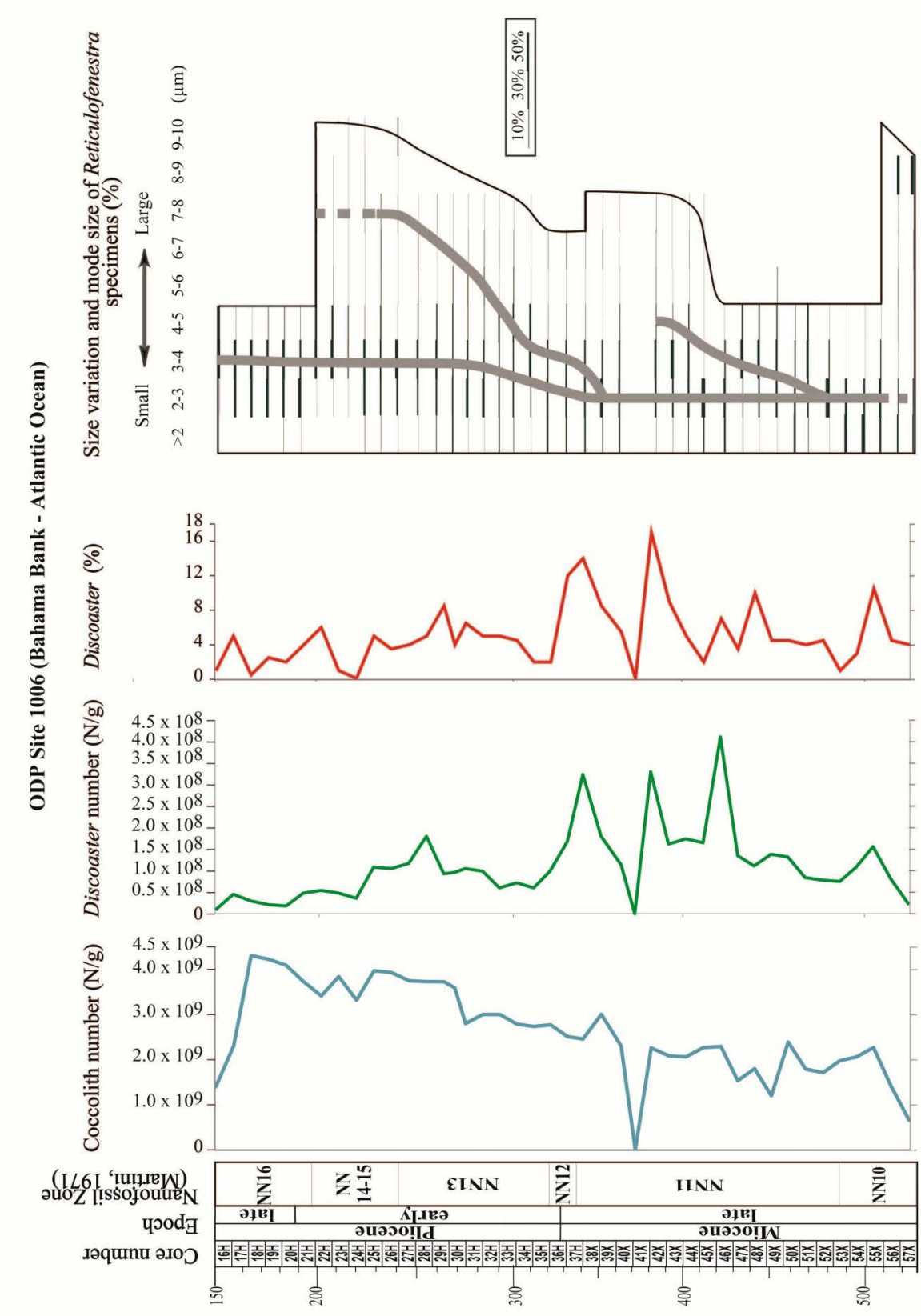

Figure 6.9. A comparison of coccolith number (N/g), *Discoaster* productivity, percentage of *Discoaster*, and mode size variation of *Reticulofenestra*, in ODP Site 1006 (Bahama Bank of Caribbean Sea, Atlantic Ocean).

VII. Paleoceanographic Episodes in the western Pacific Ocean and Bahama Bank of Caribbean

I analyze the number of coccolith productivity, *Discoaster* productivity and size variations of *Reticulofenestra* to reconstruct the Neogene paleoceanography of Bahama Bank of Atlantic and western Pacific Ocean (Figure 7.1, Figure 7.2).

The coccolith productivity of site 782 is characterized by the increase from NN6 to the lower part of NN8-NN10 Zone while the relative abundant of *Discoaster* species shows opposite trends in this interval. The mode and maximum size of the *Reticulofenestra* show five times increasing patterns while the mode indicates bimodal (Figure 7.1). The relative abundance of *Discoaster* which lived in the lower photic zone under the stable sea with nutricline and thermocline, decreased step by step at NN10/NN11, NN11, NN15/NN16, and in NN17/NN18 boundaries.

The maximum size of *Reticulofenstra* is indicated by the decrease during 14 Ma to recent. The change in relative abundance and productivity of coccolith are also closely related to the stepwise change in the modal size of *Reticulofenestra* in NN10, NN11, NN17 and NN19 Zone (Figure 7.1). Meanwhile, in the upper part of NN8-NN10 show the coccolith productivity decreased. At 8.8 Ma, the sea surface stability of Western Pacific Ocean was changed from oligotrophic to the eutrophic condition. The collapse of sea surface water condition (from oligotrophic to eutrophic) since Miocene to Quaternary in 8.8 Ma was related to the Asian Monsoon Intensify. Furthermore, decreasing temperature at the late Miocene is predicted as the closing of the Indonesia seaway or/and global cooling (Akmaluddin et al., 2000).

Although the coccolith and *Discoaster* productivity of Site 1007 located in the

Bahama Bank is not changed clearly during Miocene sequence, coccolith productivity suddenly increased in the early Pliocene of NN12 to NN16 (Figure 7.2). The mode and maximum size of the *Reticulofenestra* show two times increasing patterns while the mode indicates bimodal (Figure 7.2). The dominance of small *Reticulofenestra* in 8.8 Ma are a positive correlation with coccolith productivity. Around that period (late NN10 to early NN11), Young (1990) termed it as "small *Reticulofenestra* interval", as well as Takayama (1993) also investigated that dramatic size reduction event occurring in the late Miocene (NN10).

The dominance of small placolith (*Reticulofenestra*) indicates upwelling (Okada and Wells, 1997). As the occurrence of the large size, *Reticulofenestra* indicates the oligotrophic/warm water species and stable sea surface ocean condition, the drastic decreasing of the maximum size of *Reticulofenestra* recorded in the Site 1007 at 8.9 Ma, 5.3 Ma and at 3.75 Ma (Figure 7.2).

Although, the relative abundance of *Discoaster* did not have change for fluctuated number during middle Miocene to Pliocene in site 1007 at Bahama Bank. However in site 1006 were showed relative abundant of *Discoaster* decreased from the upper part of NN10 throughout NN14-15 boundary with negative correlation with the peak of productivity of coccolith. The presence of larger size *Reticulofenestra* species also show the oligotrophic conditions of sea surface stratification with thermocline were showed in NN10 boundary in Site 1006 of Caribbean Sea (Figure 7.3).

The results indicate that lower photic zones species *Discoaster* were decreased at NN12 boundary. This means that thermo- and nutricline developed in NN12 to lower NN14-15 Zone. As the occurrence of the large size, *Reticulofenestra*

indicates the oligotrophic/warm water species and stable sea surface ocean condition, the drastic decreasing of the maximum size of *Reticulofenestra* recorded in the Site 1006 at 8.7 Ma, 5.4 Ma and at 3.75 Ma.

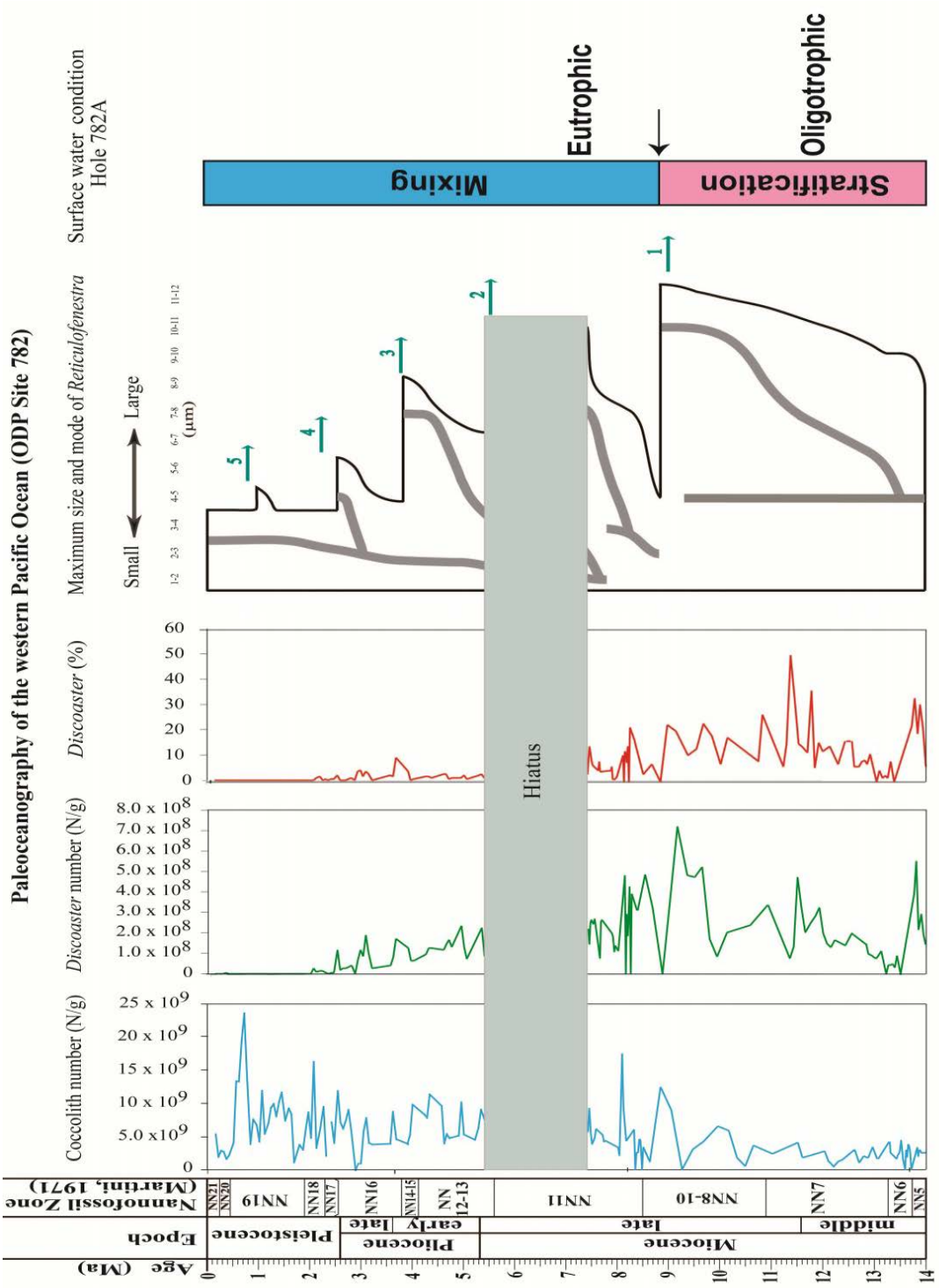

Figure 7.1. A summary correlation between coccolith number (N/g), *Discoaster* productivity, percentages of *Discoaster*, and size distribution of *Reticulofenestra*, with changes of surface water condition in ODP Hole 782A.

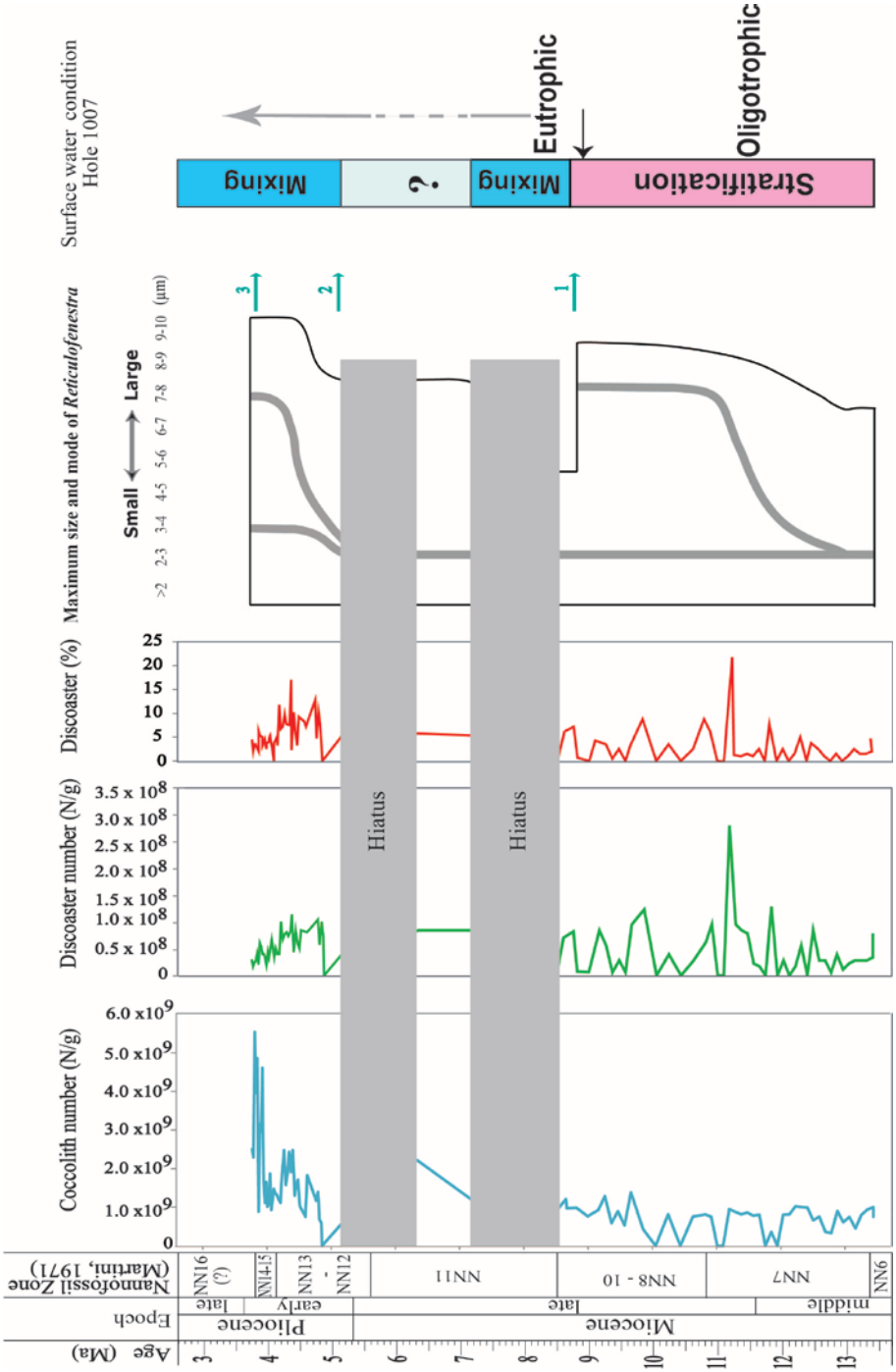

Figure 7.2. A summary correlation between coccolith numbers (N/g), *Discoaster* productivity, the percentage of *Discoaster*, and size distribution of *Reticulofenestra*, with changes of surface water condition in ODP Site 1007.

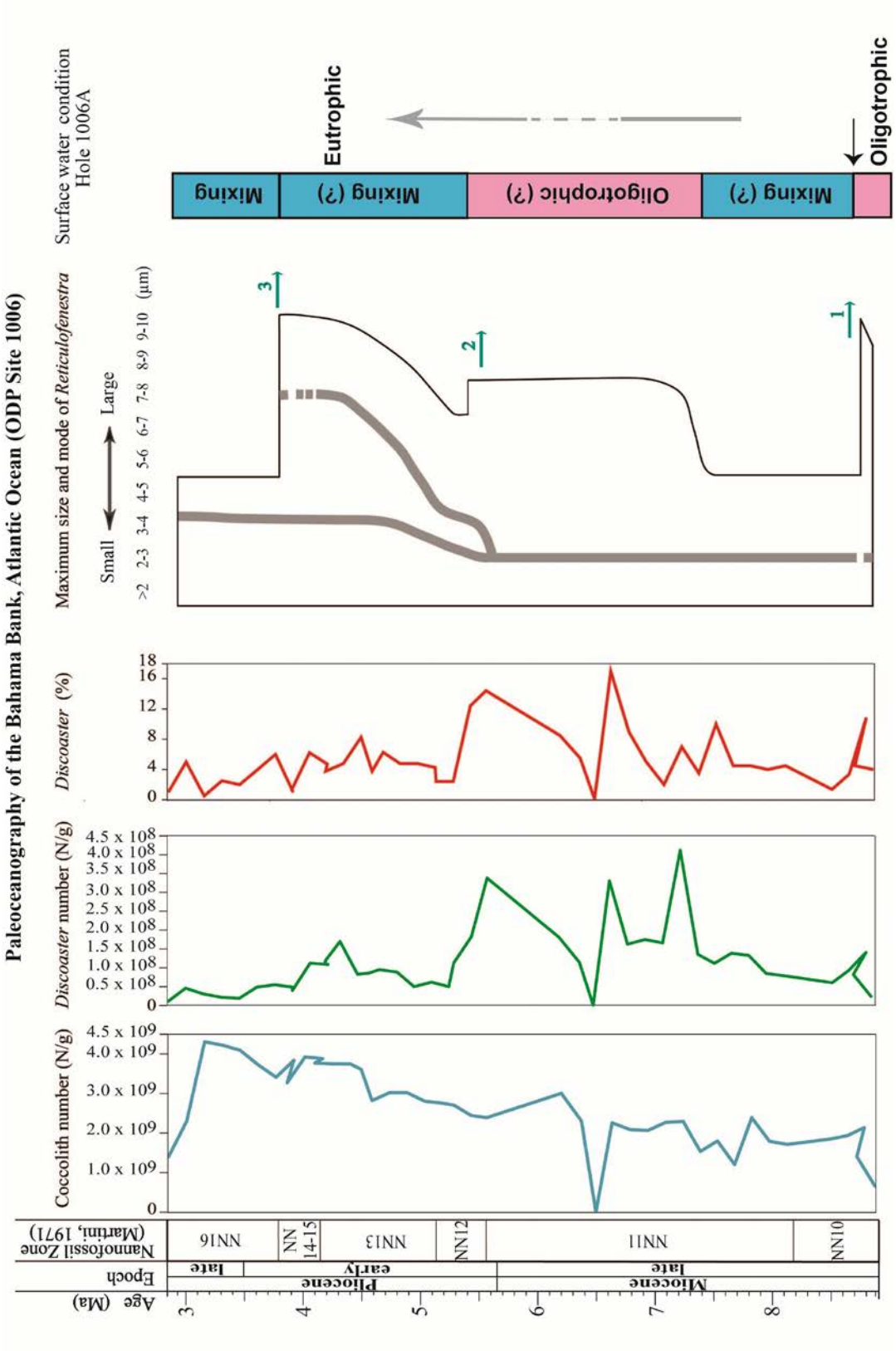

Figure 7.3. A summary correlation between coccolith numbers (N/g), *Discoaster* productivity, the percentage of *Discoaster*, and size distribution of *Reticulofenestra*, with changes of surface water condition in ODP Site 1006.

VIII. Global Sea surface stability and significant paleoceanographic episodes of the Indian Ocean, Bahama Bank of Caribbean, northwestern Pacific and the western Pacific Ocean

The additional goal of this study is to make special references for the formation of petroleum source rock based on calcareous nannofossil assemblages' distribution and productivity in the worldwide. This study discusses the paleoceanographic events through the Neogene by comparing the paleoceanographic results of the western Pacific and the Atlantic Ocean with those of the Indian Ocean (Young, 1990) and the northwestern Pacific Ocean (Imai *et al*., 2015). It also interprets the cause of the events based on the correlation with global tectonic and climatic events.

Figure 8 shows the correlation of coccolith number, the relative abundance of Discoasters and maximum size of *Reticulofenestra* between sites 782, 1006 and 1007.

The drastically decreasing of the maximum size of *Reticulofenestra* at 8.8 Ma in the late middle Miocene and 3.75 Ma in the late early Pliocene is found in Site 782, 1006 and Site 1007. Nannofossil has been described as a good tool for reconstructing the oceanographic condition when doing a paleoceanography analysis. Molfino and McIntyre (1990) described the utility of *Florisphaera profunda* assemblages which shows the stability of sea surface condition. However, as *Florisphaera profunda* first appeared in late Neogene, it was impossible to analyze the Neogene paleoceanographic conditions based on *Florisphaera profunda* assemblages. Recently, Sato and Chiyonobu (2009) focused on Discoasters for paleoceanographic

analysis.

Discoasters had been believed as the warm water species based on distributions in low latitude region (Haq, 1980; Bukry, 1971; Bukry, 1973). However, Aubry (1992), Chepstow-Lusty (1989), Stoll *et al*. (2007) and Sato and Chiyonobu (2009) described that Discoasters lived in a lower photic zone of oligotrophic environment and its ecology was similar to *Florisphaera profunda*. This means that abundant occurrence of *Discoaster* indicates the distribution of stable sea surface condition with thermocline and nutricline.

On the other hand, distinct size variations of *Reticulofenestra* in the Miocene sequence are reported by many authors (Pujos, 1987; Young, 1990; Kameo et al., 2000; Kameo et al., 1999; Chiyonobu et al., 2006; Sato et al., 2009; Farida et al., 2012; Imai et al., 2015). Hagino *et al*. (2000) suggested that small specimens of *Reticulofenestra* were more abundant in eutrophic surface waters than in oligotrophic surface waters. Recently, Sato and Chiyonobu (2009) studied the size variations of *Reticulofenestra* in the middle Miocene sequence in the Pacific Ocean and described that the presence of large size *Reticulofenestra* shows the stable and oligotrophic sea surface condition (Sato et al., 2009).

On the basis of the these phenomena, Farida *et al*. (2012) suggested that the collapse of thermo- and nutri-cline occurs step by step during Miocene to Quaternary at ODP Hole 805B in the western equatorial Pacific Ocean based on *Discoaster* relative abundance and the *Reticulofenestra* size variations (Farida et al., 2015). These studies also indicated that the collapse of the stability of the sea surface stratification in the equatorial western Pacific Ocean changed gradually from oligotrophic to eutrophic conditions during the Miocene to Quaternary. Based on

these results, I interpret the paleoceanographic environment in the study area and correlation both of study sites.

The results indicate that abundances of *Discoaster* species have a positive correlation with a size change and mode of *Reticulofenestra*, and negative correlation with the productivity of coccolith in the western Pacific Ocean. The maximum size of *Reticulofenestra* increased until 8.8 Ma which shows the oligotrophic conditions with sea surface stratification and thermocline. However, the maximum size of *Reticulofenestra* suddenly decreased at 8.8 Ma, 5.4 Ma, 3.75 Ma and 2.516 Ma.

This means that the stabilization of the Ocean condition in the western Pacific Ocean collapse at 8.8 Ma, 5.4 Ma, 3.75 Ma and 2.516 Ma as a result of the change to eutrophic sea surface conditions (Figure 8). This indicates that the mode size decreased four times throughout the sequence in 8.8 Ma, 6.4 Ma, 5.4 Ma and in 3.75 Ma (1, 2, 3, 4 in Figure 8). Changes in the mode coccolith size of *Reticulofenestra* during the late Miocene to early Pliocene did not occur uniformly in Site 1007 and 1006 of Caribbean Sea (Figure 8). The mode size of *Reticulofenestra* coccolith decreases two times (8.8 Ma and 5.4 Ma) and shows a negative correlation with coccolith number. Although the relative abundance of lower photic zone species *Discoaster* does not change in Site 1007, persistently abundant small *Reticulofenestra* coccoliths are observed in 8.8 Ma which indicates strong eutrophication at the sea surface in the Bahama Bank of Caribbean (Figure 8).

Meanwhile, NN11 Zone shows a gradual increase of the number of coccolith productivity and relative abundance of *Discoaster* also increase but the size variation of *Reticulofenestra* coccolith demonstrates that large coccolith occurred in Site 1006. These results are interpreted eutrophic and oligotrophic in question during NN11

Zone.

The observations on the coccolith productivity, low relative abundances of *Discoaster*, and high relative abundance of small *Reticulofenestra*, portray that the correlation of paleoceanographic condition between western Pacific and Bahama Bank of Atlantic Ocean lies on the sea surface stability which collapsed at 8.8 Ma, resulting in eutrophication of the surface waters.

The high relative abundance of small *Reticulofenestra* shows strong eutrophication which appears at 8.8 Ma and 3.75 Ma in the Bahama Bank of Caribbean and the western Pacific Ocean. The nannofossil events recognized in this study illustrate that the drastic changes of paleoceanography in the world occur four times throughout the Neogene and especially when the events are distinct in the Pacific Ocean.

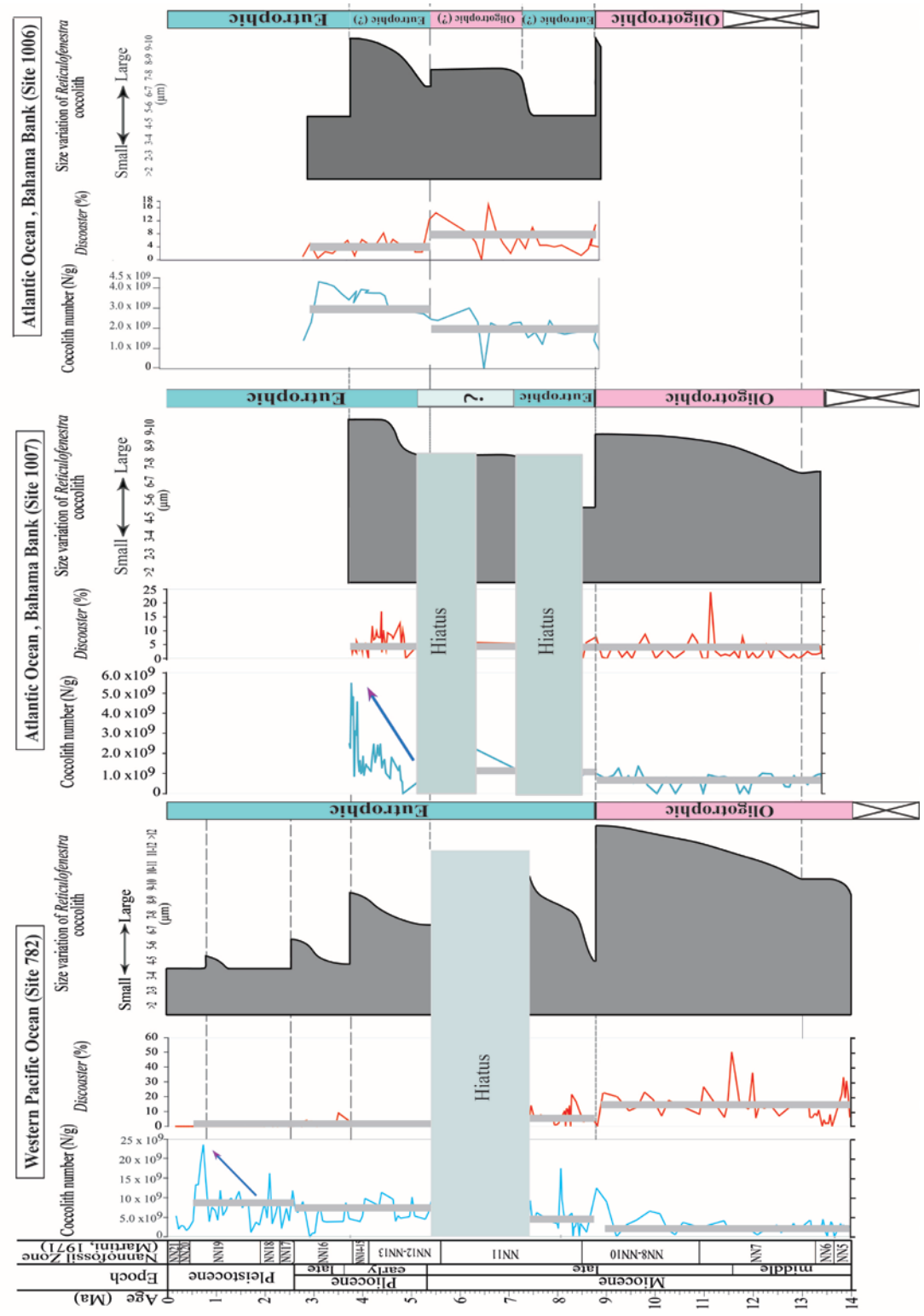

Figure 8.1 The correlation between Paleoceanography conditions based on calcareous nannofossil assemblages throughout the middle Miocene to Pleistocene sections in the western Pacific Ocean (Site 782), and Bahama Bank of Atlantic Ocean (Site 1007 and 1006) and Global climate events.

IX. Correlation between the Global Tectonic Events and Paleoceanography of the Western Pacific and Bahama Bank of Atlantic Ocean

Many global tectonic and climatic events occurred in the Neogene have been studied. I compare the presently investigated results of the size variation of *Reticulofenestra* in the Pacific Ocean and Caribbean sea with those in the Indian Ocean (Young, 1990), northwestern Pacific (Imai et al., 2015) and Equatorial Pacific Ocean (Farida et al., 2012) (Figure 9). A bimodal size distribution of coccoliths of the genus *Reticulofenestra* was found in the upper Miocene to upper Pliocene interval in the Pacific and Indian oceans (Young, 1990; Kameo et al., 2010; Farida et al., 2012).

Young (1990) present three bimodalization occurred in the Indian Ocean sites from NN6 to NN16 Zone at 8.8 Ma; 5.4 Ma; and 3.75 Ma (Figure 9.1). The strong decreased maximum size of *Reticulofenestra* coccoliths is present in 8.8 Ma. These events are responsible for the change of the sea surface stability in the Indian Ocean. Imai *et al*. (2015) studied calcareous nannofossil assemblages from ODP holes 1210A in the northwestern Pacific Ocean also present the large number of *Reticulofenestra* coccolith indicates a shallow thermo- and nutricline is drastically changed to the small size in six times (in 8.8 Ma, 6.4 Ma, 5.4 Ma, 3.75 Ma, 3.4 Ma and 2.75 Ma) in this sites.

Farida et al. (2012) described the collapse of sea surface stability in the equatorial Pacific Ocean based on correlation between *Discoaster* abundances and the size change and the mode of *Reticulofenestra*. The results indicated that the lower photic zone *Discoaster* species decreased step by step and thermo- and nutri-cline

developed at NN10/11 boundaries, and have a positive correlation with size change of *Reticulofenestra*. The sea surface of the equatorial Pacific Ocean has been changed from oligotrophic to eutrophic conditions during the Miocene to Quaternary in 8.8 Ma and strong eutrophication was observed in 6.4 Ma, 5.4 Ma and at 3.75 Ma (Farida et al., 2012). Furthermore, compared with other sites, the northwestern Pacific Ocean is also characterized by the strong eutrophication in 8.8 Ma, 6.4 Ma, 5.4 Ma and at 3.75 Ma based on size variations.

Figure 9.1 shows the changes of mode size of *Reticulofenestra*. Changes of *Reticulofenestra* maximum and mode size which are strongly related to the collapse of stability of Ocean surface are clearly traceable to these oceans. Among these events, two of them are found in the oceans distinctly in as follows:

Event ①: Found in the uppermost NN10 Zone in the late Miocene (8.8 Ma; Figure 9)

Event ④: Found in the NN15/NN16 boundary in the Pliocene (3.75 Ma; Figure 9)

The changes of maximum size of *Reticulofenestra* are strongly influenced by the collapse of sea surface stability relating to the disappearance of nutricline by upwelling. Upwelling systems are characterized by their high primary productivity of phytoplankton that is caused by the displacement of nutrient-depleted water in the photic zone by nutrient-rich subsurface water. Based on the characteristics of the relationship between size variability and nutrient condition, these nannofossil events are interpreted as changes to a high nutrient condition which resulted in the changes of the Global climate system. During 8 Ma and 10 Ma is characterized by the intensification of Asian Monsoon caused by uplift of Tibetan Plateau (Burbank et al.,

1993; Filippelli, 1997; Zhisheng et al., 2001; Zachos et al, 2001).

This means that Event ① recognized in 8.8 Ma in the Indian Ocean, Bahama Bank of Atlantic Ocean, western Pacific and Equatorial Pacific Ocean are strongly influenced by the intensification of Asian Monsoon.

Event ④ of 3.75 Ma is strongly related to the formation of Panama Isthmus. Haug and Tiedman (1998) described that current system across the Panama Seaway changed from 4.6 Ma and intensification of the northern hemisphere glaciation was pronounced between 3.1 Ma and 2.5 Ma. Kameo and Sato (2000), Sato *et al*. (2004), and Bartoli *et al*. (2005) also described the final closure of Panama Isthmus was established around 2.75 Ma based on nannofossil assemblages and isotope stratigraphy. On the basis of these facts, a drastic decrease of the maximum size of *Reticulofenestra* occurred in 3.75 Ma was strongly influenced by the closure of Panama Isthmus.

The additional events ② and ③ in Figure 9.1 found in northwestern Pacific, Equatorial Pacific Ocean and Indian Ocean (Figure 9.1) which are indicated by maximum size changes of *Reticulofenestra*, are correlated to the formation of hiatus in the western Pacific Ocean and Bahama Bank (Figure 9.1). These two events are correlated in 6.4 Ma and 5.4 Ma. The age of these events is also respectively correlated to global events such as the formation of western Antarctic ice sheet and Messinian salinity crisis. Krijgsman *et al*. (1999) presented astronomically calibrated chronology for the Messinian salinity crisis. They show that the onset of the Messinian salinity crisis at 5.96±0.02 Ma and also isolation from the Atlantic Ocean has established between 5.59 and 5.33 Ma. Messinian salinity crisis event brought an influence to the changes of sea surface stability conditions in

the global sea level (Hodell et al., 2001; Warny et al., 2003). This indicates that the event ③ in 5.4 Ma indicated by size changes of *Reticulofenestra*, is strongly influenced by Messinian Salinity Crisis.

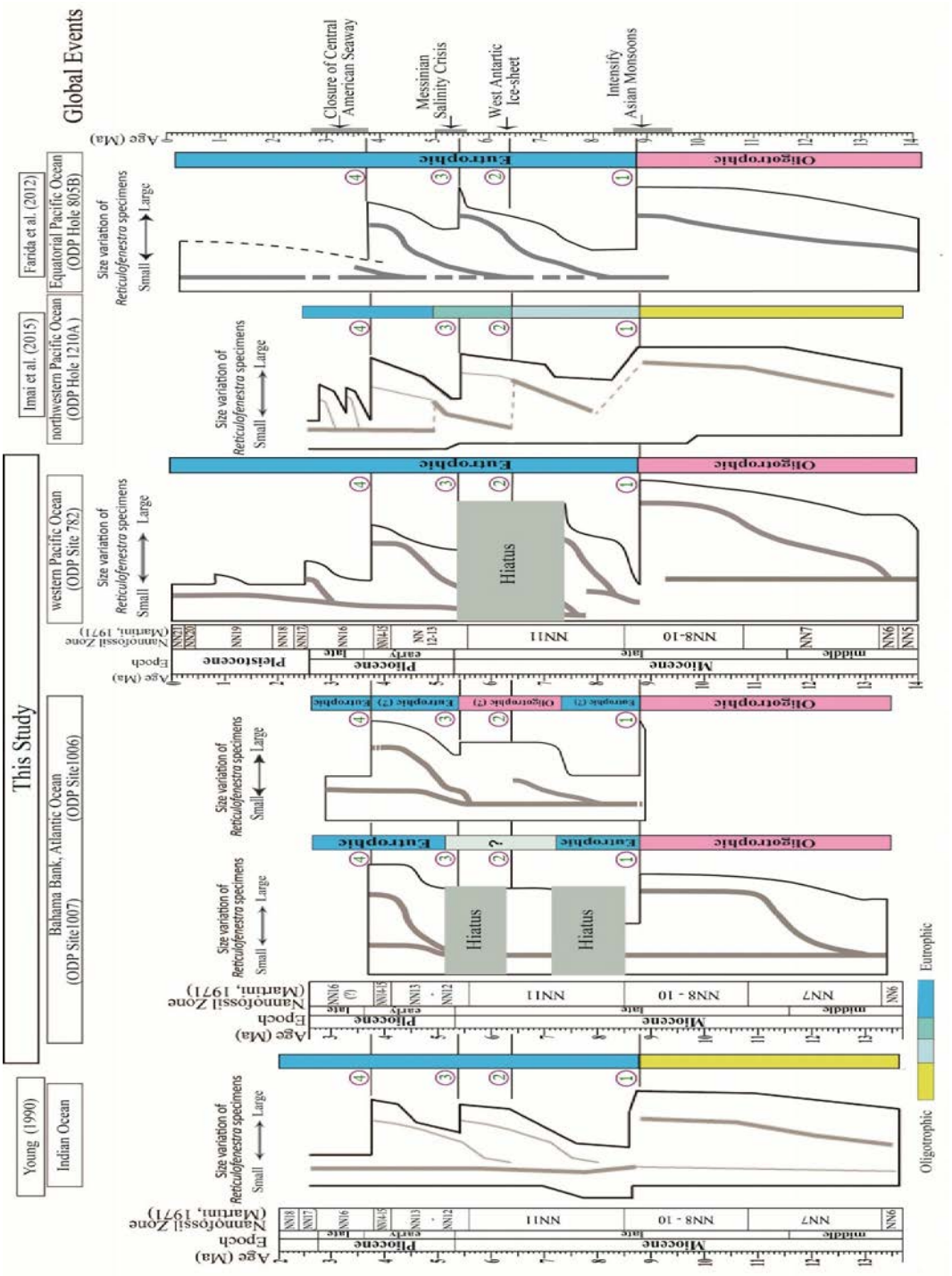

Figure 9.1 A summary of *Reticulofenestra* coccoliths size distribution in the Indian Ocean, Bahama Bank of Atlantic, western Pacific, northwestern Pacific and the Equatorial Pacific Ocean, and the interpretation of the paleoceanography condition.

Eutrophication Zone, Global Climatic/Tectonic Events and Petroleum Source Rocks

Organic content for the petroleum source rocks is controlled largely by biological productivity and oxygenation of the water column and sediment. The amount and type of organic material incorporated into a source rocks are controlled in part by depositional and environmental conditions.

The most area along the coast is well-aerated by circulation, the wind, and wave action. In some areas, however, the aeration is hindered by physical barriers such as reefs or shoals, and in deeper waters far offshore, the water below a certain depth is depleted of oxygen. In such environment, organic waste materials and dead organisms can sink to the bottom and be preserved in an anaerobic environment instead of being decomposed by oxidizing bacteria. The accumulation and compaction of impermeable clay along with the organic matter help to seal the organic matter off from dissolved oxygen. Thus isolated, it becomes the raw material that is transformed into petroleum by the heat and pressure of deeper burial (The University of Texas, 2014).

The mechanism by which oil and gas are generated varies from basin to basin depending on sedimentary facies, burial history, tectonic events process (McCarthy et al., 2011). Sedimentation in areas of high organic productivity and preservation of organic matter in sediment are good sources of rocks form for oil and gas.

Much of the world's oil (85 %) has been sourced from marine source rocks. Changes in facies associated with the geological events and a long-term increase in

upwelling and paleo-productivity are possibly connected with the migration of plate or tectonic events in the worldwide. The productivity of coccolith plays a pivotal role playing in the largely of distribution petroleum source rock and associated with the geological and tectonic activity. The increase or changes of the upwelling were superimposed on a changing stratigraphic record composed of several sequences transgressive or regressive cycle deposits in dynamically changing basin and sub-basin which is important for the accumulation of source rocks.

The efficient of nutrient recycling depends on the winds, surface nutrient, and paleoclimate changes which affected the Ocean productivity as well as eutrophication and stratification zone. In addition, the stratification condition is initiated by an influx or fresh water to semi-isolated basins, either as excess rainfall or glacial melting or a combination of both. The development of stratification is caused by the preferentially greater heater of the surface ocean layer than the deep water masses during an episode of regional or global climatic changes.

The global events of Asian Monsoon intensification (8.8 Ma) are influenced by the change of sea surface ocean condition from oligotrophic to eutrophic condition which in this study occurred in Atlantic, western Pacific, northwestern Pacific, Equatorial Pacific and Indian Ocean sites (Figure 9.1). The characteristic of eutrophication condition determined by the high productivity of coccolith and the drastic decrease of the maximum size of *Reticulofenestra* are strongly related to the appearance of nutricline in the sea surface ocean. A deep nutricline indicates eutrophic condition consequently, a higher abundance of small sized *Reticulofenestra* coccolith occurs.

Zisheng et al (2001) demonstrated that the significant increases in altitude of

the Tibetan plateau were thought to occurrence about 10 to 8 Ma while the record of the microfossils increase or the occurrence of the upwelling was influenced by the development of intensification of Asian Monsoon. During the periods of enhanced monsoonal activity which were characterized by humid conditions and stronger winds, mixing of the enhanced wind stress that improved vertical mixing and led to an entrainment of nutrients into the surface waters. This resulted in an increase of primary production or increase of coccolith productivity.

Such increases mean that the eutrophication condition occurred in 8.8 Ma in the Bahama Bank of Atlantic Ocean, the western and northwestern Pacific, equatorial Pacific and the Indian Ocean are traceable worldwide. They also signaled the occurrence of petroleum source accumulation (high productivity of phytoplankton). Events 3 or the additional events occurred in this study when the eutrophication sequence occurred in the Indian and northwestern Pacific Ocean is Messinian Salinity crisis (Figure 9.1). The timing of high productivity of coccolith related with the petroleum source potential is available as a reference for the Pacific and the Indian Ocean sites. The idea that the Mediterranean Sea dried out completely during the late Miocene (Messinian 5-6 Ma) is now widely accepted (Hardie et al. 2004) and the first published in 1972 grew out of the interpretation by Deep Sea Drilling Project (DSDP) Leg 13 in 1970. That was the last expedition focusing on the Messinian salinity crisis. During the timing of Messinian salinity crisis (5-6 Ma), the sapropels occurred relatively from DSDP Leg 13 data (Kidd et al., 1973).

The development of eutrophic conditions coincided with the rising sea level and the overflow of saline waters from the Mediterranean Sea (Arthur et al. 2004). The event 4 at 3.75 Ma which is traceable in the Indian, Pacific and Atlantic Ocean is

Closure of Panama Isthmus shows the high peak of coccolith productivity. The high nutrient condition is also a time reference to the high source rock potential for the petroleum. The closure of the Central American Seaway severed the communication between the equatorial Pacific and Atlantic and Caribbean Sea. Consequently, this event increases in the surface salinity of the Caribbean Sea and the western Atlantic Ocean. Such climatic event influenced the change in the oceanic circulation, sedimentation rates, and marine climatic condition both in the Atlantic and the Pacific Ocean associated biologic reorganization (Ibaraki, 1996).

The closure of Central American Seaway process led to higher evaporation and a more moisture supply to the high latitude and fueling the buildup of the northern hemisphere ice sheets (Bartoli et al., 2005). The stability of sea surface Ocean collapses to eutrophication condition which was by the decrease of large size *Reticulofenestra* specimens during the timing of this event. The primary and important event recognized in 8.8 Ma in the Indian Ocean, Bahama Bank of Atlantic Ocean, western Pacific and Equatorial Pacific Ocean is strongly influenced by the intensification of the Asian Monsoon. The timing clearly shows the high productivity of phytoplankton is traceable worldwide and applicable for the formation of petroleum source rocks.

Meanwhile, the basin development is inferred by the global tectonic events. Oxygen depletion may occur in the underlying bottom-waters as oxygen supply is overwhelmed by the demand created by degradation of dead organic matter. Source beds of marine petroleum source rocks may develop in enclosed basins with restricted water circulation (reducing oxygen supply), or in open shelves and slopes with upwelling into the zone of ODD (oxygen-depleted/-deficient) (Satyana, 2004).

The examples Miocene petroleum source in the Pacific Ocean is developed in Japan which means that the event in 8.8 Ma is somehow correlated with the Asian Monsoon intensification and is clearly relevant to the reference of petroleum source rock distribution. Figure 9.2 shows the major oil and gas fields in Japan area located in the northeastern part of Honshu island which is from the Onnagawa The Onnagawa Formation is rich in organic matter and represents the principal or primary source rock in the Akita Basin (Taguchi, 1975 and Aoyagi and Iijima, 1987). The Onnagawa Formation has produced 5.4 million kl of oil and 790 million m^3 of gas. The average content of organic carbon and hydrocarbon in source rocks of the Onnagawa Formation shows the highest values of any Neogene unit in the area. The Onnagawa Formation in Akita mainly composed of hard mudstone, siliceous shale, diatomaceous mudstone and acidic pyroclastic rocks (Aoyagi et al., 1981). Figure 9.3 shows correlations of Neogene-Quaternary units in this region. The Onnagawa Formation can correlate to the lower part of the Monterey Formation which has been reported as about 4.5-15 Ma (Addicott, 1978). The best-known sequences of Neogene strata in western Japan are present in the subsurface beneath the Akita-Niigata oil producing area and the adjacent Oga Peninsula area where Miocene diatomaceous sedimentation is represented by the Onnagawa and Funakawa Formations (Ingle et al., 1981). Formation in Akita included the Fukubezawa, Kurokawa, Toyokawa, Yabase and Asahikawa fields (Figure 9.4).

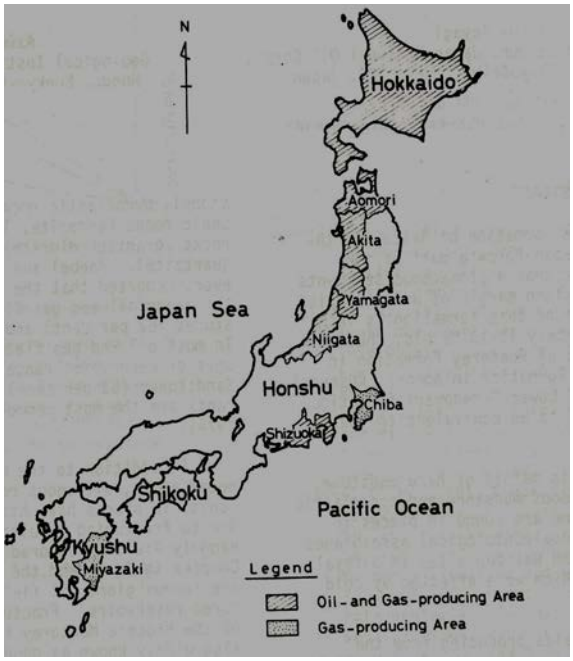

Figure 9.2 Locality map showing the oil- and gas-producing areas in Japan (Aoyagi et al. 1983).

Geological Age (Ikebe et al., 1977)			Aomori	Akita	Yamagata	Niigata
Quaternary	Holocene		Alluvium Terrace Deposit	Alluvium Terrace Deposit	Alluvium Terrace Deposit	Alluvium Terrace Deposit
	Late Pleistocene		——	Katanishi Fm.	Shohnai Gr.	Oguni Fm.
			Tsurugasaka Fm.	Shibikawa Fm.		Tsukayama Fm. / Wanazu Fm.
	Early Pleistocene		Narusawa Fm.	Sasaoka Fm.	Kannonji Fm.	Haizume Fm.
	Pliocene		Maido Fm.	Upper Tentokuji Fm.	Maruyama Fm.	Nishiyama Fm.
				Lower Tentokuji Fm.	Tateyama Fm.	Hamatsuda Fm.
Neogene	Miocene	Late	Akaishi Fm.	Upper Fnakawa Fm.	Kitamata Fm.	Shiiya Fm. / Araya Fm.
				Lower Fnakawa Fm.		Upper Teradomari Fm.
		Middle	Daidoji Fm.	Onnagawa Fm.	Kusanagi Fm.	Lower Teradomari Fm.
			Tanosawa Fm.	Nishikurosawa Fm.	Aosawa Fm.	Nanatani Fm.
		Early	Sawabe Fm.	Daijima Fm.	Zenpoji Fm.	Tsugawa Fm.
			Iwadate Fm.	Monzen Fm.	Atsumi Gr.	Aikawa Gr.
				Akashima Fm.		

Figure 9.3 Geological correlation of Neogene-Quaternary Units in northeastern Honshu, Japan (modified after Aiba, 1982)**.**

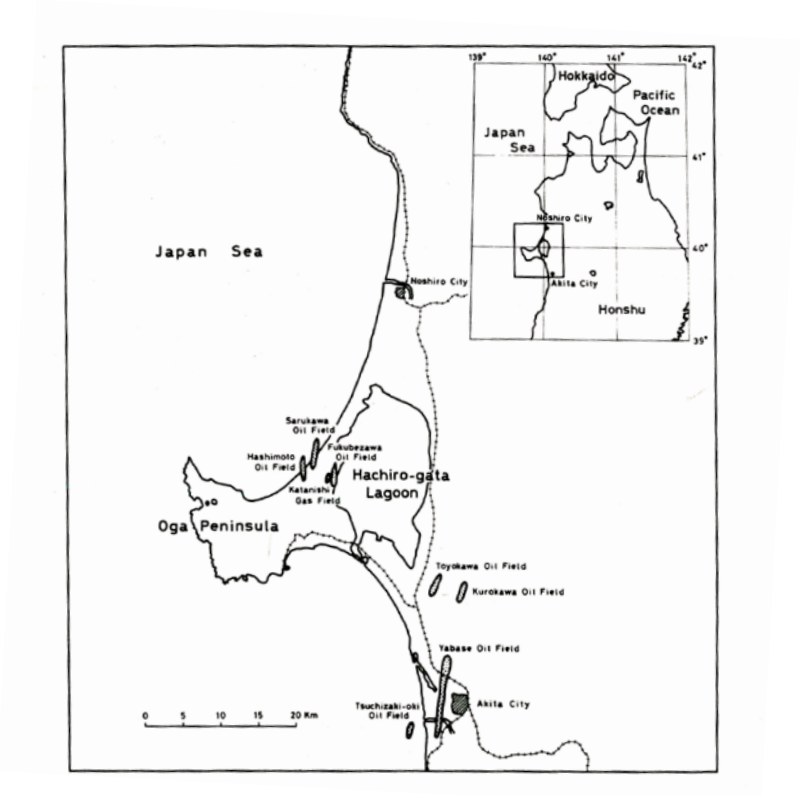

Figure 9.4 Locality map showing the major oil and gas fields producing from the Miocene Onnagawa Formation in Akita, Japan (Aoyagi et al. 1983).

Initial subsidence and marine transgression in this area are represented by the litoral and shelf deposits of the mid-Miocene Nishikurosawa Formation. Rates of subsidence increased in the later mid-Miocene and late Miocene with deposition of massive and laminated diatomites od Onnagawa and lower Funakawa formations on slopes and basins in which sill depth intersected a well-developed oxygen minimum layer (Asano, Ingle, and Takayanagi, 1969). The organically rich diatomaceous deposits of the Onnagawa and Funakawa formations are the principal source beds for petroleum in this area (Figure 9.5).

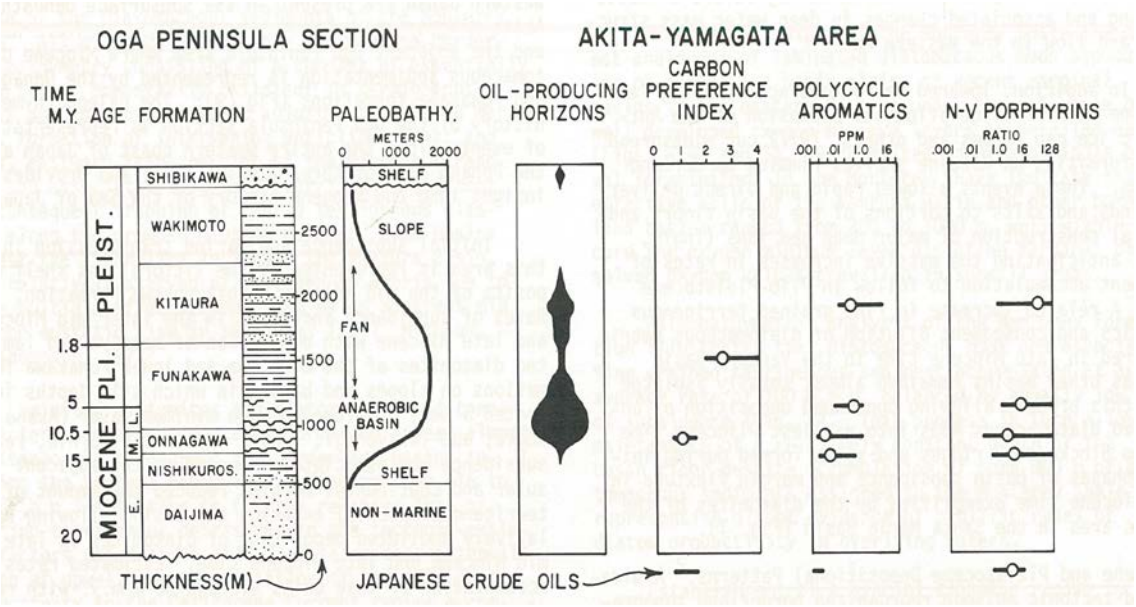

Figure 9.5 Relationship of stratigraphy, age, and paleoenvironments of the Oga Peninsula section, Japan to the general occurrence and maturity of hydrocarbons found in these units within the adjacent Akita-Yamagata area of northwestern Honshu (Taguchi, Sasaki, Sato, Sato, and Hayashida (1977)).

The Onnagawa and Nishikurosawa formations of Middle Miocene age have been considered as the major source rocks for the Yabase oil. Approximately 20 oil and gas deposits, including Yabase oil field, have been discovered in this basin. These deposits are characterized by a high content (up to 60–70%) of biogenic silica. The organic matter in each formation is predominantly Type II kerogen. Most of the oil and gas–oil fields are related to steeply-dipping reverse faults and folds trending northeast–southwest. Detailed geological descriptions of the Akita basin and the geochemical characteristics of possible source rocks and oils were published by Sakata et al. (1988) and Kikuchi et al. (1991). The other part of an oil field in Japan is Hokkaido. Waseda et al. (1998) described that the biomarker distributions from an oil field in Hokkaido and the marine oils are closely correlated to the Miocene marine shales. They suggested that the marine shale's in the Miocene formations should be the major source rocks for the marine oils in both western and eastern Hokkaido.

The other important examples for middle-late Miocene petroleum source related with those results and global tectonic event are Los Angeles and California petroleum source rock. The Miocene Monterey Formation is widely considered to be the primary source rock for hydrocarbons in California (Isaacs and Petersen, 1987). Total organic carbon (TOC) in the Monterey can be as high as 23% (34% organic matter by weight), but averagely between 2% and 5%, with large sample to sample variation, depending on lithology and depositional setting (Isaacs and Petersen, 1987). Deposition of the Monterey and its equivalents coincided with or followed major changes in Miocene ocean circulation, global climate, and tectonics (Pisciotto and Garrison, 1981; Vincent and Berger, 1985; Barron, 1986a). This means that the timing of high productivity of phytoplankton as an important factor for essential elements in petroleum is affected by the global climatic events.

The timing of the collapse of sea surface conditions in the Ocean influences the changes of coccolith size while the size distribution of coccolith is developed through the thermocline and nutricline (Figure 9.1). Kennett (1977) described that Monterey deposition also encompassed the important middle Miocene cooling step in which the Southern Hemisphere cryosphere expanded into the western Antarctica. Weaver et al. (1981) reported that regional intensification of upwelling and increased affinity with higher latitude assemblages in the late Miocene was indicated by most planktonic taxa.

The co-occurrence of all these events in the middle to late Miocene has led many to attribute or relate the character of Monterey deposits to this important reorganization of the Earth's cryosphere-hydrosphere atmosphere system, both as the

cause and the effect (Pisciotto and Garrison, 1981; Vincent and Berger, 1985; Barron, 1986a).

Richter et al. (1992) suggested that although the accumulation of organic carbon in the Monterey Formation alone was probably insufficient to account for this shift, the Monterey was clearly deposited within the context of an important transition in Cenozoic cooling associated with cryospheric expansion, thermohaline circulation reorganization and possibly accelerated flux of nutrients to the ocean related to Himalayan uplift. The widespread lower calcareous mudstone facies of the Monterey were largely deposited during an interval of early to middle Miocene gradual warming.

The middle and upper Miocene Monterey Shale is not only one of the first formations described in California (Blake, 1855; Martin, 1912; Hanna, 1928) but one of the most extensive and important formations in the state. In fact, similar approximately coeval rocks occur also in Baja, California, Japan and elsewhere, both onshore and offshore, in the circum-Pacific area (Redwine, 1981). Figure 9.6 shows oil fields in the Santa Maria area. The Monterey Shale in the Santa Maria area consists of a complex suite of predominantly siliceous rocks, diatomaceous mudstone, and shale, siliceous, partly porcelaneous shale to subordinate, cherty shale containing nodules, lenses (Bramlette, 1946) (Figure 9.7).

Figure 9.8 shows the other example source rocks distribution during the middle to late Miocene boundary in the Los Angeles basin correlate with this study. Stratigraphy source rocks distribution in the Los Angeles basin, Palos Verdes Hills (Monterey formation) and Santa Monica mountains showed that the source rocks was founded during the middle to the late Miocene age. The character of the source rock

was inferred from the geochemistry of each family and their distinct stratigraphic occurrence (Peters et al., 2014).

Walker et al. (1983) reported that the Santa Monica Mountains (NW and NE basin) consist of brown to brownish gray diatomaceous shale with interceded and that the phosphatic “nodular shale” in those mountains contains up to 10 wt. % TOC. The distinctive of formations composed of laminated diatomites and genetically related porcelanites and cherts of lower Miocene through lower Pliocene age occur within many bathyal marine sequences deposited around the North Pacific rim is showed in figure 9.9.

Modern concepts regarding the origin of Neogene marine diatomites and related siliceous rocks have emerged with the recognition of the association between the oxygen minimum layer, exclusion of bottom in fauna, and consequent preservation of laminated diatomaceous muds in anaerobic and near-aerobic Recent marine basins off southern California and in the Gulf of California (Emery, 1960; Byrne and Emery, 1960; Ingle, 1967, 1972, 1980; Soutar and Crill, 1977).

The developed oxygen minimum layer is an important oceanographic feature of intermediate water impinging against the continental margins of the eastern Pacific. Basically, vigorous upwelling induced by seasonal winds and the Coriolis Effect lead to high productivity in surface waters of the eastern Pacific as nutrient-rich water is brought to the surface from the upper portion of the oxygen minimum layer (Figure 9.9).

The key to limiting nutrients accumulate in the oxygen minimum layer and are transported to the photic zone and surface via upwelling completing the recycling process and triggering acceleration of primary productivity. Correlation of selected

Neogene marine sequences along the Pacific Coast of North America, North Pacific Ocean, and the Sea of Japan containing well developed Miocene diatomites and genetic related porcelanites and cherts are showed in figure 9.10.

Significantly, diatomaceous deposition appears to have been initiated between 16 and 14 m.y.b.p. around the entire North Pacific rim with an equal synchronous and widespread termination of this lithofacies between 5 and 4 m.y.b.p. with the exception of topographically isolated highs such as Meiji Guyot (Figure 9.10).

The depositional setting the lower Miocene-mid Miocene lithofacies change from calcareous clay to diatomaceous ooze and clay at DSDP Site 192 on Meiji Guyot and offers solid evidence of the dramatic mid-Miocene increase in upwelling and siliceous productivity induced at higher latitudes by the onset of glacial climate (Ingle, 1981).

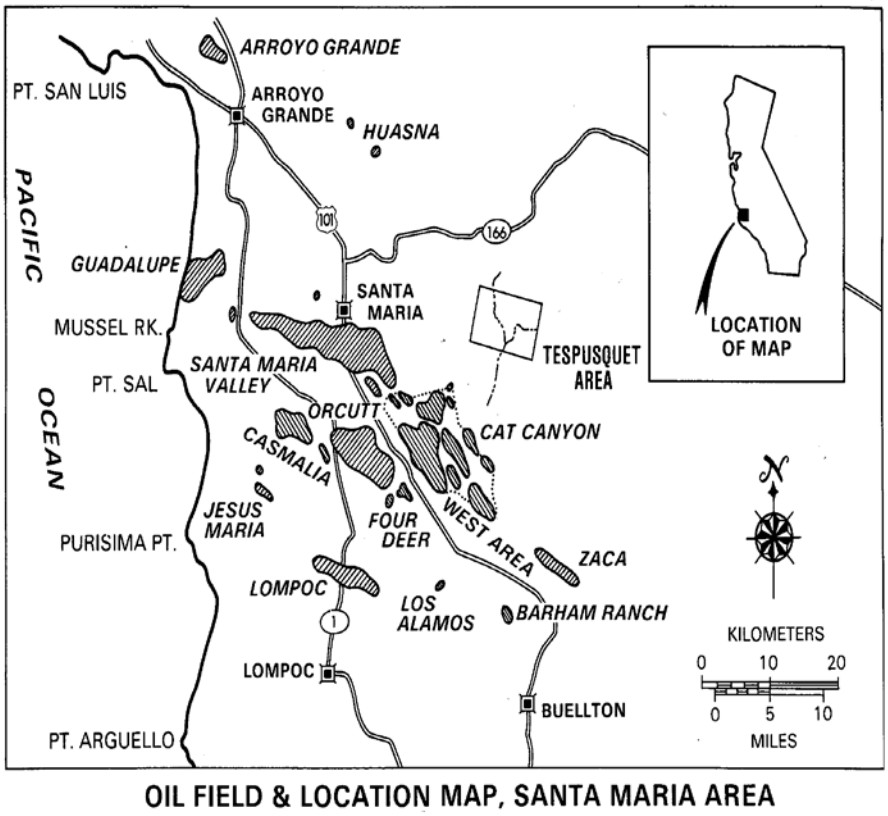

Figure 9.6 Oil fields in the Santa Maria area and localities. Fields area indicated by hatched area and slanted lettering.

The dominantly bioclastic composition of many of the diatomaceous units demands a severe reduction in the delivery of terrigenous detritus to the various marginal basins during mid through late Miocene time. Peak in productivity accompanying maximum periods of refrigeration almost certainly led to intensification and expansion of the oxygen minimum layer in the northeastern Pacific whereas this same event would have led to increased delivery of oxygen-rich Antarctic Intermediate water in the southwestern Pacific maintaining the relatively thin oxygen minimum layers in this area despite increased production of biologic debris (Ingle, 1981).

Ingle (1981) concluded that the wide distribution of Pacific Miocene diatomites has been controlling by a mid-Cenozoic tectonic episode and climatic controlled with induced acceleration of diatoms productivity beginning 15 m.y.b.p. provided the required volumes of diatomaceous sediments as well as the intensification of oxygen

minima. It can be concluded that the eutrophication condition during the late Miocene sequence is relevant to the age of source rocks distributed in that area. Based on that relationship the results of this study suggest that paleoceanography correlated with global climatic events is important for the formation of petroleum source rocks.

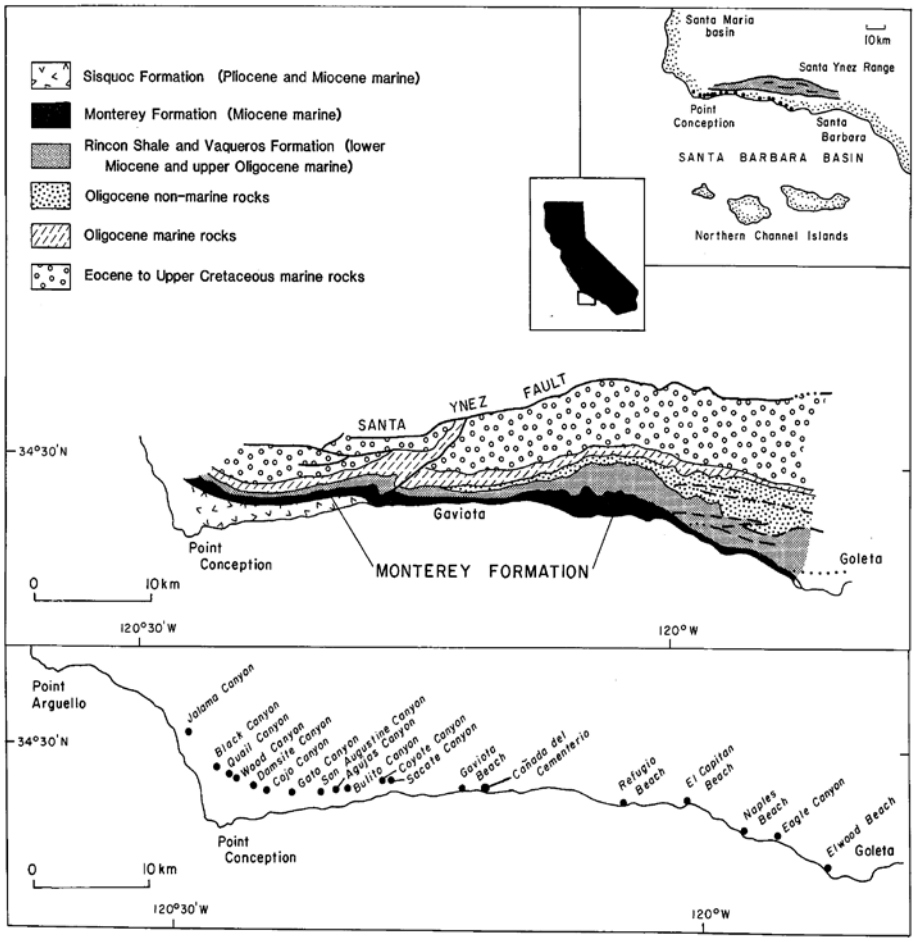

Figure 9.7 Location of sections and geologic setting of the Monterey Formation along the coast west of Santa Barbara, between Golata and Point Conception. Geology adapted from Dibblee (1950, 1966).

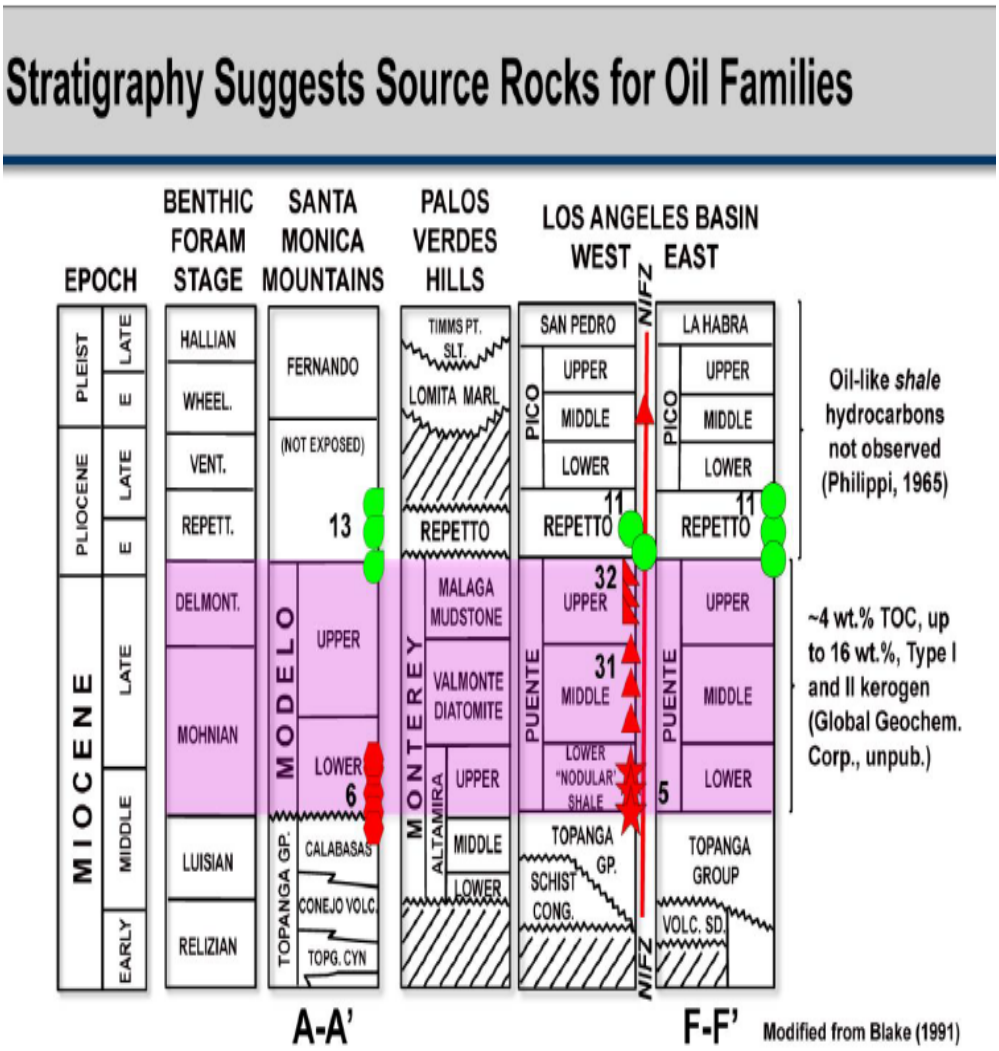

Figure 9.8 Stratigraphy suggests source rocks in the Los Angeles basin (Peters et al., 2014).

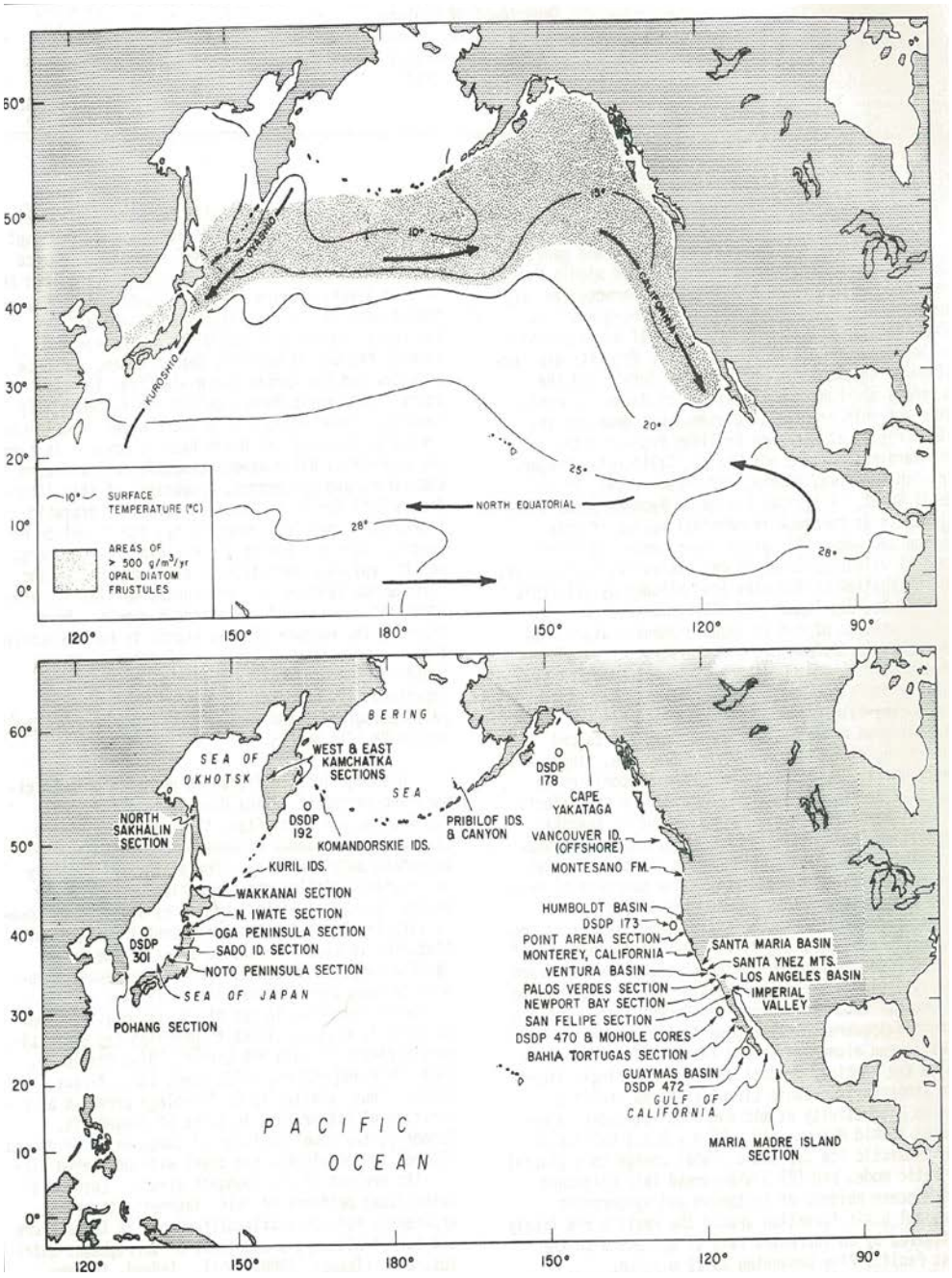

Figure 9.9 Important locations, Deep Sea Drilling Project (D.S.D.P) sites, and stratigraphic section around the North Pacific margin containing well developed Neogene diatomite facies and genetically related porcelaneous shales and cherts. Modern surface current and surface isotherm patterns from Ingle (1967). Area of highest annual diatom productivity and associated production of opaline diatom frustules adapted from Lisitzin (1972).

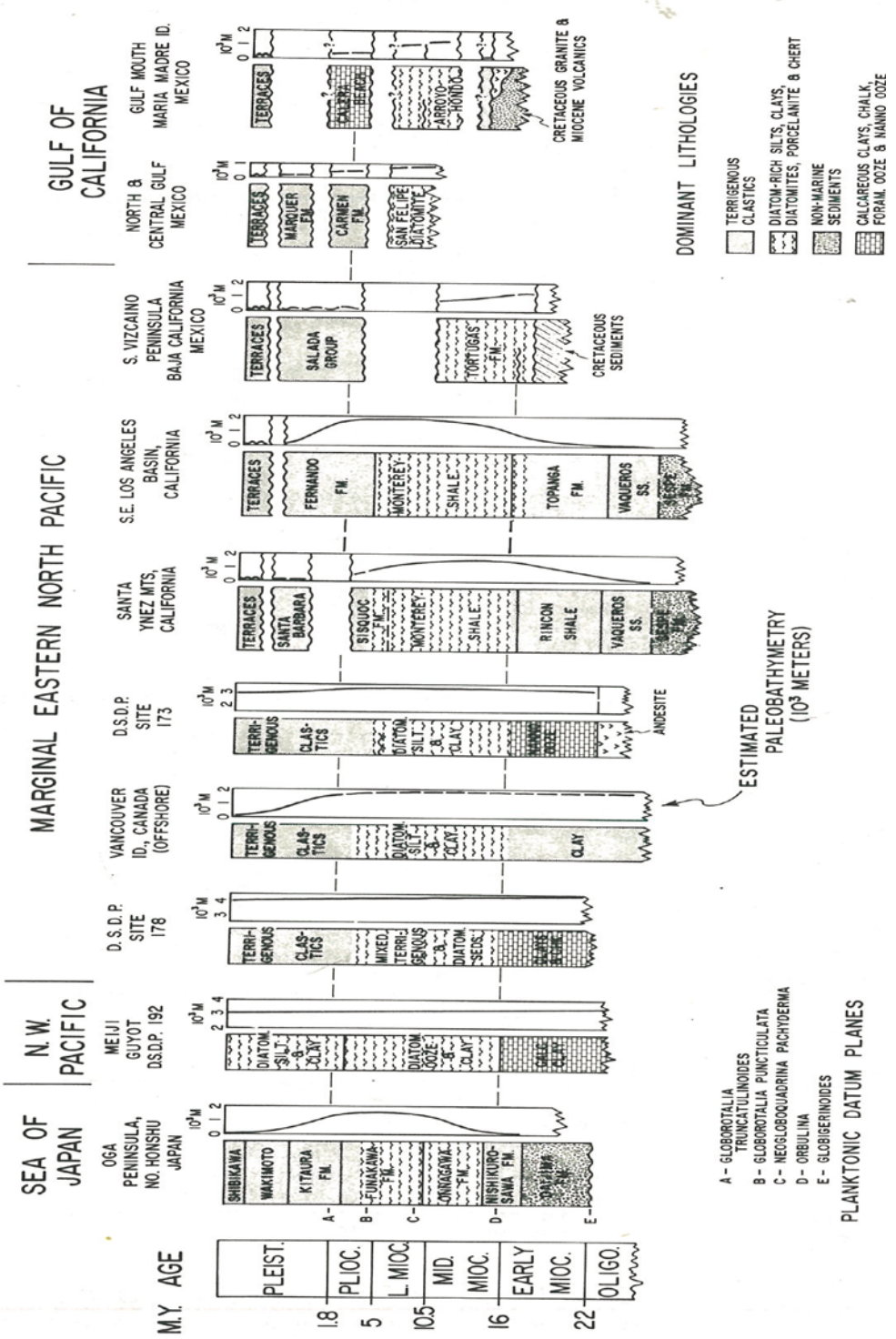

Figure 9.10 Correlation of selected Neogene marine sequences along the Pacific Coast of North America, North Pacific Ocean, and the Sea of Japan containing well developed Miocene diatomites and genetic related porcelanites and cherts. Estimated paleobathymetry of each sequence is based on analysis of benthic foraminiferal biofacies using methods detail by Ingle (1980); figure modified from Ingle (1973b).

X. Conclusions

The coccolith abundance, *Discoaster* productivity, and *Reticulofenestra* species size distribution through the Neogene sequences in the western Pacific and the Bahama Bank of Caribbean were studied to reconstruct the ocean surface stability. The difference of geographic distribution pattern of calcareous nannofossil assemblages in sedimentary records was controlled by the condition of sea surface water mass and related with the global climatic events response. The stability of sedimentation rate and a high of phytoplankton productivity are important factors for the development of petroleum source rocks and Calcareous nannofossils which the one of phytoplankton are traceable in the worldwide. At least 59 species of calcareous nannofossils were determined in ODP Hole 1006A, 50 species of nannofossils in ODP Hole 1007B.C and 61 species of calcareous nannofossils in ODP Hole 782A.

Size change and mode of *Reticulofenestra* have a positive correlation with *Discoaster* abundances, which is coccolith (*Reticulofenestra* spp.) step by step decreased size distribution, as well as *Discoaster* abundances.

The abundant of *Discoaster*, coccolith productivity and large coccoliths from species belonging to the genus *Reticulofenestra* suggest a deep thermocline and nutricline, typical of oligotrophic conditions. And the low *Discoaster* abundance, high productivity of coccolith and large numbers of small *Reticulofenestra* coccoliths indicated a shallow thermocline and nutricline, typical of mixing (eutrophic) conditions. In the case of the Bahama Bank of Caribbean (Atlantic Ocean), the relative abundance of *Discoaster* indicates no significant changes in Site 1007 but it decreased continuously from the late Miocene to late Pliocene in Site 1006.

Floral distribution patterns showed a positive correlation with an abundance of coccolith in the Atlantic Ocean sites. Size changes recognized in the sequence of the Bahama Bank sites clearly showed that the mode of the maximum size of *Reticulofenestra* decreased in the Zones NN8-NN10 (8.8Ma), NN12-NN13 (5.4 Ma), and NN14-NN15 (3.75 Ma).

The results indicated that the size of *Reticulofenestra* increased five times throughout the section. However, it drastically decreased in NN8-10 (8.8 Ma), NN12-13 (5.4 Ma), NN14-NN15 (3.75 Ma), NN17/NN18 (2.514 Ma) and in NN19 Zone (0.8 Ma) in the western Pacific site.

Size variations of nannofossil assemblages (*Reticulofenestra*), *Discoaster* productivity and relative abundance of coccolith- the parameters being studied - indicated that the thermocline and nutricline developed during the Neogene sequences at ODP Hole 782A (western Pacific Ocean) and Bahama Bank of Caribbean (1006A, 1007B, and 1007C) and collapsed at 8.8 Ma resulting in eutrophication of the surface waters. The strong of mixing or eutrophic ocean condition change to stronger in 5.4 Ma and high eutrophic species abundant in the 3.75 Ma.

These changes of *Reticulofenestra* maximum size which are strongly related to the collapse of stability of Ocean surface are clearly traceable to Bahama Bank, western and the northwestern Pacific Ocean and the Indian Ocean. Among them, two events found in 8.8 Ma and 3.75 Ma, are respectively correlated to the intensification of the Asian Monsoon and the closure of Panama Isthmus.

The timing of eutrophication of high productivity coccolith is important as the reference to the formation of petroleum source rock. Organic carbon- rich facies

accumulate preferentially during major transgressive episodes. Asian Monsoon Intensify affected the changes of current systems and the Global climate systems on the basic of the Geographic distribution patterns calcareous nannofossils. The Asian Monsoon intensify also has a profound effect on petroleum basins. This means that the event 8.8 Ma when the eutrophication zone occurrence with the high productivity of nannofossil was the key timing for the formation of petroleum source rock in the Pacific, Atlantic and Indian Ocean.

The upwelling of nutrient-rich oceanic waters may give rise to exceptionally high organic productivity. Transgressive seas also create circumstances that lead to the seasonally or longer-term enhanced water-column stratification and the development of anoxia in combination with eutrophication. The timing correlated to the Japan oil field in which source rocks of petroleum in Hokkaido, Niigata and Akita at Japan oil field area was established in the late Miocene sequences.

Monterey Formation on Santa Barbara, Los Angeles basin, Palos Verdes Hills and Santa Monica Mountains basin showed that the source rocks was founded during the middle to the late Miocene age. This study suggests that the timing of the collapse of sea surface condition or eutrophication condition (8.8 Ma) is related and applicable to the formation of petroleum source rock.

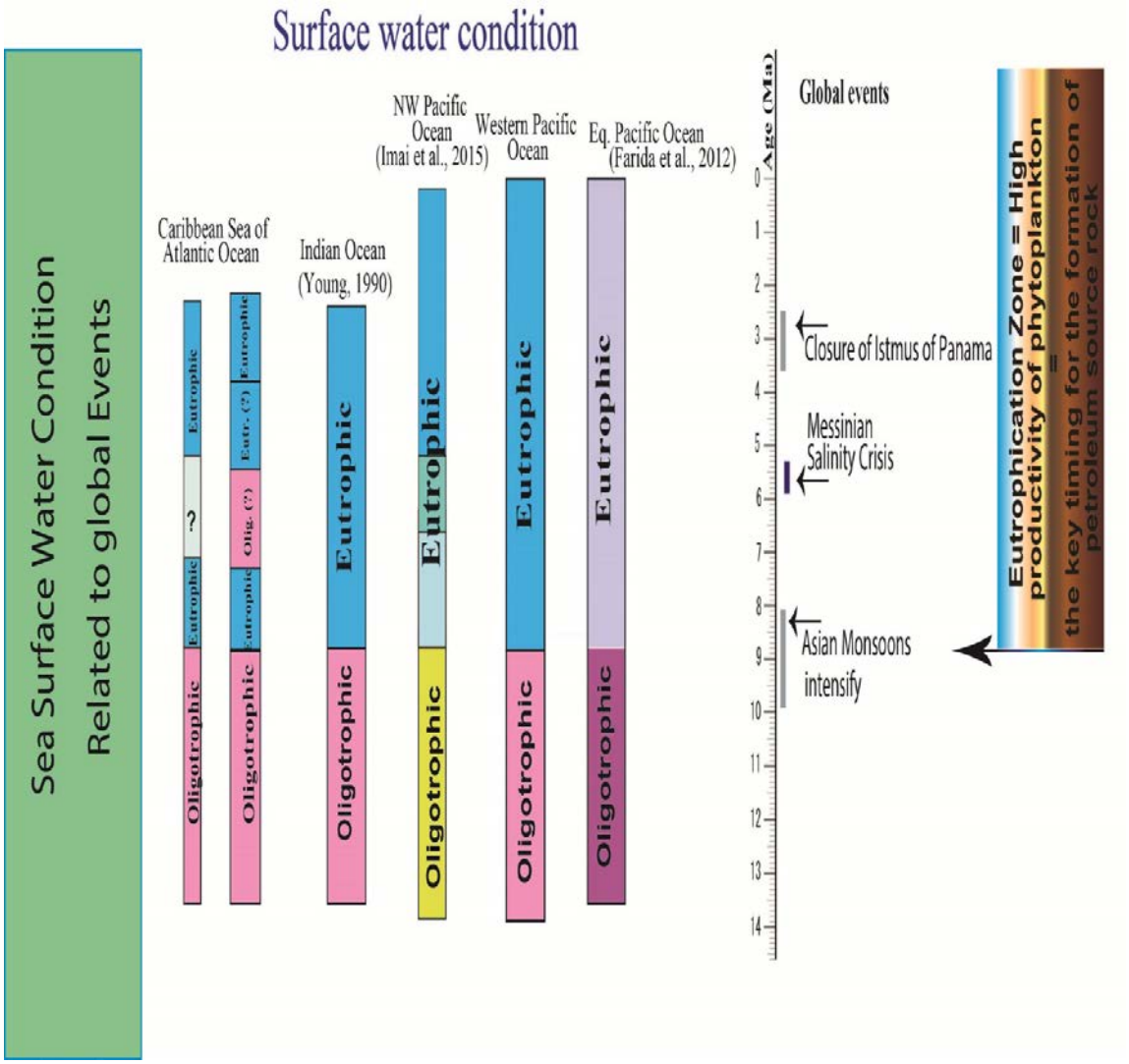

Figure 10.1 Summarize of sea surface water condition related to global event results at Caribbean Sea, Indian Ocean, NW Pacific, western Pacific, and Equatorial Pacific, in interpretation of the timing of petroleum source.

REFERENCES

[1] Okada, H. and Honjo, S. (1973) The distribution of oceanic coccolithophores in the Pacific. Deep-Sea Research, 20, 355–74.

[2] Molfino, B. and McIntyre, A. (1990) Precession forcing of nutricline dynamics in the equatorial Atlantic. Science, 249, 766–9.

[3] Haq, B.U. and Lohmann, G.P. (1976) Early Cenozoic calcareous nannoplankton biogeography of the Atlantic Ocean. Marine Micropaleontology, 1, 119–120.

[4] Bukry, D. (1978) Biostratigraphy of Cenozoic marine sediment by calcareous nannofossils. Micropaleontology, 24, 44-60.

[5] Aubry, M. P. (1992) Late Paleogene calcareous nannoplankton evolution: a tale of climatic deterioration. In: Prothero, D.R., Berggren, W.A., Ed., Eocene–Oligocene climatic and biotic evolution, Princeton Univ. Press, NJ, 272–309.

[6] Stoll, H.M., Shimizu, N., Archer, D. and Ziveri, P. (2007) Coccolithophore productivity response to greenhouse event of the Paleocene-Eocene thermal maximum. Earth and Planetary Sciences Letters, 258, 192-206.

[7] Takahashi, K. and Okada, H. (2000) The paleoceanography for the last 30 000 years in the southeastern Indian Ocean by means of calcareous nannofossils. Marine Micropaleontology, 40, 83–103.http://dx.doi.org/10.1016/S0377-8398(00)00033-5

[8] Sato, T. and Chiyonobu, S. (2009) Cenozoic paleoceanography indicated by size change of calcareous nannofossil and Discoaster number (in Japanese with English abstract). Fossils (Palaeontol. Soc. Japan.), 86, 12–19.

[9] Farida, M., Imai, R. and Sato, T. (2012) Miocene to Pliocene Paleoceanography of the western equatorial Pacific Ocean based on Calcareous Nannofossils, ODP

Hole 805B. Open Journal of Geology, 2, 72–79.
http://dx.doi.org/10.4236/ojg.2012.22008

[10] Imai, R., Farida, M. and Iryu, Y. (2015) Evidence for eutrophication in the northwestern Pacific and eastern Indian oceans during the Miocene to Pleistocene based on the nannofossil accumulation rate, Discoaster abundance, and coccolith size distribution of Reticulofenestra. Marine Micropaleontology, 116, 15-27.

[11] Young, J.R. (1990) Size variation of Neogene Reticulofenestra coccoliths from Indian Ocean DSDP Cores. Journal of Micropalaeontology, 9, 71–86.
http://dx.doi.org/10.1144/jm.9.1.71

[12] Shipboard Scientific Party. (1990) Site 782. In: Fryer, P., Pearce, J.A., Stokking, L.B., et al., Ed., Proceedings of the Ocean Drilling Program, Initial Reports 125, College Station, Texas, 197–252.

[13] Shipboard Scientific Party. (1997) Site 1007. In: Eberli, G.P., Swart, P.K., Malone, M.J., et al., Ed., Proceedings of the Ocean Drilling Program, Initial Reports 166, College Station, Texas, 289–345.

[14] Martini, E. (1971) Standard Tertiary and Quaternary calcareous nannoplankton zonation. In: Farinacci, A., Ed., Proceedings of the Second Planktonic Conference, Roma, Tecnoscienza, 739–785.

[15] Haq, B.U. (1980) Biogeographic history of Miocene calcareous nannoplankton and paleoceanography of the Atlantic Ocean. Micropaleontology, 26, 414-443.

[16] Bukry, D. (1971) Discoaster Evolutionary Trends. Micropaleontology, 17, 43-52.

[17] Bukry, D. (1973) Coccolith and silicoflagellate stratigraphy, Tasman Sea and Southwestern Pacific Ocean, Deep Sea Drilling Project Leg 21. In: Burns, R.E.,

Andrew, J.E., et al., Ed., Initial Reports of the Deep Sea Drilling Project 21, U.S. Government Printing Office, Washington, 885–893. http://dx.doi.org/10.2973/dsdp.proc.21.127.1973

[18] Chepstow-Lusty, A., Backman, J. and Shackleton, N.J. (1989) Comparison of upper Pliocene Discoaster number variations from North Atlantic sites 552, 607, 658, 659, and 662: Further evidence for marine plankton responding to orbital forcing. In: Ruddiman, W., Sarnthein, M., et al., Ed., Proceedings of the Ocean Drilling Program, Scientific Results 108, College Station, Texas, 121–141.

[19] Pujos, A. (1987) Late Eocene to Pleistocene medium–sized and small-sized "reticulofenestrids". Abhandlungen der Geologischen Bundesanstalt, 39, 239–277.

[20] Kameo, K. and Takayama, T. (1999) Biostratigraphic significance of sequential size variations of the calcareous nannofossil genus Reticulofenestra in the Upper Pliocene of the North Atlantic. Marine Micropaleontology, 37, 41–52.

[21] Kameo, K. and Sato, T. (2000) Biogeography of Neogene calcareous nannofossils in the Caribbean and the eastern equatorial Pacific– floral response to the emergence of the Isthmus of Panama. Marine Micropaleontology, 39, 201–218.

[22] Chiyonobu, S., Sato, T., Narikiyo, R. and Yamasaki, M. (2006) Floral changes in calcareous nannofossils and their paleoceanographic significance in the equatorial Pacific Ocean during the last 500000 years. Island Arc, 15, 476–482. http://dx.doi.org/10.1111/j.1440-1738.2006.00543.x

[23] Hagino K., Okada H. and Matsuoka H. (2000) Spatial dynamics of coccolithophore assemblages in the Equatorial Western-Central Pacific Ocean. Marine Micropaleontology, 39, 53–72.

[24] Burbank, D.W., Derry, L.A. and France-Lanord, C. (1993) Reduced Himalayan

sediment production 8 Myr ago despite an intensified monsoon. Nature, 364, 48–54.

[25] Filippelli, G.M. (1997) Intensification of the Asian monsoon and a chemical weathering event in the late Miocene–early Pliocene: Implications for late Neogene climate change. Article in Geology, 25, 27-30.

[26] Zhisheng, A., Kutzbach, J.E., Prell, W.L. and Porter, S.C. (2001) Evolution of Asian monsoons and phased uplift of the Himalaya-Tibetan plateau since Late Miocene times. Nature, 411, 62–66. http://dx.doi.org/10.1038/35075035

[27] Zachos, J., Pagani, M., Sloan, L., Thomas, E. and Billups, K. (2001) Trends, rhythms, and aberrations in global climate 65 Ma to Present. Science, 292, 686–693.

[28] Haug, G.H. and Tiedemann, R. (1998) Effect of the formation of the Isthmus of Panama on Atlantic Ocean thermohaline circulation. Nature, 393, 673–676.

[29] Sato, T., Yuguchi, S., Takayama, T. and Kameo, K. (2004) Drastic change in the geographical distribution of the cold-water nannofossil Coccolithus pelagicus (Wallich) Schiller at 2.74 Ma in the late Pliocene, with special reference to glaciation in the Arctic Ocean. Marine Micropaleontology, 52, 181–193.

[30] Bartoli, G., Sarnthein, M., Weinelt, M., Erlenkeuser, H., Garbe-Scho¨nberg, D. and Lea, D.W. (2005) Final closure of Panama and the onset of northern hemisphere glaciation. Earth and Planetary Science Letters, 237, 33-44. http://dx.doi.org/10.1016/j.epsl.2005.06.020

[31] Krijgsman, W., Hilgen, F., Raffi, I., Sierro, F. and Wilson, D. (1999) Chronology, causes and progression of the Messinian salinity crisis. Nature, 400, 652-655. http://dx.doi.org/10.1038/23231

[32] Hodell, D.A., Kanfoush, S.L., Shemesh, A., Crosta, X., Charles, C.D. and Guilderson, T.P. (2001) Abrupt cooling of Antarctic surface waters and sea ice

expansion in the South Atlantic sector of the Southern Ocean at 5000 cal yr B. P. Quaternary Research, 56, 191–198. http://dx.doi.org/10.1006/qres.2001.2252

[33] Warny, S.A., Bart, P.J. and Suc, J.-P. (2003) Timing and progression of climatic, tectonic and glacioeustatic influences on the Messinian Salinity Crisis. Palaeogeography, Palaeoclimatology, Palaeoecology, 202, 59–66. http://dx.doi.org/10.1016/S0031-0182(03)00615-1

[34] De Vargas, C., Aubry, M-P., Probert, I., Young, J. (2007): Origin and evolution of coccolithophores: From coastal hunter to oceanic farmers. *Eds*., *Evolution of Primary Producers in the sea*, 251-285, Elsevier.

[35] Nathan, S. A and Leckie, R.M. (2009): Early History of the Western Pacific Warm Pool during the Middle to Late Miocene (~13.2–5.8 Ma): Role of Sea-Level Change and Implications for Equatorial Circulation. *Palaeogeography, Palaeoclimatology, Palaeoecology*, 274, 140-159.

[36] Von der Heydt, A and Dijkstra, H.A. (2008): The effect of gateways on ocean circulation pattern in the Cenozoic. Global and Planetary Change, 62, 132-146.

[37] Qiu, B. (2002): The Kuroshio Extension system: Its large-scale variability and role in the midlatitude ocean-atmosphere interaction. *Journal of Oceanography*, **58**, 57–

[38] Krammer, R., Baumann, K-H. and Heinrich, R. (2006): Middle to late Miocene fluctuations in the incipient Benguela upwelling system revealed by calcareous nannofossil assemblages (ODP Site 1085A), *Paleoceanography*, *Paleoclimatology*, *Paleoecology*, 230, 319-334.

[39] Cane, M.A and Molnar, P. (2001): Closing of the Indonesian seaway as a precursor to east African aridification around 3-4 Million years ago. *Nature*, 411, 157-162.

[40] Ruddiman, W.F. (1997): Tectonic Uplift and Climate Change. Plenum Press, New York.

[41] Akmaluddin., Watanabe, K., Kano, A. and Rahardjo, W. (2010): Miocene warn tropical climate: Evidence based on Oxygen Isotope in Central Java, Indonesia. *World Academy of Science, Engineering and Technology*, 71, 66-70.

[42]Yasuda, I. (2003): Hydrographic structure and variability in the Kuroshio-Oyashio transition area. *Journal of Oceanography*, **59**, 389– 402.

[43] McCarthy, K., Rojas, K., Niemann, M., Palmowski, D., Peters, K., Stankiewicz, A. (2011) Basic Petroleum Geochemistry for Source Rock Evaluation. Oilfield Review Summer 2011: 23, 2. Schlumberger.

[43] Shipboard Scientific Party. (1970). DSDP Leg 13. Initial report of the Deep Sea Drilling Project, 42, Part 1: Washington DC.

[44] Waseda, A., Nishita, H. (1998). Geochemical characteristics of terrigenous- and marine-sourced oils in Hokkaido, Japan. *Org. Geochem*, 28, 1/2, 27-41.

[45] Awang H. Satyana (2004). Petroleum Potential in Frontier Areas of Indonesia. The 38th IPA Pre-Convention Course, Jakarta 19-20 May 2014. Aoyagi, K., Iijima, A., 1987. Petroleum occurrence, generation, accumulation in the Miocene siliceous deposits of Japan. In: Hein, J.R. (Ed.), Siliceous Sedimentary Rock-Hosted Ores and Petroleum. Van Nostrand Reinhold, pp. 117–137.

[46] Taguchi, K., 1975. Geochemical relationships between Japanese Tertiary oils and their source rocks. In Ninth World Petroleum Congress Proceedings, Vol. 2,

Geology. Applied Science Publishers, pp. 193–194.

[47] Arthur, M, A. and ageman, B, B. (2004). Sea-level control on source-rock development: perspectives from the Holocene black sea, the mid-cretaceous western interior basin of North America, and the late Devonian Appalachian basin. The Deposition of Organic-Carbon-Rich Sediments: Models, Mechanisms, and Consequences SEPM Special Publication No. 82.

[48] Sakata, S., Suzuki, N. and Kaneko, N. (1988). A biomarker study of petroleum from the Neogene Tertiary sedimentary basins in northeast Japan. Geochem. J., 22, 89–105.

[49] Kikuchi, Y., Tono, S. and Funayama, M. (1991). Petroleum resources in the Japanese island-arc setting Episodes, 14, 236–241.

[50] Sato, T., and Oda, M., (2013). 新盤日化石マニュアル。朝から書店。

[51] The University of Texas at Austin. (2014). Practical Petroleum Geology (2nd edition). USA

[52] Blake, G.H., 1991, Review of the Neogene biostratigraphy and stratigraphy of the Los Angeles basin and implications for basin evolution, in Active Margin Basins: AAPG Memoir 52, p. 135-184.

[53] Peters, K.E., Ramos, L.S., Zumberge, J.E. and Wright, T.L. (2014). Petroleum Systems in the World's Richest Petroliferous Basin, Los Angeles, California. AAPG Annual Convention and Exhibition, Houston, Texas, April 6-9, 2014.

[54] Isaacs, C. M., and Petersen, N. F. (1987). Petroleum in the Miocene Monterey Formation, California, in Hein, J. R., ed., Siliceous sedimentary rock-hosted ores and petroleum: Evolution of ore fields: New York, Van Nostrand Reinhold, p. 83–116

[55] Petersen, N. F., and Hickey, P. J. (1987). California Plio-Miocene oils: Evidence

of early generation, in Meyer, R. F., ed., Exploration for heavy crude oil and natural bitumen: American Association of Petroleum Geologists Studies in Geology 25, p. 351–359.

[56] Walker, A. L., McCulloh, T. H., Petersen, N. F., and Stewart, R. J. (1983). Anomalously low reflectance of vitrinite, in comparison with other petroleum source rock maturation indices, from the Miocene Modelo Formation in the Los Angeles Basin, California, in Isaacs, C. M., and Garrison, R. E., eds., Petroleum generation and occurrence in the Miocene Monterey Formation, California: Los Angeles, Pacific Section, Society of Economic Paleontologists and Mineralogists, p. 185–190.

[56] Pisciotto, K. A., and Garrison, R. E. (1981). Lithofacies and Depositional Environments of the Monterey Formation, California, in Garrison, R. E., and Douglas, R. G., eds., The Monterey Formation and related siliceous rocks of California: Los Angeles, Pacific Section, Society of Economic Paleontologists and Mineralogists, p. 97–122.

[57] Vincent, E., and Berger, W. H. (1985). Carbon dioxide and global cooling in the Miocene: The Monterey hypothesis, in Sundquist, E. T., and Broecker, W. S., eds., The carbon cycle and atmospheric CO2: Natural variations Archean to present: American Geophysical Union Geophysical Monographs 32, p. 455–468.

[58] Richter, F. M., Rowley, D. B., and DePaolo, D. J. (1992). Sr isotope evolution of seawater: The role of tectonics: Earth and Planetary Science Letters, v. 109, p. 11–23.

[59] Barron, J. A., and Isaacs, C. M. (1999).Updated chronostratigraphic framework for the California Miocene, in Isaacs, C. M., and Ruellkötter, J., eds., The Monterey Formation: From rocks to molecules: New York, Columbia.

[60] Kennett, J. P. (1977) Cenozoic evolution of Antarctic glaciation, the

circumAntarctic Ocean, and the impact on global paleoceanography: Journal of Geophysical Research, v. 82, p. 3843–3860.

[61] Weaver, F. M., Casey, R. E., and Perez, A. M. (1981). Stratigraphic and paleoceanographic significance of early Pliocene to middle Miocene radiolarian assemblages from northern to Baja California, in Garrison, R. E., and Douglas, R. G., eds., The Monterey Formation and related siliceous rocks of California: Los Angeles, Pacific Sec.

[62] Isaacs, C. M., and Petersen, N. F. (1987). Petroleum in the Miocene Monterey Formation, California, in Hein, J. R., ed., Siliceous sedimentary rock-hosted ores and petroleum: Evolution of ore fields: New York, Van Nostrand Reinhold, p. 83–116.